NATIONAL ENERGY TECHNOLOGY LABORATORY

Integration of H_2 Separation Membranes with CO_2 Capture and Compression

November 30, 2009

DOE/NETL- 401/113009

U.S. DEPARTMENT OF ENERGY

INTEGRATION OF H_2 SEPARATION MEMBRANES WITH CO_2 CAPTURE AND COMPRESSION

DOE/NETL-401/113009

FINAL REPORT
November 30, 2009

NETL Contact:
Eric Grol
Chemical Engineer
Office of Systems, Analysis, and Planning

National Energy Technology Laboratory
www.netl.doe.gov

ACKNOWLEDGEMENTS

This report was prepared by *JM* Energy Consulting, Inc. for Technology & Management Services, Inc. (TMS), at the request of the U.S. DOE National Energy Technology Laboratory (NETL). This study was conducted over a forty-three month period beginning in April 2006.

Project Managers

Mr. Eric Grol (Dec. 2008 - Nov. 2009)
Mr. Jared Ciferno (Apr. 2006 - Nov. 2008)
U.S. Department of Energy
National Energy Technology Laboratory
Pittsburgh, PA

Mr. Steven Ostheim
Technology & Management Services, Inc.
National Energy Technology Laboratory
Pittsburgh, PA

The author would like to express his appreciation Mr. Jared Ciferno, who developed many of the IGCC simulation and economic models and data used for this analysis, and was instrumental in the development of the framework used for this assessment.

Others who contributed their reviews, comments, and suggestions include:

Mr. Jim Acquaviva	Pall Corp.	Mr. Nicholas Means	Parsons/NETL
Dr. Kathyrn Berchthold	LANL	Dr. Bryan Morreale	DOE/NETL/ORD
Dr. Richard Ciora	Media & Process Technology	Dr. Kevin O'Brien	SRI International
Mr. Jose Figueroa	DOE/NETL/SCC	Mr. Ron Schoff	Parsons/NETL
Mr. Eric Grol	DOE/NETL/OSAP	Mr. Brian Sylcott	TMS/NETL
Dr. David Luebke	DOE/NETL/ORD	Mr. Tom Tarka	DOE/NETL/OSAP
Mr. Michael Matuszewski	DOE/NETL/OSAP	Ms. Jenny Tennant	DOE/NETL/SCC

Your help was invaluable.

DISCLAIMER

Any conclusions, comments or opinions expressed in this report are solely those of the author and do not represent any official position held by TMS, NETL, DOE, or the U.S. Government. Information contained herein was based on the best data available to the author at the time of the report's preparation. In many cases, it was necessary to interpolate, extrapolate, estimate, and use engineering judgment to fill in gaps in these data. Therefore, all results presented here should be interpreted in the context of the specific requirements for accuracy dictated by any intended end use application of these data.

EXECUTIVE SUMMARY

A core mission of the U.S. Department of Energy's (DOE) Carbon Sequestration Program is to foster the development of commercially-ready technologies for CO_2 capture and sequestration. R&D goals have been established for electric power generation from next-generation Integrated Gasification Combined Cycle (IGCC) plants and for future coal-to-hydrogen fuel plants.

Currently for carbon capture, the best available coal gasification system employs a two-stage physical-absorption system for H_2S removal and CO_2 capture. Coal is fed to a high-efficiency gasifier, and the conversion of CO in the raw syngas to H_2 is maximized in a water-gas shift (WGS) reactor. For IGCC applications, the acid gas removal (AGR) system located downstream of the WGS produces a hydrogen-rich fuel gas that is combusted in a gas turbine (GT) topping cycle. H_2S removed in the AGR is sent to a Claus sulfur plant; while the CO_2 recovered is dehydrated and compressed for transport to an appropriate sequestration site. When hydrogen is the desired product, the optimal design is slightly different; less shifting of the raw syngas is required and the AGR is followed by a pressure swing adsorption (PSA) system to recover high-purity hydrogen for compression and sale. The by-product gas from the PSA, which contains H_2, CO and CO_2, is combusted with oxygen in a combined-cycle power system to generate electric power for plant use. The CO_2 from the AGR and the exhaust from the combined-cycle is dehydrated and compressed for transport and sequestration.

R&D supported by the U.S. DOE is investigating alternatives to absorption for capturing CO_2 that may exceed the performance of existing technologies and achieve the DOE program goals. Membrane gas separation has been touted as one possible approach. Membranes have a number of advantages, in that they are usually compact, have no moving parts, have low maintenance, and are highly reliable. In this assessment, alternative flowsheets incorporating membranes that may out-perform current technologies for CO_2 capture were investigated. An initial screening study identified several novel integrations of membranes for IGCC applications. For IGCC, the use of a N_2 sweep gas along with integration of the membrane within the CO_2 compression train is particularly attractive since high-purity hydrogen is not required for power generation. Potential advantages of this approach in addition to the elimination of the two-stage absorption unit are:

- The hydrogen membranes operate at a high feed pressure with a large partial-pressure differential across the membrane
- The use of a sweep gas improves the driving force across the membrane and also serves as the GT diluent
- Hydrogen re-compression is eliminated and the hydrogen fuel and sales gas are delivered at the required pipeline and turbine pressures, respectively.
- The membrane is placed well downstream of the gasifier at a location where most of the contaminants in the raw syngas have been removed

The option described above can be coupled with bulk H_2 recovery from the syngas after the WGS. This enables a high-purity side stream to be produced for use in other applications. PSA can be used for bulk separation with H_2 recoveries in the range of 50% to 80%. This plant configuration allows for maximum flexibility in either the production of hydrogen for sale, or of power generation and sale, or both.

Membranes may also be integrated with the WGS reactors to enhance reaction equilibrium and improve the yield of hydrogen. Screening of various alternatives indicated the best approach here is to eliminate the low-temperature WGS reactor and place membranes before and after the second-stage reactor.

Based on the configurations discussed above membrane selectivity and cost targets were developed to provide guidance in the selection of new and the evaluation of existing CCS Program R&D projects. Permselectivities for H_2 relative to CO_2 will need to exceed 40 for the IGCC system to achieve the 90% CO_2 capture goal. The integration of gas separation membranes by itself cannot achieve the R&D cost goal for a maximum increase in COE of 10% for CCS. However, membrane technologies do hold promise of achieving costs less than current state-of-the-art CO_2 absorption technologies, when coupled with new technologies for lowering the cost and efficiency penalty associated with CO_2 compression and for improving the overall efficiency of IGCC electric power generation.

A major challenge for implementing these CO_2 capture strategies is the development of membrane materials with high selectivities for H_2 relative to CO_2. The IGCC process with CO_2 capture using gas separation membranes, along with a similar process co-producing hydrogen and power, have been modeled with the Aspen process flowsheet simulator. Cases were developed for both warm and cold gas clean-up, and for no gas clean-up, where both CO_2 and H_2S are co-sequestered. Based on the results of this modeling, membrane development performance and cost targets are being developed.

TABLE OF CONTENTS

LIST OF FIGURES

LIST OF TABLES

LIST OF ACRONYMS

AGR - Acid Gas Removal
ASU - Air Separation Unit
BFD - Block Flow Diagram
CC - Combined Cycle
CCS - Carbon Capture and Sequestration
CTH - Coal-To-Hydrogen
DOE - Department of Energy
EOR - Enhanced Oil Recovery
EPRI - Electric Power Research Institute
GE - General Electric
GPU - Gas Permeation Units
GT - Gas Turbine
HF - Hollow Fibers
HHV - Higher Heating Value
HPS - High Pressure Steam
HRSG - Heat Recovery Steam Generator
HTS - High Temperature Shift
IEA - International Energy Agency
IGCC - Integrated Gasification Combined Cycle
LANL - Los Alamos National Laboratory
LHV - Lower Heating Value
LPS - Low Pressure Steam
LTS - Low Temperature Shift
M - 1,000
MDEA - Methyl-Diethanol Amine
MF - Moisture Free
MM - 1,000,000
MTS - Medium Temperature Shift
MW - Megawatt
NETL - National Energy Technology Laboratory
OSAP - Office of System Analysis and Planning (NETL)
ORD - Office of Research and Development (NETL)
PBI - Polybenzimidazole
PEI - Princeton Environnemental Institute
PM - Particulate Matter
PRB - Powder River Basin
PSA - Pressure Swing Adsorption
SCC - Strategic Center for Coal (DOE)
SCF - Standard Cubic Feet (60^{o}F, 1 atm)
SCFD - Standard Cubic Feet per Day
SI - Système International
SOTA - State Of The Art
SRU - Sulfur Recovery Unit
ST - Steam Turbine

STP - Standard Pressure and Temperature (0^{o}C, 1 atm)
SWS - Spiral-Wound Sheets
TGT - Tail Gas Treating
tPD - tonnes (1,000 kg) per day
TPD - Tons Per Day
WGS - Water Gas Shift

I. INTRODUCTION

A number of technical and economic evaluations have been performed on H_2/CO_2 separation membranes in recent years. These include studies sponsored by the U.S. DOE National Energy Technology Laboratory (NETL) [1-7]. The focus of these studies was the production of high-purity hydrogen from coal-derived syngas (*i.e.* coal-to-hydrogen, CTH). These evaluations estimated the performance of conceptually advanced membrane systems (*i.e.* so called water-gas-shift (WGS) membrane reactors), but did not address the performance of more near-term membrane separation options.

The Princeton Environmental Institute (PEI) has investigated hydrogen production from coal as well as the use of membranes to capture CO_2 from integrated-gasification combined-cycle (IGCC) power plants [8,9]. PEI identified a number of key factors that could significantly improve the performance and economics of pre-combustion CO_2 capture using gas separation membranes. It is advantageous that the H_2 be produced at the gas turbine (GT) inlet pressure to eliminate the need for re-compression and that nitrogen, available from the air separation unit (ASU), be used both as a sweep gas for the membrane to increase H_2 recovery, and as a diluent for the gas GT feed to increase power output. PEI and others have also considered the sequestration of "dirty" CO_2 (CO_2 containing H_2S) as a low-cost alternative to H_2S removal and sulfur recovery.

In all of the studies cited above, the question of where in the process flowsheet the membrane might best perform its function of separating H_2 and CO_2 was not considered. How membrane technologies can be coupled with other existing or advanced separation technologies to improve the performance of the total system has also not been examined in any detail. In the analysis reported on here, a scoping study was performed to pre-screen process flowsheet configurations prior to the initiation of more detailed analyses. The most attractive options were then used to develop detailed plant material and energy balances, followed by equipment sizing and costing, and economic evaluation. Based on this analysis, gas separation membrane process and economic performance targets were developed to guide future research relating to the development of hydrogen separation membranes for CO_2 capture from future IGCC power plants.

II. GAS SEPARATION MEMBRANE PLACEMENT

Gas separation membranes are used for hydrogen recovery in petroleum refineries and ammonia plants, and for CO_2 removal in natural gas processing. These large-scale commercial applications share a number of distinct characteristics, which result in competitive advantages for membranes versus other gas separation technologies. These characteristics are:

1) The feed gas contains moderate to high concentrations of the more permeable gas
2) The feed gas is at moderate to high pressure
3) The gas species being separated display moderate to high selectivities
4) Absolute purity of the product gas is not required
5) High recovery of the product gas is not required
6) The feed gas is at moderate temperature
7) The feed gas is relatively clean, requiring little or no pretreatment
8) Low to moderate volumes of gas are being processed

The transport mechanism employed in most gas separation membranes is favored in situations where characteristics 1 - 5 hold. Large partial pressure differences across the membrane are desirable to facilitate gas transport, this implies high feed gas pressures, low permeate gas pressures, and high feed concentrations of the more permeable gas. However, without high selectivity, membrane transport may be rapid, but gas separation will be poor.

Characteristics 6 and 7 allow membranes to be manufactured from relatively inexpensive materials, such as polymers. This significantly reduces material and manufacturing costs. Many polymers can be fabricated into hollow fibers (HF) or spiral-wound sheets (SWS), allowing extremely large area-to-volume packing densities per module[1]. Commercial polymer membranes used for gas separations are limited to temperatures less than the glass transition temperature of the polymer[2]. While many materials are resistant to exposure to water and particulates, coalescing filters for entrained liquids and particulate removal, may be required upstream of the membrane module. It is critical that no liquids be present on the feed-side of the membrane, since this will degrade membrane performance. Therefore, this stream should also remain above the dew point of all gas components to ensure no condensation occurs within the module. Performance of a membrane may also be reversibly or irreversibly damaged by the presence of trace amounts of fouling or otherwise corrosive compounds[3].

[1] Greater than 1,000 ft^2/ft^3 [3,000 m^2/m^3] for HF and 300 ft^2/ft^3 [1,000 m^2/m^3] for SWS membrane modules.

[2] On the order of 120°C (250°F), and no greater than 150°C (300°F) for commercial polymer membranes.

[3] Hydrogen sulfide (H_2S) and aromatic compounds, if present at significant levels, may permanently damage many polymer membrane materials.

Characteristic 8 reflects that membrane units are modular, and separation capacity requirements are met by employing multiple duplicate modules configured in parallel. While this is an advantage from a process flexibility standpoint, it also means that the cost of adding membrane capacity scales nearly linearly with gas throughput. Other competing gas separation technologies have scaling exponents significantly less than one and exhibit improved economies in large scale operations. Existing gas separation applications employing membranes process gas volumes significantly less than what is anticipated with pre-combustion CO_2 capture and sequestration from IGCC power plants. For example, the largest commercial applications of membranes for hydrogen recovery from natural-gas derived syngas, produce on the order of 50 MM SCFD of H_2, requiring more than 100 individual modules. By comparison, it is estimated that a future 500 MW IGCC power plant will require the production of about 250 MM SCFD of H_2, five times as much.

Table 1 compares the application of gas separation membranes for CO_2 capture from an IGCC power plant and H_2 recovery and purification from a CTH plant to the commercialization characteristics discussed above.

Table 1. Characteristics of IGCC & CTH Processes Relating to Membrane Integration

	Conventional Materials		Advanced Materials
	IGCC	CTH	
Feed has moderate to high concentrations of more permeable gas	TRUE	TRUE	SAME
Feed at moderate to high pressure	TRUE	TRUE	SAME
Absolute purity of product not required	TRUE	FALSE	SAME
High product recovery not required	TRUE	FALSE	SAME
Feed of low to moderate volume	FALSE	FALSE	SAME
Gas species display moderate to high selectivities for H_2/CO_2	FALSE	FALSE	TRUE
H_2 displays high permeance	TRUE	FALSE	TRUE
Feed at required membrane temperature	TRUE	FALSE	TRUE
Feed within membrane contaminant tolerances	TRUE	FALSE	TRUE
Relatively inexpensive materials	TRUE		FALSE
Modules have high area to volume ratio	TRUE		FALSE

The second and third columns of Table 1 compare the application of gas separation membranes, based on conventional materials used in current commercial applications (*i.e.* polymers). The fourth column indicates what may be possible with future advanced technologies. In this comparison, it is assumed that the gas separation membrane is

placed at the same location in the IGCC process currently occupied by the AGR system, which is downstream of the WGS reactors, and is integrated with the WGS for the CTH process. The top section of Table 1 lists process characteristics particular to these locations, and the bottom section lists characteristic that relate directly to specific material properties of membranes.

It can be seen that polymer membranes are more applicable to CO_2 capture from IGCC plants, than to H_2 recovery and purification from CTH plants, based on today's technology. However, both applications face two major obstacles, the H_2 selectivity relative to CO_2 of current polymers (and most other materials) is poor, and the processing volumes are very large for these applications. The potential cost disadvantage relative to competing technologies can only be overcome by the development of cheaper and more permeable materials of construction with lower costs of fabrication. Unfortunately, advanced materials with high selectivities are likely to be manufactured from more expensive and less versatile materials than polymers.

Most existing and potential uses for H_2 produced from coal beyond power generation, require the H_2 to be delivered at high purities (greater than 95-98%) and high pressures (greater than ~450 psia [31 bar]). This makes high H_2 selectivity and permeability a prerequisite. Most materials, other than Pd and similar precious metals, exhibit an inverse relationship between permeability and selectivity, making it difficult to achieve high levels of H_2 recovery and purity simultaneously.

For IGCC applications, the challenge is to achieve high H_2 recoveries; purity of the H_2 is less critical. CO_2 purity is a greater concern, since it is to be transported by pipeline to a suitable sequestration site. Low H_2 recoveries result in a CO_2 stream containing undesirable levels of H_2, a potentially flammable component, and in the loss of valuable H_2 fuel for power generation. Temperature and contaminant tolerances are also bigger issues for CTH than for IGCC. These are discussed in more detail in the next section.

The last column in Table 1 indicates that materials are available or are currently being investigated that can solve many of the remaining technical issues for the use of H_2 separation membranes in IGCC and CTH plants. However, no single material has yet been identified that can simultaneously meet all of these challenging and sometimes conflicting process and economic requirements.

A. Placement Options

Unlike other gas separation technologies (*e.g.*, absorption and adsorption), membranes are compact and modular, and can be placed at more than one location to separate H_2 from CO_2 and other gas components. Figure 1 identifies areas where membranes might be effectively integrated into the IGCC process. Each area has potential benefits and drawbacks that must be considered for any proposed CO_2 removal technology. Currently, the best available technology is a two-stage physical absorption technology employing a solvent such as Selexol™. H_2S is removed in the first stage and CO_2 in the second.

Process conditions, gas composition, pressure and temperature, are different at the various locations identified in Figure 1. Each location has its own unique set of advantages and disadvantages in regards to hydrogen separation and recovery. In addition, other technologies under development, such as warm or hot-gas clean-up processes (*e.g.*, H_2S AGR - acid-gas removal), may impact selection of a H_2/CO_2 separation technology, and may or may not complement the membrane separation.

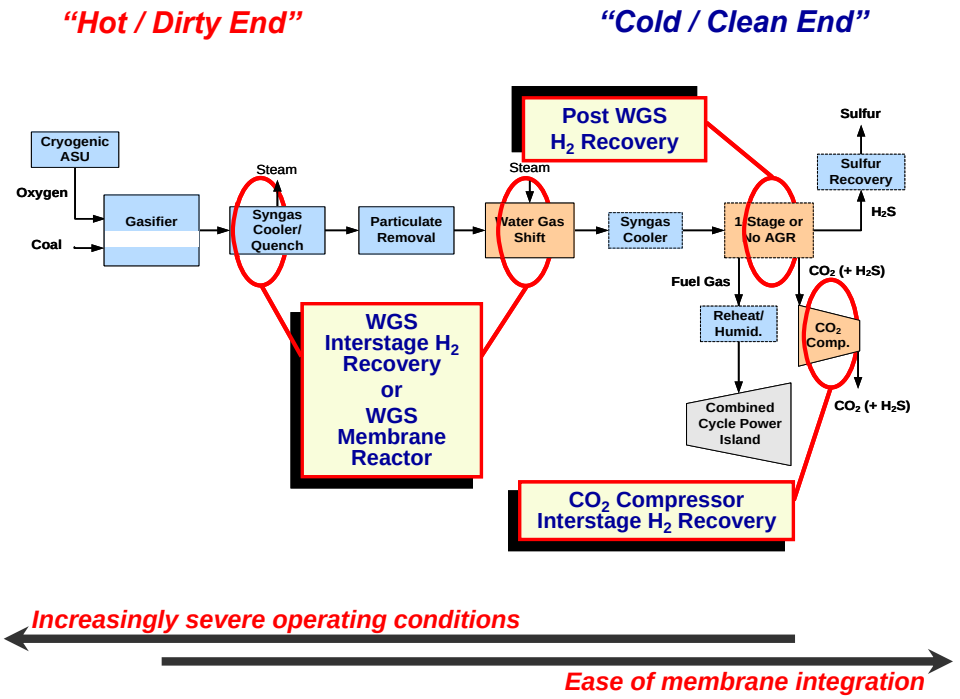

Figure 1. Integration of Membrane-Based Gas Separations with IGCC

Intuitively, the operating envelope for any given membrane technology should match the conditions where it will be placed in the process. If this is possible, the feed and product gases need not be compressed/expanded or heated/cooled. These additional operations can only lower the overall efficiency and raise the overall cost of an IGCC plant. Proper placement of a membrane unit in the process flowsheet is critical, and it seems unlikely that a single membrane material can perform adequately at all feasible locations in the process. Therefore, the challenge is to take advantage of the unique characteristics of individual membrane materials and technologies, while mitigating any shortcomings.

The four locations identified in Figure 1 are described below:

Post WGS H_2 Recovery – This is the current location for H_2S and CO_2 absorption systems in the IGCC process. The syngas at this point has been cleaned of all impurities that might have harmful effects on membrane materials. Current technologies operate at "cold-gas" temperatures that require the syngas leaving the water-gas-shift reactors to be cooled prior to entering the absorption process. Syngas cooling condenses water present in the syngas and lowers plant efficiency, since the fuel gas must be reheated prior to firing in the gas turbine and condensation decreases the mass flow to the turbine. "Warm-

gas" H_2S removal systems are being developed to improve efficiency; however, they will be ineffective if the syngas must be cooled anyway to remove CO_2.

Current two-stage absorption processes produce CO_2 at relatively low pressures (45-150 psia [3-10 bar]), maximizing the compression required to deliver the CO_2 for sequestration. Gas separation membranes located here would replace the second-stage of the absorption process, and also the first stage, if H_2S and CO_2 can be co-sequestered. The CO_2 is delivered to the compression train at a high pressure; however, the recovered H_2 must be re-compressed unless a diluent such as N_2 is used as a sweep gas to lower the H_2 partial pressure on the permeate side of the membrane. The diluent will also increase the mass flow to the gas turbine. If warm-gas H_2S removal is employed, it is desirable that the membrane be permeable to H_2O to avoid later condensation of this water in the CO_2 compression train. This integration is shown in Figure 2a.

CO_2 Compressor Interstage H_2 Recovery – Placement of membranes here has the advantage that the high feed gas pressures will improve the driving force for H_2 transport across the membrane; thus, maximizing H_2 recovery or minimizing membrane area requirements. Use of a sweep gas is still advantageous. For this option, CO_2 compression is minimized, and H_2 can be delivered at the required service pressure without re-compression. Though, some H_2 will be over compressed as it passes through the CO_2 compression train prior to recovery. The process can be optimized by locating multiple membrane units prior to compression, between stages, and post compression. As with post WGS H_2 recovery, the feed gas to the membrane has been cleaned to remove contaminants. This type of integration is shown in Figure 2b.

Figure 2. Gas Separation Membrane Integrations

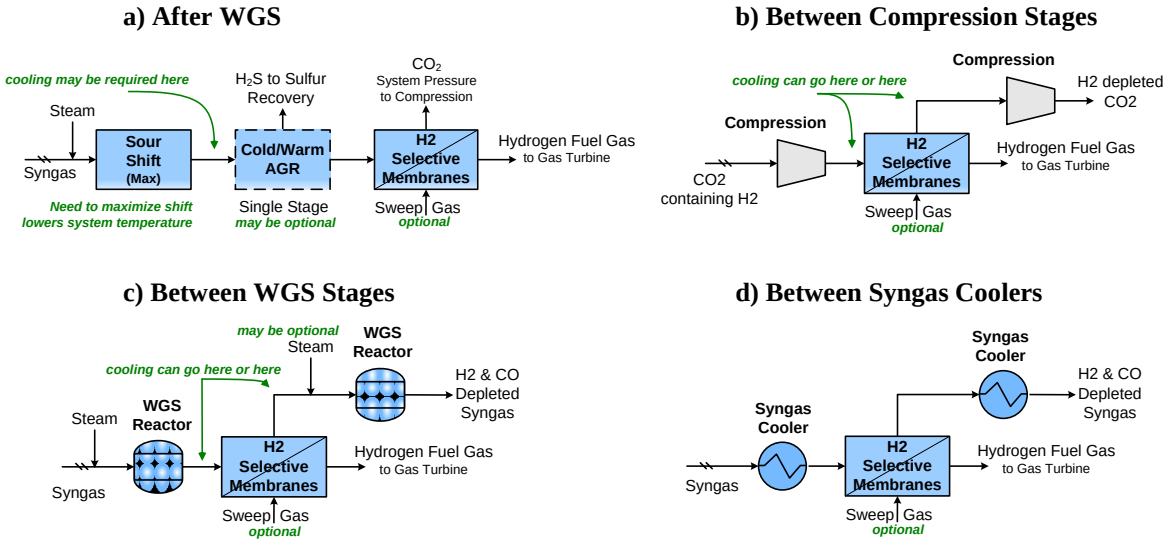

WGS Interstage H_2 Recovery – Removing H_2 between reactor stages drives the water-gas-shift reaction:

$$H_2O + CO \leftrightarrows H_2 + CO_2$$

toward completion by shifting equilibrium in favor of H_2 production. The membrane must be sufficiently impermeable to water for this approach to be advantageous. Interstage H_2 recovery allows the catalyst volume to be minimized, and possibly decreases the number of shift reactors required. It also enables any excess steam co-fed to the reactor and the amount of interstage cooling to be reduced, possibly improving the efficiency of the process. One drawback, however, is that any unconverted water vapor left may be lost to the fuel gas, decreasing the mass flow to the turbine.

Normally, a sulfur-tolerant shift catalyst is employed with H_2S removed downstream of the WGS via absorption-based, cold-gas AGR. As mentioned above, warm-gas removal technologies are still under development. A membrane integrated here would need to be resistant to sulfur compounds. Alternatively, hot-gas H_2S removal could be performed upstream of the WGS. In this case, iron and copper-based shift catalysts would be employed. This integration is shown in Figure 2c.

If the membrane unit is integrated within the syngas cooling step, the homogeneous WGS reaction will occur at the elevated temperatures found here. This location is the most severe, and any membrane placed here would need to have a high tolerance for a wide range of impurities, including particulates, sulfur and nitrogen compounds, and trace metals present in the raw syngas leaving the gasifier. Use of a sweep gas is even more advantageous when coupled with the WGS reaction, since it will enhance H_2 removal and improve the WGS equilibrium further in favor of H_2 production. This is shown in Figure 2d.

WGS Membrane Reactor – By integrating the membrane separation with the WGS reaction, the benefits described above can be maximized. This can be accomplished by packing the retentate flow-space with WGS catalyst or by employing a membrane with a surface that is catalytically active for the WGS reaction. However, this presents a very challenging operating environment for the membrane. In addition to the sulfur tolerance discussed above, the membrane would need to be resistant to a number of other compounds, such as methanol, high molecular-weight hydrocarbons, and coke (carbon deposition), produced as side-products from the catalyzed WGS reaction. The membrane would also be subject to temperature gradients resulting from the exothermic heat of reaction, and some form of internal cooling might be required, complicating the design and fabrication of the membrane reactor. A schematic of a WGS membrane reactor is shown in Figure 3.

Figure 3. WGS Membrane Reactor [10]

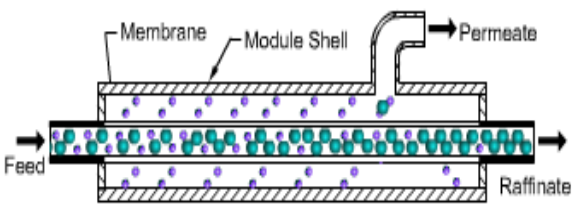

B. Temperature & Pressure Considerations

Table 2 lists the operating temperatures for the locations in the IGCC flowsheet shown in Figure 1. The low and high ranges given for interstage cooling are based on whether the gasifier employs a syngas quench or radiant cooler, respectively. Similarly for the WGS, the low range corresponds to conditions after the interstage coolers and the high range to the outlet temperatures of the reactors. AGR systems under development may operate in a number of different temperature regimes. For interstage compression, the low value is after cooling, upstream of the next stage of compression, and the high range corresponds to possible compressor discharge temperatures.

Table 2. Preferred Membrane Operating Temperatures for IGCC Applications

Location	Temperature Range, °C	
	interstage syngas cooling	
Water Quench / Convective Cooler	200 - 425	
Radiant Cooling / Gas Quench	700 - 900	
	inlet	*outlet*
WGS Reactor - HTS	300 - 350	400 - 500
- LTS	200 - 260	240 - 320
Post Cold-Gas AGR	40 - 100	
Post Warm-Gas AGR	100 - 450	
Post Hot-Gas AGR	> 450	
Compressor	*inlet*	*outlet*
CO_2 Compressor Interstage	~40	65 - 200

WGS - Water-Gas-Shift LTS - Low-Temperature Shift
HTS - High-Temperature Shift AGR - Acid-Gas Removal

Gas separation membranes integrated with WGS will be required to operate in a significantly higher temperature regime than encountered in current polymeric membrane applications, which are limited to about 120°C. The operating temperatures of existing cold-gas AGR systems, or between compressor stages, are within the range of existing polymeric membrane materials.

Table 3 lists IGCC operating pressures. The ranges given are indicative of two common modes of gasifier operation. Lower pressures are normally employed in systems using amine-based AGR, while higher pressures are more representative of a system employing a physical solvent for absorption. For membrane-based gas separation, the high pressure mode is more desirable. At the CO_2 compressor inlet, the ranges given correspond to possible pressures exiting any upstream H_2S/CO_2 AGR process. The compressor outlet is the desired delivery pressure to the CO_2 transport pipeline. The preferred permeate pressure is set by the gas turbine design employed in the IGCC topping-cycle.

Table 3. Preferred Membrane Operating Pressures for IGCC Applications

Location	Pressure Range bar (psia)		H_2 Concentration[a] (wet)	
	gasifier			
	low	*high*		
Syngas Cooling	~28 (400)	~70 (1,000)	16 - 29%	
Water Gas Shift	↓	↓	~42%	
Gas Clean-Up	~21 (300)	~45 (650)	~54%	
	cold-gas	*warm/hot gas*		
CO_2 Compression - Inlet	3.4 - 10 (50-100)	21 - 45 (300-650)	-	
CO_2 Compression - Outlet	110-150 (1,600-2,200)		< 2%	
	for power	*for chemicals*	*for power*	*for chemicals*
H_2 Permeate	24 - 31 (350-450)	>31 (>450)	44 - 80%	> 99%

[a] Based on gasification of typical Eastern U.S. bituminous coal.

The low range reported in Table 3 is typical for IGCC power plant applications designed without CO_2 capture. The lower CO_2 outlet pressure corresponds to the requirements for geological sequestration at or near the IGCC plant; whereas, the high pressure corresponds to requirements for pipeline transport to a sequestration site remote from the plant. It should be kept in mind that the H_2 partial pressure difference is the true driving force for membrane separation, not the total pressure differential across the membrane (total differential does, however, have direct bearing on membrane structural integrity).

Approximate molar H_2 concentrations are also listed in Table 3. The potential benefit of operating the gasifier at high pressure can be seen by examining the pressures and concentrations for the syngas prior to gas clean-up. For instance, the H_2 partial pressure after the WGS is roughly 11 (0.54×21) bar for low-pressure operation, versus 24 (0.54×45) bar for high-pressure operation (a pressure ratio of 24/11 or 2.2). Depending on the desired H_2 delivery pressure, operating at high pressures can significantly improve the driving force for separation. For example, if the H_2 delivery pressure is 5 bar, then the partial pressure differential is 19.3 ($0.54\times45 - 1.00\times5$) bar versus 6.3 ($0.54\times21 - 1.00\times5$) bar, for high and low-pressure operation, respectively. Thus, the partial pressure driving force is 3.1 (19.3/6.3) times higher when operating at the higher pressure. Note that this ratio is greater than the ratio of feed gas pressures. The higher the delivery pressure the greater the benefit of operating at a higher pressure.

The use of a sweep gas is also desirable; however, this is limited by the operating parameters of the gas turbine, and availability and pressure of the diluent employed. Advanced turbines are being designed for a fuel gas with a lower heating value of approximately 4.3 kJ/Nl (120 Btu/scf). This corresponds to a minimum H_2 concentration in the fuel gas of about 44%. For existing gas turbines, the heating value may be as high as about 8 kJ/Nl (220 Btu/scf). The benefits of the sweep gas can be illustrated using the

example described above. For high-pressure operation the partial pressure driving force with the use of a sweep is 22.1 (0.54×45 – 0.44×5), 1.15 (22.1/19.3) and 3.5 (22.1/6.3) times higher for the high-pressure and low-pressure operations, respectively. Alternatively, the sweep gas allows the H_2 delivery pressure to be raised to better match the requirement of the gas turbine.

C. Materials Considerations

Gas separation membranes can be classified based upon separation mechanism and materials of fabrication. Various mechanisms are shown schematically in Figure 4. The first five mechanisms shown involve porous membranes, such as ceramic, zeolite or carbon-based materials. Under viscous-flow conditions, the pores are so large that no separation occurs. With smaller pores, separation occurs through Knudsen diffusion in the gas phase. For H_2/CO_2 separation, the selectivity is only about five for Knudsen Diffusion. This is too low to be of practical use in commercial applications. At even smaller pore diameters, separation occurs based on the size of the gas molecules, through a molecular-sieving effect. However, the ratio of CO_2/H_2 kinetic diameters is surprisingly small, only about 1.15. Again, this is too low to be of practical use industrially; though research efforts continue on tuning nanoporous materials for H_2/CO_2 separation. However, porous ceramic and metallic materials have found applications as support materials for other dense membrane materials.

Figure 4. Mechanisms for Membrane-Based Gas Separations

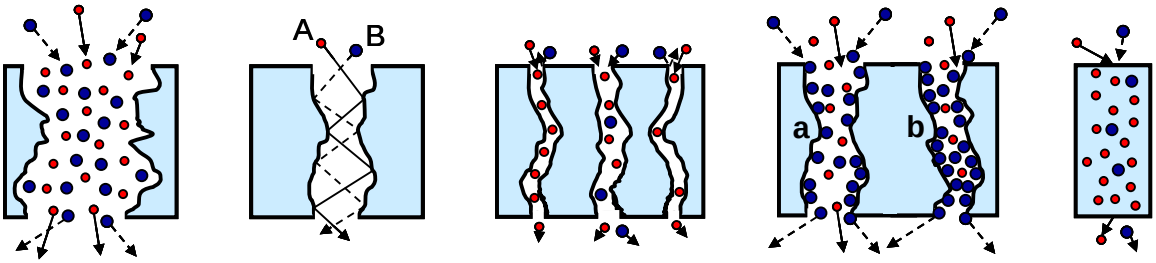

				Surface Adsorption
Viscous Flow	**Knudsen Diffusion**	**Molecular Sieve**	**with Surface Diffusion**	**with Solution Diffusion**
***Separation based on*:**				
None	Molecular Weights	Kinetic Diameter	Multiple Phenomena	Solubility & Diffusion
***Pore Diameter, d_P*:**				
d_P > ~0.1 μm	5-10 Å < d_P < ~0.1 μm	kin.dia.< d_P < 5-10 Å	kin.dia.< d_P < ~0.1 μm	

If one of the gas molecules of interest is preferentially adsorbed on the pore surface, separation can be strongly affected, either positively or negatively. This case is labeled 'Surface Adsorption with Surface Diffusion' in Figure 4. A number of interesting phenomena can occur within the pore structure of the membrane based upon the pore size distribution, relative sizes of the gas molecules, and how strongly one or more components is adsorbed on the surface. In 'a' above, the larger molecule B is adsorbed and separation can be influenced by surface diffusion along the pore walls. If molecule B is sufficiently large relative to the pore diameter, as in 'b', the pore can become plugged and only surface diffusion can occur. It is also possible for molecule B to sufficiently

plug the pores to cease the gas-phase transport of B, but still allow room for the passage of molecule A. Similar phenomena can occur if the smaller molecule A is the strongly adsorbed species. In regards to H_2/CO_2 separation, it is CO_2 which is the more condensable of the two gases. While it is possible to design a gas separation system based upon the preferential transport of CO_2 through a membrane, this is undesirable in IGCC applications, since the CO_2 must be compressed up to pressures much higher than that of the membrane feed gas.

The mechanism labeled 'Surface Adsorption with Solution Diffusion' in Figure 4 occurs in dense membranes, no permanent pore structures are found in these materials. Gas molecules are adsorbed on the surface of the membrane, dissolve in the solid, and are transported via diffusion. As in the case of surface diffusion in porous membranes, surface adsorption can strongly affect the performance of the dense membrane if one species should significantly cover the surface. In glassy polymers, diffusion dominates and H_2 is preferentially transported. Conversely, adsorption dominates in rubbery polymers where CO_2 is preferentially transported. As discussed above, CO_2 transport is undesirable for IGCC applications. Since molecular diffusion is also related to kinetic diameter, conventional polymers are not suitable for industrial H_2/CO_2 separations.

Other materials can be used as dense membranes, including certain metals and ceramic materials. In metals, Pd and various other transition elements and alloys, the transport mechanism is more complex. H_2 disassociates on the surface and is transported through the metal as atomic hydrogen. In dense ceramics composed of rare-earth mixed-oxides, H_2 is ionized to two protons (H+), which are transported through the membrane. Ionic transport is facilitated if the membrane is also an electrical conductor. This has led to the development of ceramic/metallic composite membranes, often referred to as cermets. Non-porous silica and silica/alumina composite are also being developed for gas separations, with transport via the solution diffusion mechanism.

Table 4 summarizes materials that have been tested in the past or are currently being developed for H_2/CO_2 gas separations. Dense ceramic, metallic and hybrid membranes can have essentially infinite selectivity for H_2, as long as no structural defects are present. Whereas, dense polymers and molecular sieves are permeable to all the gases listed, and currently the best H_2/CO_2 selectivities reported are less than 100. In particular, molecular sieves possessing high selectivities cannot be consistently prepared.

Also noteworthy, the relative H_2 fluxes reported in Table 4 vary from 0.005 to 20, more than three orders of magnitude. While this would seem to rule out materials with the lowest fluxes, it should be kept in mind that current large-scale gas-separation applications employ almost exclusively polymeric membranes. A low-cost, low-permeance membrane may be just as or more attractive than a high-cost, high-permeance membrane as long as the membrane meets selectivity requirements. Polymers are relatively cheap, and can be manufactured into hollow fibers and thin sheets, allowing the membranes to be packaged into fiber bundles and spiral-wound sheets exhibiting extremely high area-to-volume ratios. This provides them with a very significant space and cost advantage relative to all of the other materials listed in Table 4.

Table 4. Comparison of Some Potential Membrane Materials H_2/CO_2 Gas Separations

Material	Transported	Normalized H_2 Flux[a]	Ideal Selectivity H_2/CO_2	H_2/CO	H_2/H_2O	H_2/N_2	Temperature °C
Dense Polymers							
Commercial	H_2	0.6 - 1.4	2.5 - 7	30 - 100	~0.1	60 - 200	<110
Advanced - PBI	H_2	0.01 - 0.3	40 - 58	~86	~0.2	-	<400
Molecular Sieves[a]							
Ceramic-Based	H_2	~3	2 - <30	-	-	-	150 - 700
Zeolite-Based	H_2	0.01 - 9	1 - <90	-	-	1.5 - 12	150 - 450
Carbon-Based	H_2	2 - 5	10 - <60	40 - 150	~0.8	50 - 150	150 - 550
Dense Ceramics							
Silica-Based	H_2	0.1 - 2.8	>1,000	>1,000	>1,000	>1,000	150 - 550
Doped Rare-Earth Oxides	H+,e-	<0.005	>1,000	>1,000	>1,000	>1,000	600 - 900
Dense Metallic							
Palladium	H	2 - 5	>1,000	>1,000	>1,000	>1,000	320 - 450
Palladium Alloys	H	5 - 15	>1,000	>1,000	>1,000	>1,000	320 - 450
Asymmetric Composites	H	3 - 20	>1,000	>1,000	>1,000	>1,000	320 - 450
Hybrids							
Ceramic/Nickel	H+,e-	0.01 - 0.04	>1,000	>1,000	>1,000	>1,000	600 - 900
Ceramic/Palladium	H+,e- & H	0.01 - 8	>1,000	>1,000	>1,000	>1,000	600 - 900

[a] Feed pressure of 51 bar; permeate pressure zero; temperature is variable.

Based on the operating limitation for the membrane materials listed in Table 4 and the IGCC process temperature data reported in Table 2, it is possible to make some inferences in regards to membrane selection. A comparison is shown graphically in Figure 5. This figure also identifies current factors limiting the operating temperatures of the various materials. Clearly, all of the membranes described could in principle be used for H_2/CO_2 separation in the IGCC process. Based on the wide variations in temperature encountered in the IGCC process, no single membrane material will be the best choice at all possible locations. This is unlikely to change. Furthermore, most materials will only be optimal over much narrower ranges.

Lastly, a critical factor which must also be considered is the tolerance of the membrane material to the composition of the gas stream being separated. Hydrogen can cause embrittlement of metallic membranes, leading to failure. CO and H_2O can also have damaging effects on certain materials. And as discussed previously, depending upon the location of the membrane, the syngas may contain particulates, sulfur and nitrogen compounds, and trace metals. Sulfur poisons the surface of palladium, and much research is being conducted to improve the sulfur tolerance of palladium-based membranes.

Appendix A contains a short tutorial on membrane-based gas separations that includes a more detailed discussion of membrane separation mechanisms, nomenclature and units of measure, historical development, and current industrial membrane applications.

Figure 5. Temperature Match for Membrane/IGCC Integration

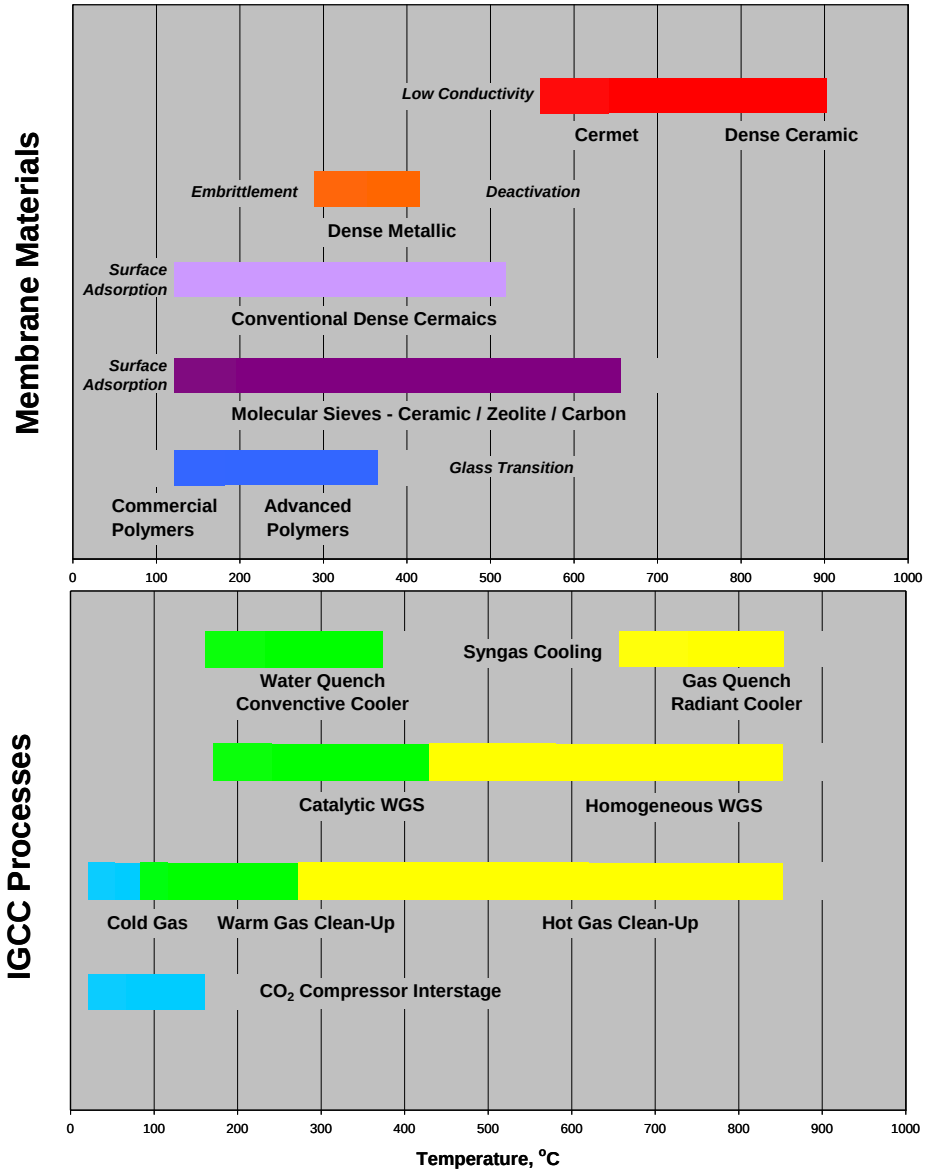

D. Summary

Membranes are modular and may be attractively integrated into a number of locations in the IGCC process. Since CO_2 will need to be further compressed to 150 bar (2,200 psia), it is desirable to recover CO_2 at high pressures; therefore, a H_2 selective membrane is preferred. By the same token, it is also desirable to minimize recompression of the H_2 permeate. Since the required H_2 purity of the fuel gas may be as low as 44%, a sweep gas (preferably N_2 to minimize cycle efficiency losses) can be used both as a fuel-gas diluent and to increase H_2 recovery.

In order to maximize H_2 recovery, gas separation membranes should be placed at locations with high H_2 partial pressures (high total pressure and/or high H_2

concentration). Prior to the first-stage WGS reactor, the H_2 partial pressure driving force for separation is relatively low, after the WGS it can be significantly higher. A likely operating range is 28-50 bar H_2 (100-400 psia). Syngas quality also improves the farther downstream a gas separation membrane is placed from the gasifier. At a minimum, particulate matter will need to be removed prior to gas separation. For the most part, the effect of other syngas impurities will be dependent on specific membrane materials of construction.
Pinch analysis could prove quite useful for optimal placement of H_2/CO_2 separation membranes within the IGCC process.

High selectivity is a prerequisite for successful process integration, since the required selectivity is directly related to the 90% CO_2 capture goal. Low-cost, low-permeance membranes may be more attractive than high-cost, high-permeance membranes as long as the selectivity requirement is met. High selectivity is still an issue for many H_2/CO_2 separation membranes under development. H_2 and CO_2 molecules are similar in size, and this poses an obstacle for the development of molecular sieve and dense polymer membranes. However, these materials are permeable to H_2O, and would be ideal for cold-gas integration.

III. SYSTEM DEVELOPMENT & EVALUATION

The synthesis of IGCC processes employing membranes for CO_2 capture presents some significant design challenges. Most membrane separation systems of interest are only now at bench-scale development. Key parameters are un-optimized or may be unknown, and process scale-up involves a great deal of uncertainty. In addition, technologies upstream and/or downstream of the membrane may or may not complement membrane-based gas separation. Other technologies under development may impact selection of H_2/CO_2 separation technology; examples include upstream, warm-gas clean-up processes for H_2S removal, and downstream, advanced H_2-combustion turbines for heat and power generation[4]. Also of importance specifically to gas separation membranes, are limitations resulting from trade-offs between product purity, recovery and delivery pressure.

Placement of the membrane system within the process flowsheet is critical. Many previous studies have tried to interchange solvent-based CO_2 capture with membrane-based processes. This is not the best approach. Since it is not feasible to consider all combinations of parameters and configurations, the design strategy taken here is evolutionary. Some simplistic alternatives are formulated that take advantage of unique characteristics of membrane-based gas separations while mitigating their shortcomings. These are analyzed and are accepted or rejected. The best alternatives are used to synthesize improved membrane configurations, which are evaluated in more detail to determine membrane process and economic performance targets satisfying DOE R&D Program Goals.

Finally, this assessment is not aimed at determining what might be achievable with a particular membrane material (*i.e.* material science issues) or how this might be accomplished (*i.e.* module design issues). Experts in the field of membrane gas separation are in the best position to make such determinations. Rather, by formulating membrane process and economic performance targets, this assessment provides qualitative guidance to membrane researchers useful for formulating R&D strategies to move gas-separation membrane technology toward commercialization for CO_2 capture applications[5].

A. Membrane Assessment Methodology

The methodology used in this evaluation is summarized in Figure 6. It consisted of five phases.

[4] Detailed analysis of these other technologies is not considered explicitly here; rather sensitivity cases are analyzed to quantify their impact on gas separation membrane requirements related to process and cost performance targets.

[5] Depending on the current state of development for a given membrane, the results of this assessment provide guidance as to which membrane parameters are critical for meeting the DOE R&D Program Goals. For example, should further efforts be focused on improving selectivity, permeance, or cost? The researcher can decide how this is to be accomplished, such as by reducing membrane thickness, changing materials formulations, alternative module designs, etc. The relative importance of these parameters is strongly dependent on the specific membrane and its current state of development.

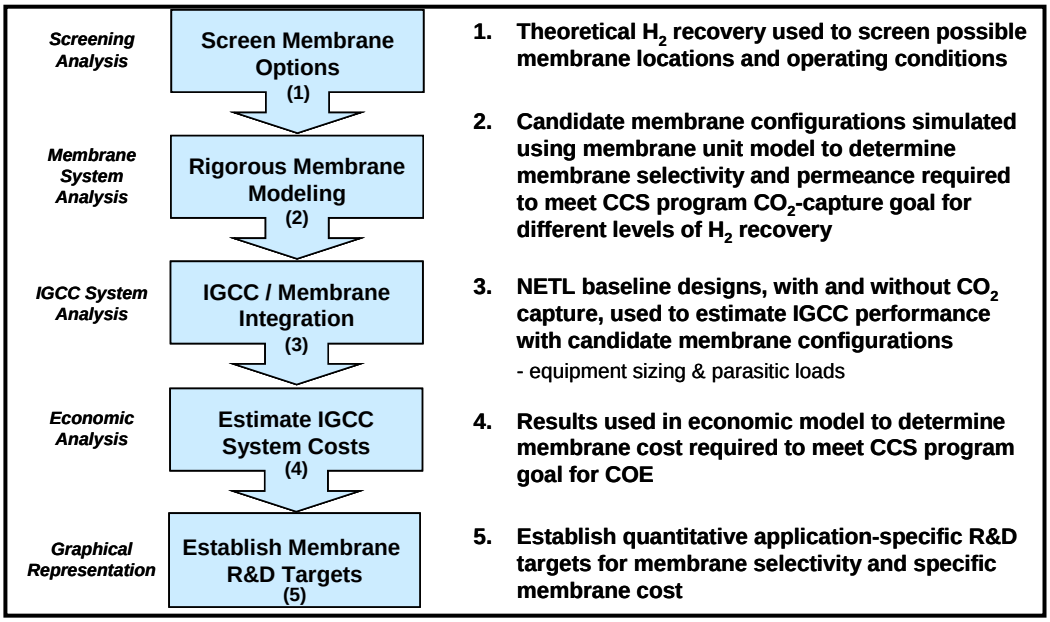

Figure 6. Membrane Assessment Methodology

Phase 1: Screening analyses quantify the benefits and penalties for a range of membrane operating parameters and locations in the IGCC flowsheet. A hybrid system employing pressure swing adsorption (PSA) along with membrane-based gas separation was also analyzed. Screening is performed using simplifying modeling assumptions and theoretically-derived equations relating hydrogen recovery to membrane operating pressures and initial H_2 content of the membrane feed gas. The equations assume that the membrane is only permeable to hydrogen. Parameters studied included membrane feed pressure and hydrogen content, hydrogen permeate pressure and purity, total pressure differential across the membrane, and hydrogen-pinch pressure.

A detailed description of the screening methodology is provided in Appendix B, and derivations of the equations used to predict H_2 recovery are given in Appendix C through E. Appendix C derives the theoretical H_2 recovery when there is no water-gas-shift (WGS) activity within the membrane module (Eq. C11); Appendix D, the theoretical CO conversion in a WGS reactor with no separation (Eq. D19); and Appendix E, the theoretical H_2 productivity (H_2 recovery with CO conversion) for a WGS membrane reactor (Eq. E23). Equation C11 is used for screening WGS inter-stage and post-WGS H_2 recovery options, and Equation E23 is used for WGS/membrane reactors.

Insights gained during the screening analysis were used to develop more detailed process flowsheets integrating multiple membrane units capable of achieving the DOE R&D goals for pre-combustion CO_2 capture from advanced IGCC power plants.

Phase 2: This phase involved the rigorous simulation of the H_2 recovery membrane configurations developed in Phase 1. This was accomplished using a finite-difference numerical model of a single membrane unit developed for execution within an Excel™ workbook. The finite-difference model breaks the membrane unit into a large number of increments to approximate the governing differential equations for flow on either side of

the membrane, and transport of all permeable species across the membrane barrier. For this assessment, it was assumed that the retentate and permeate streams flow co-currently along the length of the membrane[6]. It was also assumed that other mass-transfer resistances between the bulk retentate and permeate streams can be ignored. These resistances will be minimized for successful membrane technologies during rigorous module design.

The membrane networks of interest involve multiple interconnected membrane units. In order to simulate the performance of a network of membrane units, individual membrane workbooks are linked together within Excel to enable the flowrates and compositions of individual streams predicted by the membrane model to be transferred between the specified membrane units. The system equations thus modeled are solved to determine the H_2 permeance, membrane area and H_2/CO_2 selectivity necessary to achieve varying degrees of H_2 recovery. This information is used later in the IGCC system design and economic analysis.

Appendix F contains a more detailed description of the membrane model used for this assessment. Input data for the model are described in Appendix G.

Phase 3: The simulated results from the second step must be integrated with the IGCC power plant. The National Energy Technology Laboratory (NETL) has developed rigorous baseline designs for IGCC power plants, with and without CO_2 capture, using the Aspen Plus™ simulator. These baseline designs are described in more detail in the next section.

It is not practical to develop and run the multitude of process simulations required for all of the cases considered in this analysis. Therefore, the results from the rigorous membrane simulations discussed in Phase 2 were used to adjust the material and energy balances for the NETL baseline design for IGCC with capture. In most cases, tuning of results was straightforward and exact[7]; however, some approximations were required when making adjustments to the power plant steam balance. Appendix G describes in greater deal the procedures used to make these adjustments.

To ensure that the above described procedure is accurate, several rigorous process simulations were set up and executed, and the results compared. The comparisons were reasonable, and well within the accuracy desired for developing membrane technology R&D targets.

---

[6] Actual membrane modules can be designed for co-current, counter-current, cross-flow or some combination of these arrangements. Counter-current is the most efficient orientation, but is more difficult to model. For developing membrane performance targets, the simplest configuration, co-current, was used. Development of optimal membrane module designs is outside the scope of this analysis, and should only be considered for those membrane technologies that exceed or come close to meeting the targets developed here, and after adequate membrane data have been collected for use in detailed module design.

[7] For example, if a membrane capture case uses more power internally than was used in the baseline, this incremental power is subtracted from the baseline plant net power output, and vice versa if less power is required.

Phase 4: The material and energy balances generated in Phase 3 allow the IGCC plant equipment to be re-sized and re-costed. Costs for equipment present in both the original NETL baseline and the membrane-integrated IGCC designs are scaled based on changes in capacity. Costs for new equipment, other than the added membrane units, were developed using other sources.

The adjustments discussed above are made within the NETL IGCC economics model [11]. The model then computes the levelized-cost of electricity (LCOE) for the membrane-integrated design. The LCOE is calculated for two different, assumed values for installed cost of membrane area, 0 and $\$100/ft^2$. These values are used in the fifth phase of the assessment.

Appendix H contains a complete description of the economic analysis.

Phase 5: Membrane cost curves are developed using the selectivity versus H_2 recovery data generated in Phase 2, along with the COE estimates from Phase 4. The cost curves relate the change in LCOE between the membrane-integrated IGCC design and the NETL baseline without CCS to the specific cost of the membrane per unit area per unit H_2 permeance with H_2/CO_2 selectivty as a parameter. Development of the membrane cost curves and R&D targets are described in Appendix I.

B. Conceptual Design Basis and Data Sources

***a. Membrane Screening Analysis*.** The screening analysis was performed in late 2005 and early 2006. It used a different basis than the detailed system analyses that followed, since the NETL IGCC baseline designs described below were not completed until 2007. However, the number of differences is small, and these differences are not considered significant with respect to the conclusions drawn from the screening analysis.

The screening analysis only considered the performance of the membrane. Therefore, only a few process conditions needed to be specified; stream compositions, pressures and temperatures for possible feed streams to the membrane unit, and hydrogen delivery pressure and purity. The WGS feed stream composition was obtained from a coal-to-hydrogen study conducted by Parsons Corp. for NETL published in 2003 [12]. This was supplemented with additional information on three-stage WGS reactor performance obtained from Parsons [13]. Pressure and purity requirements were based on an earlier IGCC CO_2-capture study performed by Parsons for the Electric Power Research Institute (EPRI) and DOE published in 2000 [14].

This 2003 Parsons design produces hydrogen as a product and does not capture CO_2 for sequestration. Other elements of the design relevant to the screening analysis include:

- Syngas is generated from high-efficiency two-stage gasifiers based on E-Gas™ technology fed Pittsburgh No.8 bituminous coal with 2.9% sulfur. Raw syngas cooling is performed using waste heat boilers, followed by convective shell-and-tube gas coolers. Cooling is followed by particulate removal using metal candle filters.

- Only high-temperature, sulfur-tolerant, WGS reactors are required to convert about 80% of the CO in the syngas to CO_2. This was accomplished in two fixed-bed WGS reactors in series with inter-cooling. A low-temperature shift is not used since the downstream PSA unit will produce a tail gas containing residual hydrogen that is consumed as plant fuel.
- A single-stage acid-gas removal (AGR) system captures H_2S using the amine solvent MDEA, and a PSA is used to produce high-purity (99%) hydrogen from the clean syngas leaving the AGR.

This design was modified using information from the other sources to add a third-stage, low-temperature WGS reactor capable of boosting overall CO conversion to about 98%, as required for IGCC operation with CO_2 capture. The 2000 IGCC CO_2-capture study also replaces the single-stage MDEA-based AGR system with a two-stage Selexol™ system capable of removing both H_2S and CO_2, and adds CO_2 drying and compression to 1,200-2,200 psia (82-150 bar). PSA to separate and purify hydrogen is replaced by combined-cycle power production employing General Electric's H-type advanced gas turbine.

b. IGCC System Analysis. The design basis for the IGCC system analysis employing H_2 separation membranes for CO_2 capture was obtained from the NETL 2007 report *Cost and Performance Baseline for Fossil Energy Plants* [15]. Case 3 from this study is a state-of-the-art IGCC plant without CCS, and Case 4 is the same plant fitted with state-of-the-art CO_2 capture. Figure 7 depicts the major differences in the flowsheets for these two designs.

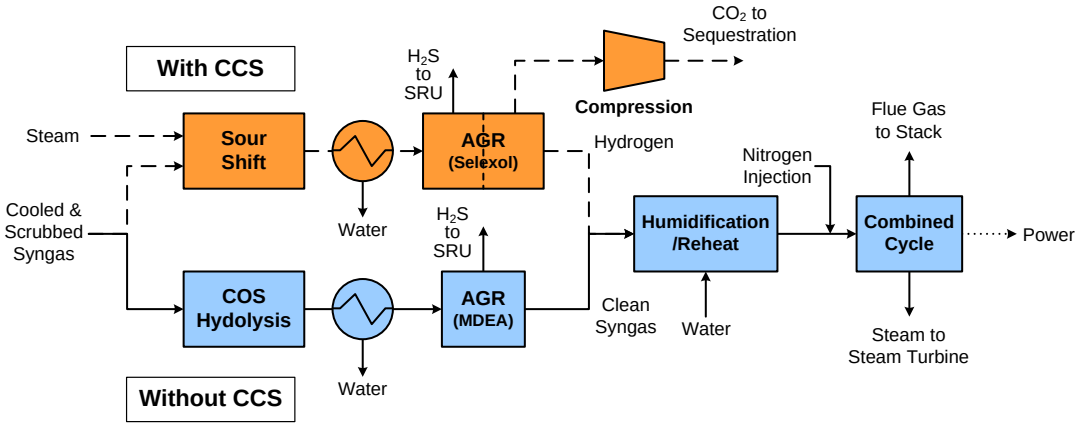

Figure 7. IGCC Flowsheet Changes Required for CCS

Important elements of the Case 3 design are:

- Syngas is generated using high-efficiency two-stage gasifiers based on E-Gas™ technology fed Illinois No.6 bituminous coal with 2.5 wt% sulfur and 11.2 wt% moisture as received (AR). The coal is ground and slurried with water to a solids concentration of 63 wt%, before being fed to the gasifiers at a pressure of 850 psia (58 bar). Oxygen required for gasification is supplied at 95% purity by cryogenic air

separation units (ASU). Two gasification trains, with a combined feed of 5,567 TPD AR (5,050 tPD) of coal, are required for an IGCC plant producing 623.4 MW of electricity (net).

- Raw syngas leaves the second-stage of gasification at a temperature of 1,850°F (1050°C), and is cooled to 700°F (371°C) within a heat-recovery, steam generator (HRSG). Particulates are removed from the cooled gas via a cyclone followed by a ceramic candle filter. Following particulate removal, the syngas is cooled to 330°F (166°C) prior to entering a syngas scrubber, where a water wash is used to remove chlorides and any remaining particulate. The syngas exits the scrubber saturated at 305°F (152°C) and 555 psia (37.8 bar). It is then reheated to 400°F (205°C) and enters a COS hydrolysis reactor, where about 99.5% of the COS is converted to CO_2 and H_2O. The exiting gas passes through a series of condensers to lower the syngas temperature to 39°C (103°F) and to separate entrained water, and is then treated in a carbon bed to remove 95% of the Hg present in the gas.
- Cool, particulate-free syngas is fed to an absorber at 103°F (39°C) and 495 psia (33.8 bar), where H_2S is preferentially removed from the gas stream by contact with the chemical solvent MDEA. The absorber column is operated at 80°F (27°C) by refrigerating the lean MDEA solvent. The acid-gas stream recovered from the solvent stripper, containing of 29% H_2S and 70% CO_2, is sent to a Claus unit. Overall sulfur recovery is 99.5%. Tail gas from the Claus unit is recycled to gasification.
- Clean syngas exits the MDEA absorber at 99°F (37°C) and 494 psia (33.7 bar) and is partially humidified, diluted with nitrogen, and then reheated before being fed to the combustion turbine at a temperature of 385°F (196°C) and pressure of 479 psia (32.7 bar). Humidification is used rather than nitrogen because there is insufficient nitrogen produced in the ASU to provide the level of dilution required to reach the target syngas heating value of 120 Btu/scf (4.3 kJ/Nl) (LHV basis).
- The GE advanced F Class combustion turbines produce 464 MWe. Heat is recovered from the hot exhaust from the turbine in the heat-recovery steam generator. The steam raised in the HRSG is used to power an advanced, commercially available steam turbine using a steam cycle operated at 1800 psig/1,050°F/1,050°F (123 barg MP/566°C/566°C). The steam turbine produces 278.5 MWe for an IGCC plant output of 742.5 MWe gross and 623.4 MWe net. Net plant efficiency is 39.3% (HHV basis).
- The levelized cost of electricity for this IGCC plant is 7.80 ¢/kWh.

The modifications required for CO_2 capture shown in Figure 7 result in the following changes for Case 4:

- The total coal feed to gasification is increased to 5,735 TPD (5,203 tPD).
- COS hydrolysis is replaced by two parallel sets of fixed-bed WGS reactors; each set consisting of three reactors (high, low, and medium temperature shift) in series. In addition to shifting the syngas, the sour-gas shift reactors also perform the dual function of hydrolyzing COS. Steam is injected upstream of the first WGS reactor to

adjust the syngas H_2O-to-CO molar ratio to 2:1 on a molar basis. Cooling is provided between the WGS reactors to control the exothermic temperature rise. The temperature and pressure of the shifted syngas leaving the last WGS reactor are 457°F (236°C) and 516 psia (35.2 bar), respectively.

- Following cooling and Hg removal, the shifted syngas is fed to the first stage of a two-stage Selexol absorption unit at 93°F (34°C) and 471 psia (32.1 bar), where H_2S is removed and sent to the sulfur recovery unit (SRU) as before. The second stage removes CO_2 at three pressure levels: 22, 160, and 300 psia (1.5, 10.9 and 20.5 bar). The low and medium pressure CO_2 streams are compressed, and then combined with the high pressure stream. The combined CO_2 is further compressed to a supercritical state of 2,215 psia (150 bar), consistent with pipeline transmission requirements. During compression, the CO_2 stream is dehydrated to a dew point of -40ºF (-40°C). The raw CO_2 stream from the Selexol process contains over 93% CO_2 with the balance primarily nitrogen. Further purification of this stream is required prior to transport and storage.
- Clean syngas exits the Selexol unit at 99°F (37°C) and 469 psia (32 bar); and as in Case 3, is partially humidified, diluted with nitrogen, and then reheated before being fed to the combustion turbine at a temperature of 385°F (196°C) and pressure of 453.5 psia (31 bar). The advanced F Class combustion turbines produce 464 MWe as in Case 3; however, the steam turbine output is lower, 229.8 MWe. In this case, the steam cycle is operated at 1800 psig/1,000°F/1,000°F (123 barg MP/538°C/538°C). The IGCC plant output is 693.8 MWe gross and 518.2 MWe net. The net output is significantly reduced relative to Case 3, since the gross power plant output is constrained by the capacity of the two combustion turbines, and since the CO_2 capture and compression process increases the auxiliary load on the plant. The net plant efficiency drops to 31.7% (HHV basis).
- The levelized cost of electricity for this IGCC plant is 10.29 ¢/kWh.

A major difference between the Case 4 design from the 2007 NETL baseline and the earlier IGCC CO_2-capture study design from 2000 is the operating pressure in the syngas clean-up section of the plant. The 2000 study has a pressure of 825 psia (55.6 bar) for the syngas entering the AGR, versus 471 psia (32.1 bar) from the 2007 study. As a result, additional power can be generated by expanding the fuel gas prior to combustion. The expander is located after humidification, before nitrogen is injected. As will be seen later, a higher pressure for the syngas is necessary when considering gas separation membranes as an alternative to absorption for CO_2 capture.

It should be noted that the GE advanced F Class turbine selected for the baseline designs was assumed to be available by 2010 for both conventional and high H_2 content syngas representative of the CO_2 capture Case 4. High H_2-content fuel combustion issues like flame stability, flashback and NOx formation were assumed to be solved in the time frame considered by this study. In addition, the minimum, fuel-gas LHV specification for the F Class turbine is 100 Btu/scf (3.6 kJ/Nl), less than the 120 Btu/scf (4.3 kJ/Nl) used in Cases 3 and 4. Permeate dilution is also beneficial for improving H_2 recovery using membrane-based separation. However, this change to the NETL design has

implications for the overall performance and efficiency of the IGCC plant, which are outside the scope of this assessment. Therefore, this modification was not considered.

The Case 4 baseline design provides few details on the design used for the second stage of the Selexol system. The system achieves 99.4% recovery of hydrogen. In addition, only 93% CO_2 purity is obtained directly by the Selexol system as designed. As a result, it is assumed that a secondary, but unidentified, process will be employed to boost CO_2 purity to 100%. In the open literature on Selexol absorption technology, nitrogen is often employed to strip CO_2 from the solvent.

In addition to the cases discussed above based on the ConocoPhillips E-Gas gasifier, the 2007 NETL baseline study included cases employing the GE and Shell gasifiers. Without CO_2 capture, the net plant HHV efficiency was highest with the Shell gasifier at 41.1%, followed by E-Gas at 39.3%, and GE at 38.2%. With CO_2 capture, all the gasifiers produced the same IGCC net efficiency of about 32%. However, all of the CO_2 capture cases do not manage carbon with the same proficiency. Emissions on a lb-CO_2 per MWh basis were 253 with E-Gas, 206 with GE, and only 199 with Shell. This ordering is also reflected in the maximum theoretical amount of hydrogen produced after complete shifting of the raw syngas. E-Gas has the lowest content at 53.70%, followed by GE at 57.88% and Shell at 58.18%. One of the implications of this ordering is that for a given system pressure, membrane-based H_2 recovery will be easier with the Shell and GE gasifiers than with E-Gas, at least based on these current designs. On the other hand, the levelized cost of electricity is also the highest of the IGCC plant designs employing the Shell gasifier. With regards to the present study, membrane integration into the E-Gas based IGCC plant is more challenging.

IV. SCREENING & FLOWSHEET DEVELOPMENT

The screening analysis was undertaken to examine where in the IGCC process flowsheet the membrane might be located to best perform its function of separating H_2 from CO_2. Also examined was a hybrid system that couples pressure swing adsorption (PSA) with membrane-based gas separation. The screening results were used to develop membrane system configurations involving multiple membranes strategically distributed throughout the IGCC process, which were then analyzed using more detailed models. Results of the detailed analyses are the topic of Section V of this report.

A. Screening Analysis

The screening analysis considered the performance of a single ideal membrane, which was modeled using theoretically-derived equations given in Appendices C through D. These equations enable the maximum H_2 recovery to be predicted; however, they do not provide information on equipment size or cost, nor on impacts to the IGCC system as a whole. Maximum H_2 recovery is used solely as a metric to compare the performance of various sets of membrane operating conditions and locations. High recoveries are a prerequisite for the development of a cost-competitive CO_2 capture process, since the loss of H_2 fuel gas results in the direct loss of IGCC power output.

The steps involved in estimating H_2 recoveries for the different H_2/CO_2 separation options are: determination of permeate dilution based on fuel-gas heating-value requirements; selection of membrane/PSA unit inlet and outlet pressures; selection of membrane H_2 partial-pressure approach and/or WGS reaction temperature approach to equilibrium; and estimation of H_2 recovery and purity for the H_2-rich fuel-gas and CO_2-rich capture stream. It is also assumed that the membrane is only permeable to hydrogen (*i.e.* H_2 selectivity relative to all other gas components is infinite). Any effects of an acid-gas removal (AGR) unit, if present, on H_2 recovery are ignored. Effects of these assumptions will be examined more carefully for the membrane configurations selected for detailed modeling.

A complete description of the screening methodology is provided in Appendix B. Three membrane placement options were considered for screening: post-WGS H_2 recovery, CO_2 compressor-interstage H_2 recovery (with and without post-WGS PSA), and H_2 recovery integrated with WGS. Parameters considered in the screening analysis are reported in Table 5.

Table 5. Membrane Screening Parameters

H_2 selective membrane located downstream from WGS reactors		Range
Feed Gas H_2 Content, vol%	based on maximum shifting of syngas	57.34%
Permeate H_2 Content, vol%	based on no sweep, partial, or max sweep gas, set by gas turbine	100 / 72 / 44%
Feed Gas Pressure, psia	set by gasifier design pressure and equipment pressure drops	400 / 700
Permeate Pressure, psia	design parameter for membrane; max set by gas turbine	50 / 380
H_2 Partial-Pressure Approach, psi	indicative of membrane area	0 / 10 / 25 / 50
Pressure Diff. Across Membrane, psi	limitation of membrane material and fabrication	20 - 650
H_2 selective membrane integrated with CO_2 compression		
Feed Gas H_2 Content, vol%	based on maximum shifting of syngas	57.34%
Permeate H_2 Content, vol%	based on no sweep, partial, or max sweep gas, set by gas turbine	100 / 72 / 44%
Feed Gas Pressure, psia	CO_2 compression requirements and compression ratios	800 / 1,600 / 2,200
Permeate Pressure, psia	design parameter for membrane; max set by gas turbine	50 / 380
H_2 Partial-Pressure Approach, psi	indicative of membrane area	0 / 10 / 25 / 50
Pressure Diff. Across Membrane, psi	limitation of membrane material and fabrication	420 - 2,150
PSA located downstream from WGS reactors with…		
Feed Gas H_2 Content, vol%	based on maximum shifting of syngas	57.34%
Feed Gas Pressure, psia	design parameter for PSA unit; max set by gas turbine	380
Tail Gas Pressure, psia	design parameter for PSA unit; affects compression requirements	50 / 100
...H_2 selective membrane integrated with CO_2 compression		
Permeate H_2 Content, vol%	based on no sweep, partial, or max sweep gas, set by gas turbine	100 / 72 / 44%
Feed Gas Pressure, psia	CO_2 compression requirements and compression ratios	800 / 1,600 / 2,200
Permeate Pressure, psia	design parameter for membrane; max set by gas turbine	380
H_2 Partial-Pressure Approach, psi	indicative of membrane area	0 / 10 / 25 / 50
Pressure Diff. Across Membrane, psi	limitation of membrane material and fabrication	420 - 1,820
H_2 selective membrane integrated with WGS reactors		
Feed Gas H_2 Content, vol%	based on partial shifting of syngas, set by WGS reactor design	19.3 / 39.4 / 43%
Permeate H_2 Content, vol%	based on no sweep, partial, or max sweep gas set by gas turbine	100 / 72 / 44%
Feed Gas Pressure, psia	set by gasifier design pressure and equipment pressure drops	700
Permeate Pressure, psia	design parameter for membrane; max set by gas turbine	50 / 380
H_2 Partial-Pressure Approach, psi	indicative of membrane area	0 / 10 / 25 / 50
Pressure Diff. Across Membrane, psi	limitation of membrane material and fabrication	420 - 650
WGS Temperature Approach, ^oF	indicative of catalyst requirements	0 / 10 / 20

a. Post-WGS H_2 Recovery. This membrane location results in minimum changes to the IGCC flowsheet without CO_2 capture. The membrane unit is placed after the MDEA acid gas recovery unit or first-stage Selexol unit used to remove H_2S from the syngas. Thus, it performs the function of the second stage of the Selexol unit in an IGCC plant fitted for CO_2 capture. The CO_2-rich retentate is routed to CO_2 compression and the H_2-rich permeate is routed to the gas turbine. Figure 8 depicts this option. One alternative for this configuration is complete elimination of the AGR and associated SRU. The retentate will then contain H_2S. This so-called "dirty CO_2" is then compressed for transport and sequestration. The membrane must be sulfur tolerant and also have a high selectivity for H_2 over H_2S to achieve low SOx emissions from the gas turbine.

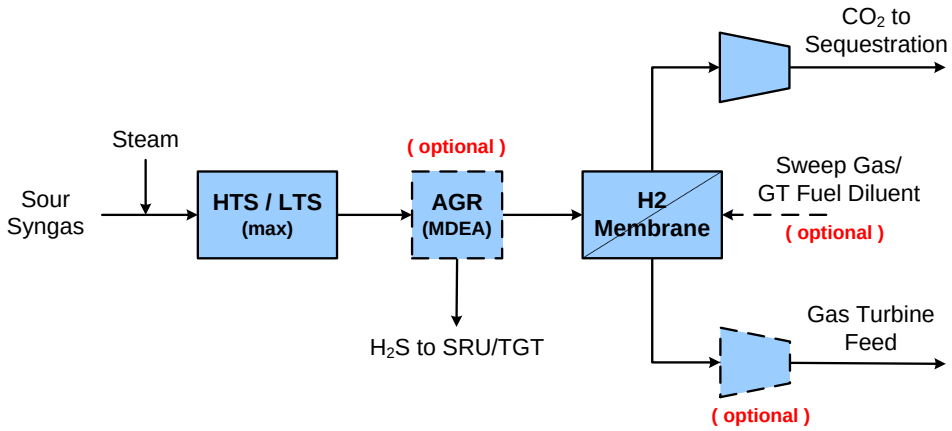

Figure 8. Post-WGS H_2 Recovery Schematic

The results of the post-WGS hydrogen recovery analysis are reported in Table 6. The baseline Case 1a assumes a membrane feed pressure of 400 psia (27 bar), which is a typical pressure used in some IGCC designs. It is desirable to recover hydrogen at the required GT feed pressure of 380 psia (26 bar). Case 1a shows that this pressure is infeasible. The total pressure differential across the membrane is too small and results in a negative H_2 partial-pressure approach for the membrane. If the permeate pressure is lowered to 50 psia (3.4 bar) as in Case 1b, recoveries up to 89.4% would be possible; however, hydrogen re-compression will be required. Case 1c maintains the desired permeate pressure of 380 psia, but uses a sweep gas to lower the H_2 partial-pressure of the permeate; achieving a modest recovery of 46.9%. Combining a low permeate pressure with the use of a sweep gas as in Case 1d can recover up to 95.7% of the feed hydrogen.

Table 6. Results of Screening for Post-WGS H_2 Recovery

Case	Description	Feed Pressure psia	Permeate Pressure psia	H_2 Press. Approach psi	Retentate (CO_2-rich) mol% H_2	Permeate (H_2-rich) mol% H_2	Hydrogen Recovery %	H_2 Recovery Sensitivity (see Nomenclature)
1a	Baseline	400	380	0	57.3%	100.0%	0.0%	-
1b	1a + Low Permeate Pressure	400	50	0	12.5%	100.0%	89.4%	-3.7 $\Delta P_P/\Delta\%_{H2\ Rec}$
1c	1a + Max Sweep	400	380	0	41.6%	43.8%	46.9%	-1.2 $\Delta\%_{H2\ P}/\Delta\%_{H2\ Rec}$
1d	1b + Max Sweep	400	50	0	5.5%	43.8%	95.7%	-8.9 $\Delta\%_{H2\ P}/\Delta\%_{H2\ Rec}$
1e	1a + High Feed Pressure	700	380	0	54.3%	100.0%	11.7%	25.7 $\Delta P_P/\Delta\%_{H2\ Rec}$
1f	1e + Low Permeate Pressure	700	50	0	7.1%	100.0%	94.3%	-4.0 $\Delta P_P/\Delta\%_{H2\ Rec}$
1g	1e + Max Sweep	700	380	0	23.8%	43.8%	76.8%	-0.9 $\Delta\%_{H2\ P}/\Delta\%_{H2\ Rec}$
1h	1f + Max Sweep	700	50	0	3.1%	43.8%	97.6%	-16.9 $\Delta\%_{H2\ P}/\Delta\%_{H2\ Rec}$
1i	1f + 1/2 Sweep	700	50	0	5.1%	71.9%	96.0%	-16.6 $\Delta\%_{H2\ P}/\Delta\%_{H2\ Rec}$
1j	1h + 10 psi Approach	700	50	10	4.6%	43.8%	96.4%	-8.7 $\Delta P_{APP}/\Delta\%_{H2\ Rec}$
1k	1h + 20 psi Approach	700	50	25	6.7%	43.8%	94.7%	-8.5 $\Delta P_{APP}/\Delta\%_{H2\ Rec}$
1l	1h + 40 psi Approach	700	50	50	10.3%	43.8%	91.5%	-8.2 $\Delta P_{APP}/\Delta\%_{H2\ Rec}$

1 atm = 1.013 bar = 14.696 psi

Case 1e employs a high feed pressure of 700 psia (48 bar), more typical of high-pressure gasification operations, and a permeate pressure of 380 psia. While this case is feasible, the recovery is only about 12%. If the permeate pressure is lowered to 50 psia as in Case 1f, the recovery is 94.3%; however, if sweep gas is employed as in Case 1g, the recovery is only 76.8%. Combining these two approaches for lowering the H_2 partial pressure in

Case 1h, results in the highest recovery at 97.6%. Case 1i shows the impact of cutting the sweep flowrate in half. This results a drop in a slight drop in H_2 recovery to 96%.

Comparing Case 1h to Cases 1j through 1l shows how the H_2 recovery is affected by the assumed partial-pressure approach across the membrane. The smaller the approach, the more membrane area required, and near the pinch point (*i.e.* an approach of zero), the amount of area increases exponentially. Changing the pinch from the limit of zero to 50 psi lowers the maximum recovery from 97.6% to 91.5%.

It can be seen from Table 6 that the lowest H_2 residual concentration in the retentate correlates with hydrogen recovery. For Scenario 1h, the CO_2-rich stream contains 3.1 vol% H_2.

The last column of Table 6 shows the relative changes to the various membrane process parameters required to improve H_2 recovery by one percent.

b. CO_2 Compressor Interstage H_2 Recovery. This process integration results in a H_2 recovery system which can include both a membrane and a PSA unit. It takes full advantage of the high pressures required for CO_2 transport and sequestration to drive the H_2/CO_2 separation. Figure 9 depicts this option. With PSA, it is very similar to the configuration previously studied by Parsons for the production of hydrogen from coal when hydrogen, and not power, is the primary product [12]. The CO_2-enriched tail gas from the PSA unit is compressed as required for sequestration. The membrane unit may be located between any of the compressor stages, after the last compressor, or in multiple locations. As was the case with post WGS hydrogen recovery, the alternative of eliminating the AGR and SRU entirely is possible.

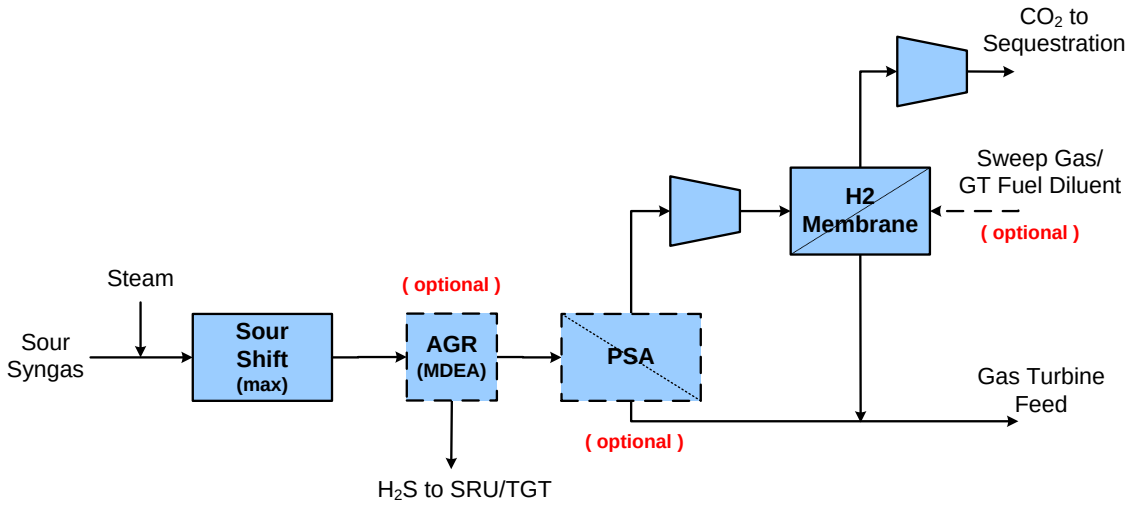

Figure 9. CO_2 Compressor Interstage H_2 Recovery Schematic

First, a series of cases were developed with interstage H_2 recovery, but without the use of PSA. These results are reported in Table 7. The baseline Scenario 2a assumes a membrane feed pressure of 800 psia, which is a typical interstage design pressure used

for CO_2 compression. Glycol dehydration of the CO_2 is performed at this pressure. For Scenario 2a, the required GT feed pressure of 380 psia was used. Scenario 2a is feasible; however, the H_2 recovery is only about 31%. Scenarios 2b and 2c raise the membrane feed pressure to 1,600 and 2,200 psia respectively. These pressures are typical of what might be required for the transport of CO_2 by pipeline for very short to long distances, respectively. The corresponding H_2 recoveries are 76.4 and 84.2%. These configurations have the serious drawback that all of the syngas is being compressed to very high pressures. Scenario 2d is a repeat of the baseline Scenario 2a, using a low permeate pressure of 50 psia. As was seen with Scenario 1d, the use of 50 psia for the permeate pressure raises the H_2 recovery into the mid nineties. Scenario 2e combines the low permeate pressure with the use of a sweep gas. The recoveries for Scenarios 2d and 2e are 94.5% and 97.7%, respectively. Note that these are very similar to the recoveries obtained in Scenarios 1d and 1e as might be expected. If the membrane separation is to be carried out on the entire syngas stream at pressures less than about 800 psia, it is preferable to produce the syngas at pressure rather than compress the entire syngas from 400 to 800 psia. Finally, Scenario 2f shows the impact of compressing all the syngas to 2,200 psia and using a permeate recovery pressure of 380 psia and a sweep gas. Again, the recovery is in the mid nineties.

Table 7. Results of Screening for CO_2 Compressor Interstage H_2 Recovery

	Membrane Only	Feed Pressure psia	Permeate Pressure psia	Pressure Pinch psi	Retentate (CO_2-rich) mol% H_2	Permeate (H_2-rich) mol% H_2	Hydrogen Recovery %
2a	Baseline	800	380	5	48.1%	100.0%	31.0%
2b	2a + 1,600 psia	1600	380	5	24.1%	100.0%	76.4%
2c	2a + 2,200 psia	2200	380	5	17.5%	100.0%	84.2%
2d	2a + Low Permeate Pressure	800	50	5	6.9%	100.0%	94.5%
2e	2d + Max Sweep	800	50	5	2.9%	37.0%	97.7%
2f	2c + Max Sweep	2200	380	5	6.6%	37.0%	94.7%

None of the Scenarios 2a - 2f are particularly attractive; however, they do suggest an opportunity to combine membrane separation with some other H_2 recovery technology. PSA is complimentary to membrane separation for this application. PSA can separate H_2 from CO_2 at the desired gas turbine inlet pressure of 380 psia, producing a tail-gas with reduced H_2 that can be compressed and run through a polymer membrane unit. Table 7 gives results for Scenarios 2g - 2r which employ a hybrid recovery system with post-WGS PSA and CO_2 compressor interstage membrane.

Scenarios 2g - 2i assume a PSA feed pressure of 400 psia and tail gas pressure of 50 psia. The tail gas pressure is the same CO_2 battery-limits pressure as obtained using the Selexol process. The PSA unit recovers about 70% of the feed H_2 with this tail gas pressure. The purity of the PSA H_2 product is greater than 99%. The tail gas, which contains the remaining 30% of the H_2 is compressed as part of preparing the CO_2 for pipeline transport. Scenario 2g assumes the membrane is placed in at an intermediate point in the compression train where the pressure is 800 psia. Scenario 2h assumes an interstage pressure of 1,600 psia, and Scenario 2i assumes the membrane is placed at the final compression delivery pressure of 2,200 psia. For all of the scenarios, the hydrogen

delivery pressure to the GT is 380 psia, and no recompression of the permeate stream is considered. For Scenario 2g, all of the H_2 recovery is accomplished by the PSA unit. The partial pressure of the remaining H_2 in the tail gas is below 380 psia. At the higher retentate pressures for Scenarios 2h and 2i, the incremental H_2 recoveries from the membrane unit are 21.4 and 47.4%, respectively. The total recoveries for the combined PSA/membrane system are respectively 76.4 and 84.2%, which are below the target H_2 recovery of greater than 95%.

Table 8. Results of Screening for Hybrid PSA/Membrane H_2 Recovery

	Hybrid - PSA / Membrane	Tail Gas Pressure psia	Retentate Pressure psia	CO_2 Product (CO_2-rich) mol% H_2	Fuel Gas (H_2-rich) mol% H_2	PSA Recovery % H_2	Membrane Recovery % H_2	Total Recovery % H_2
2g	Baseline	50	800	28.7%	100.0%	70.0%	0.0%	70.0%
2h	2g + 1,600 psia	50	1600	24.1%	100.0%	70.0%	21.4%	76.4%
2i	2g + 2,200 psia	50	2200	17.5%	100.0%	70.0%	47.4%	84.2%
2j	2g + Max Sweep	50	800	6.9%	37.0%	70.0%	81.6%	94.5%
2k	2h + Max Sweep	50	1600	3.7%	37.0%	70.0%	90.6%	97.2%
2l	2i + Max Sweep	50	2200	2.7%	37.0%	70.0%	93.1%	97.9%
2m	2j + Max Sweep + 80% PSA	17	800	4.9%	37.0%	80.0%	80.8%	96.2%
2n	2k + Max Sweep + 80% PSA	17	1600	2.6%	37.0%	80.0%	90.0%	98.0%
2o	2l + Max Sweep + 80% PSA	17	2200	1.9%	37.0%	80.0%	92.6%	98.5%
2p	2j + Max Sweep + 50% PSA	100	800	10.6%	37.0%	50.0%	82.4%	91.2%
2q	2k + Max Sweep + 50% PSA	100	1600	5.5%	37.0%	50.0%	91.3%	95.7%
2r	2l + Max Sweep + 50% PSA	100	2200	4.1%	37.0%	50.0%	93.7%	96.9%

For all Scenarios:
PSA Feed Pressure = 400 psia
PSA H_2 and Permeate Pressure = 380 psia
H_2 Partial Pressure Pinch = 5 psi

Scenarios 2j - 2l are a repeat of Scenarios 2g - 2i with the addition of the use of sweep gas to lower the permeate H_2 partial pressure further. This improves both the membrane and total H_2 recoveries dramatically. The respective membrane recoveries are 81.6, 90.6 and 93.1%, and the corresponding total H_2 recoveries are 94.5, 97.2 and 97.9%. From these results, there does not appear to be much advantage to performing the membrane separation at the highest pressure of 2,200 psia.

Scenarios 2m - 2r are a repeat of Scenarios 2j - 2l with the tail gas pressure and PSA H_2 recovery varied between the practical operating ranges of 17 to 100 psia for the pressure, and 50 to 80% for the recovery. For Scenarios 2m - 2o with a tail gas pressure of 17 psia and PSA H_2 recovery of 80%, the membrane recoveries are 80.8 - 90.6%. Since more H_2 was recovered by the PSA unit these are slightly lower than the corresponding recoveries obtained with a tail gas pressure of 50 psia. However, the corresponding total H_2 recovery is higher, ranging from 96.2 - 98.5%. For Scenarios 2p - 2r, the tail gas pressure is at the highest practical limit of about 100 psia. Correspondingly, the membrane recoveries are higher, ranging from 82.4 - 93.7%, and the total recoveries are lower, ranging from 91.2 - 96.9%. There are several trade-offs that will need to be considered when selecting the PSA operating conditions. While lower tail gas pressures and higher PSA recoveries increase the total H_2 recovery and decrease the flow rate to compression, they also result in a lower starting pressure for compression, which may result in an additional stage of compression.

Finally, it can be noted that for the highest recoveries, 98.0 and 98.5%, the residual H_2 concentration in the CO_2 is 2.6 and 1.9%, respectively.

c. WGS Interstage H_2 Recovery. This process scheme results in a system which integrates the hydrogen recovery with the water-gas shift section of the IGCC plant. The IGCC baseline plant equipped with CO_2 capture utilizes WGS reactors to convert CO and H_2O in the syngas to CO_2 and H_2 by the reaction:

$$CO + H_2O \leftrightarrow CO_2 + H_2$$

This maximizes the amount of CO_2 that can be captured. The resulting H_2 can then be combusted in the GT without the generation of additional CO_2. The yield of H_2 from the WGS reaction is equilibrium controlled and the production of H_2 is favored by low reaction temperatures. Typically, three trains of reactors are used to produce high conversion to hydrogen. The first two reactors are operated at high temperature to improve the rate of the exothermic WGS reaction, and the third reactor is operated at a lower temperature to maximize total conversion. Inter-reactor cooling is required to remove the heat of reaction. In addition, excess steam is injected with the syngas to both improve the equilibrium hydrogen yield and to prevent coking of the WGS catalyst.

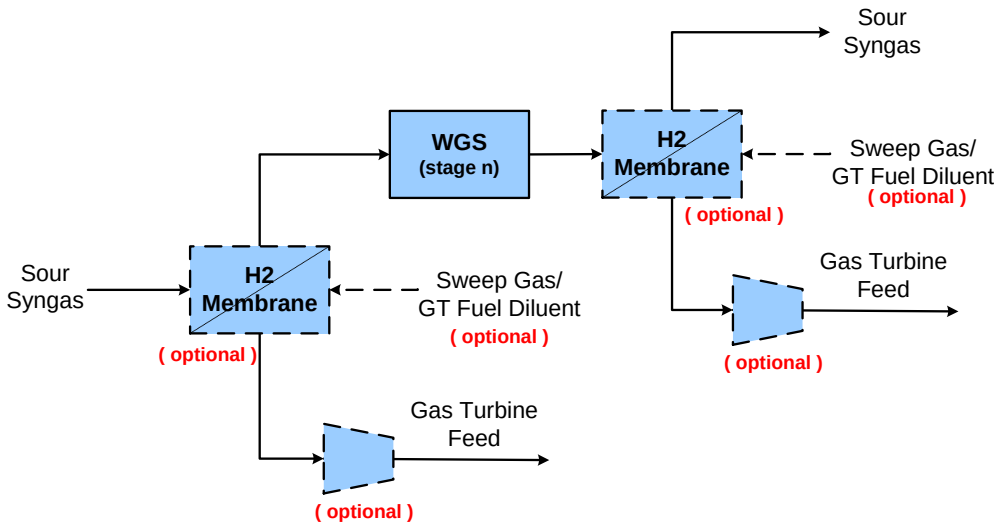

Figure 10. WGS Reactor Interstage H_2 Recovery Schematic

The results of the WGS interstage hydrogen recovery analysis are reported in Table 9

Table 9. Results of Screening for WGS Reactor Interstage H_2 Recovery Schematic

Case	Description*	Permeate Pressure psia	H_2 Press. Approach psi	Retentate (CO_2-rich) mol% H_2	Permeate (H_2-rich) mol% H_2	Hydrogen Recovery %	WGS Exit Temp °C	Total CO Conversion %
3a	Baseline (exit 3rd WGS reactor)	380	0	43.2%	100.0%	0.0%	235	97.7%
3b	3a + Low Permeate Pressure	50	0	7.1%	100.0%	89.9%	235	97.7%
3c	3a + Max Sweep	380	0	23.8%	43.8%	59.0%	235	97.7%
3d	Baseline (exit 2nd WGS reactor)	380	0	42.5%	100.0%	0.0%	295	94.6%
3e	3d + Low Permeate Pressure	50	0	7.1%	100.0%	89.6%	295	94.6%
3h	3d + Max Sweep	380	0	23.8%	43.8%	57.7%	295	94.6%
3k	Baseline (exit 1st WGS reactor)	380	0	39.4%	100.0%	0.0%	430	82.1%
3l	3k + Low Permeate Pressure	50	0	7.1%	100.0%	88.2%	430	82.1%
3o	3k + Max Sweep	380	0	23.8%	43.8%	52.0%	430	82.1%
3r	Baseline (enter 1st WGS reactor)	380	0	19.3%	100.0%	0.0%	250	0.0%
3s	3r + Low Permeate Pressure	50	0	7.1%	100.0%	67.9%	250	0.0%
3v	3r + Max Sweep	380	0	19.3%	43.8%	0.0%	250	0.0%

*Feed Pressure = 700 psia, all cases; 1 atm = 1.013 bar = 14.696 psi
Feed H_2 Conc. = 43.20%, cases a-c; 42.45%, d-g; 39.40%, h-k; 19.33%, l-o;
H_2 Approach = 0 psi; except where noted;
WGS Approach = 10 C^o (18 F^o), except where noted.

The low initial H_2-content of the syngas makes it unattractive to locate gas separation membranes upstream of the first WGS reactor. Enhancement to CO conversion resulting from integration after the first high-temperature reactor enables the low-temperature third reactor to be eliminated. However, significant hydrogen is still present in the syngas exiting the second reactor, requiring further downstream gas separation.

B. Membrane / IGCC Integration

The results from the screening analysis were used to develop more-detailed membrane system configurations and processing specifications for integrating membrane-based separations into the IGCC process. These configurations are assessed in the sections of this report that follow, using rigorous membrane modeling, detailed IGCC system design, and complete equipment sizing and costing. Six configurations, combining various features identified during screening were considered worthy of further analysis. These are described below:

Configuration Ia: This configuration is based on screening Case 1f. Membranes are integrated into the IGCC flowsheet downstream of the WGS reactors and upstream of the combustion turbine and CO_2 compression. A high gasification pressure and low permeate pressure are used to maximize the driving force for H_2 recovery.

Several options for H_2S removal prior to membrane separation are considered with this configuration: warm-gas, cold-gas and no clean-up. A sensitivity case is performed to determine the impact of having to pre-heat the membrane feed gas.

Configuration Ib: This configuration is based on screening Case 1g. As with Configuration Ia, membranes are integrated into the IGCC flowsheet downstream of the WGS reactors and upstream of the combustion turbine and CO_2 compression. The permeate pressure is considerably higher than in Ia, and matches the requirements of the gas turbine. A high gasification pressure and permeate sweep gas are used to achieve an

acceptable driving force for H_2 recovery. The sweep gas is also the diluent for the fuel-gas fed to the turbine. Note that the performance of this configuration will be superior to that estimated in the screening analysis, since the driving force will be calculated rigorously along the length of the membrane, in contrast to the screening assumption that the permeate side of the membrane is well-mixed.

As with Ia, warm-gas, cold-gas and no clean-up options for H_2S removal are considered for this configuration. Sensitivity cases are performed to determine the impact of different levels of CO_2 capture from the IGCC plant.

Configuration IIa: As the screening Cases 2d-2f indicate, Configuration Ib can be improved upon by integrating additional membranes between CO_2 compression stages, along with the use of a sweep gas. This maximizes H_2 recovery while minimizing the amount of additional compression required for any residual H_2 left in the retentate prior to compression.

As with the previous configurations, warm-gas, cold-gas and no clean-up options for H_2S removal are considered for Configuration IIa.

Configuration IIb: Based upon screening Cases 2p-2r, a hybrid Case was considered that combines PSA with membrane separation. Operation of the upstream PSA unit requires a lower pressure gas clean-up and WGS operation. However, it produces a high-purity H_2 stream that can be either used for power generation or be sold.

Configuration III: Screening Cases 3r and 3v indicate that both CO conversion and H_2 recovery suffer, if the membrane is integrated too far upstream. Therefore, a configuration based upon combining Cases 3c and 3h, and eliminating the low-temperature, third WGS reactor was developed.

V. DETAILED MODELING & ECONOMIC ANALYSIS

Based on the results from the screening analysis, a series of five process flowsheet configurations were developed for more detailed modeling and assessment. Configurations Ia, Ib, IIa, and IIb, all involve integration of the gas separation membranes after the WGS reactor section of the IGCC plant. Configuration IIb is a hybrid system employing both membranes and pressure swing adsorption (PSA). Configuration III integrates membranes within the water-gas-shift (WGS) reactor train.

Modeling of the membrane was performed using the finite-difference mathematical model described in Appendix F. This model is spreadsheet based. Since many of the membrane system configurations studied involved multiple membrane units, each unit was modeled in a separate spreadsheet. These spreadsheets were then linked together to simulate the entire membrane system, including the effects of any gas compression, heat exchange, or syngas shift. The membrane model also incorporates simplified WGS kinetics. Therefore, it can be used to model both a WGS membrane reactor and stand-alone fixed-bed WGS reactor configurations.

Multiple cases were analyzed for each configuration. These cases considered flowsheet variations, such as cold versus warm-gas clean-up for H_2S removal, CO_2/H_2S co-sequestration with no H_2S removal, and the effects of having to re-heat the membrane feed gas due to possible membrane operating limitations. Sensitivity cases were also run to examine the impact of relaxing or tightening the 90% CO_2 capture requirement. The individual cases simulated for each configuration are described in more detail below.

The material and energy balances for each case were then integrated with those for the IGCC power plant. The IGCC power plant balances were obtained from the NETL 2007 report *Cost and Performance Baseline for Fossil Energy Plants* [15]. Appendix G describes how this integration was performed. The resulting material and energy balances were used to estimate the size and cost of any new or altered equipment within the IGCC flowsheet. NETL's IGCC Economics Model was used to re-scale equipment costs, and is also described in Appendix G.

A. Configuration Ia – Membrane integration post-WGS with H_2 re-compression

This configuration is depicted in Figure 11. Four different cases are analyzed based on downstream processing of the shifted syngas:

Case Ia1: The shifted syngas is cooled, condensing residual water present in this stream, and then fed to a single-stage, cold-gas AGR unit. Unlike the IGCC plant designs that employ MDEA-based H_2S removal, this case uses a single-stage Selexol unit, which is preferred at these higher operating pressures. The clean syngas leaves the cold-gas unit at a temperature of 117°F (47°C) and a pressure of 760 psia (51.8 bar).

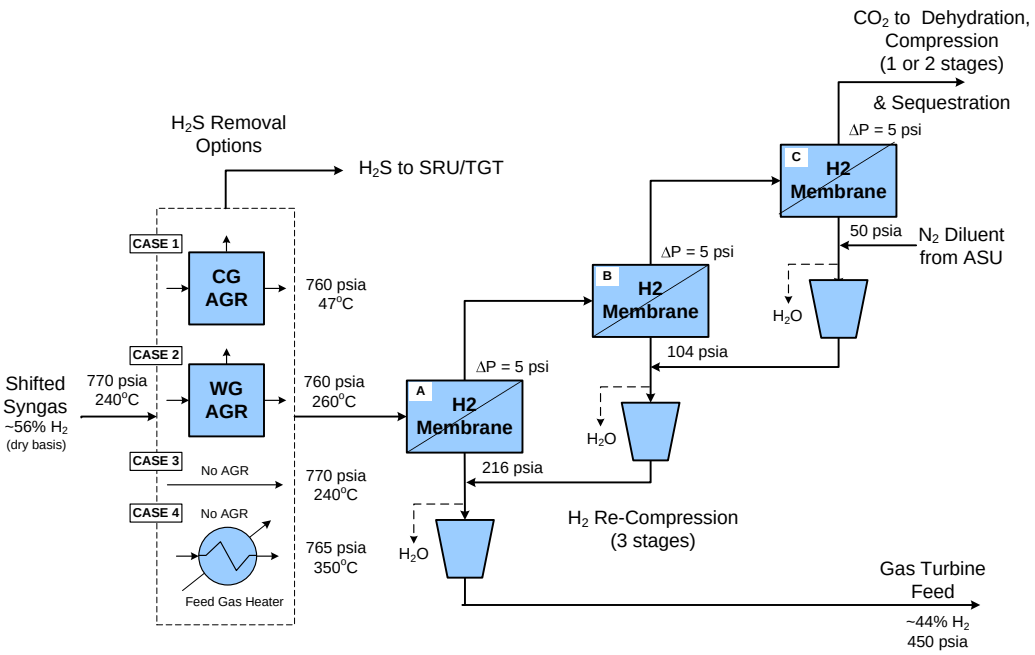

Figure 11. Configuration Ia - Membrane integration post-WGS with H_2 re-compression

Case Ia2: The shifted syngas is not cooled and no residual water is condensed. This is advantageous since it will increase the overall efficiency of the IGCC process. The shifted-syngas is fed directly to a single-stage, warm-gas AGR unit. Processes for warm-gas removal of H_2S are currently only in an early stage of development, so it has been assumed that these processes when commercialized will be able to achieve the same performance as Selexol, but at an elevated temperature. Ideally, the feed temperature to this process will match the outlet temperature of the LTS reactor. Most of the processes under development employ a solid sorbent to scavenge H_2S contained in the sour syngas. The clean syngas leaves the warm-gas unit at a slightly-elevated temperature of 500°F (260°C) due to the heat of adsorption, and a pressure of 760 psia (51.8 bar).

Case Ia3: H_2S is not removed from the syngas, but is co-sequestered with the captured CO_2. This option requires the downstream membranes to be highly impermeable to H_2S. Otherwise, H_2S that permeates the membranes will be combusted in the gas turbine resulting in unacceptable air emissions of SOx. The syngas is fed directly to the first membrane unit at a temperature of 464°F (240°C) and a pressure of 770 psia (52.5 bar).

Case Ia4: This case is similar to Ia3; accept that it is assumed the membrane cannot be operated below a temperature of 350°C. A number of membrane material considerations can result in such a limitation (see Section II). For this case, the sour syngas is pre-heated to 662°F (350°C) before being fed to the first membrane unit at a pressure of 765 psia (52.2 bar). Heating the syngas will result in some loss in IGCC plant efficiency.

For the cases involving the feeding of warm syngas to the membrane separator, it is assumed that the membrane material is highly permeable to water vapor. Otherwise, the water vapor will remain with the retentate and eventually be condensed and removed

from the CO_2 prior to sequestration. This would negate any efficiency benefits obtained from warm-gas clean-up.

The recovery of H_2 from the syngas is accomplished using three membrane units in series with the retentate from one unit being fed to the next. Three units were selected in order to minimize the parasitic power needed to compress the H_2 permeate up to the combustion turbine feed pressure of 450 psia (30.7 bar). By staging the permeate recovery pressures such that the first membrane sees the highest pressure and the last sees the lowest pressure, it is possible to minimize compression without significantly increasing membrane area requirements. The N_2 fuel-gas diluent can also be compressed along with the permeate. This dilution has the added benefit of reducing the partial pressure of water present in the permeate from the warm-gas cases, preventing condensation at the compressor discharge.

Performance of this system is comparable with conventional technology. When compared to IGCC designs employing Selexol for CO_2 capture, the post-WGS membrane design cases described above have one major advantage:

- CO_2 is available for compression at a much higher pressure, ~750 vs. 22 to 300 psia (1.5 to 20.5 bar); thus, reducing equipment and the parasitic power required for CO_2 transportation and storage

However, the post-WGS membrane design cases also have some significant disadvantages:

- Hydrogen is recovered at pressures ranging from 50 to 216 psia (3.4 to 14.7 bar) and will require re-compression to the desired fuel-gas pressure of 450 psia (bar), introducing an additional parasitic power load on the IGCC plant
- There is also a loss of power production, since the fuel-gas expander employed in the Selexol-based design has been eliminated
- H_2 recovery is likely to be lower than with Selexol
- The CO_2 stream may contain significant amounts of un-recovered H_2, as well as residual CO from WGS conversion and other impurities

B. Configuration Ib – Membrane integration post-WGS with permeate sweep

Configurations eliminate H_2 re-compression by strategic placement of multiple membrane units. A sweep gas is used to enhance the recovery of H_2 without lowering the total pressure of the H_2-rich stream leaving the membrane system. Nitrogen from the air separation unit is used as the sweep gas, and also serves as the diluent for the gas turbine fuel gas. This configuration is depicted in Figure 12. Five different cases are analyzed based on downstream processing of the shifted syngas:

Case Ib1: The shifted syngas is cooled, condensing residual water present in this stream, and then fed to a single-stage, cold-gas AGR unit. Unlike the IGCC plant designs that employ MDEA-based H_2S removal, this case uses a single-stage Selexol unit, which is preferred at these higher operating pressures. The clean syngas leaves the cold-gas unit at a temperature of 117°F (47°C) and a pressure of 760 psia (51.8 bar).

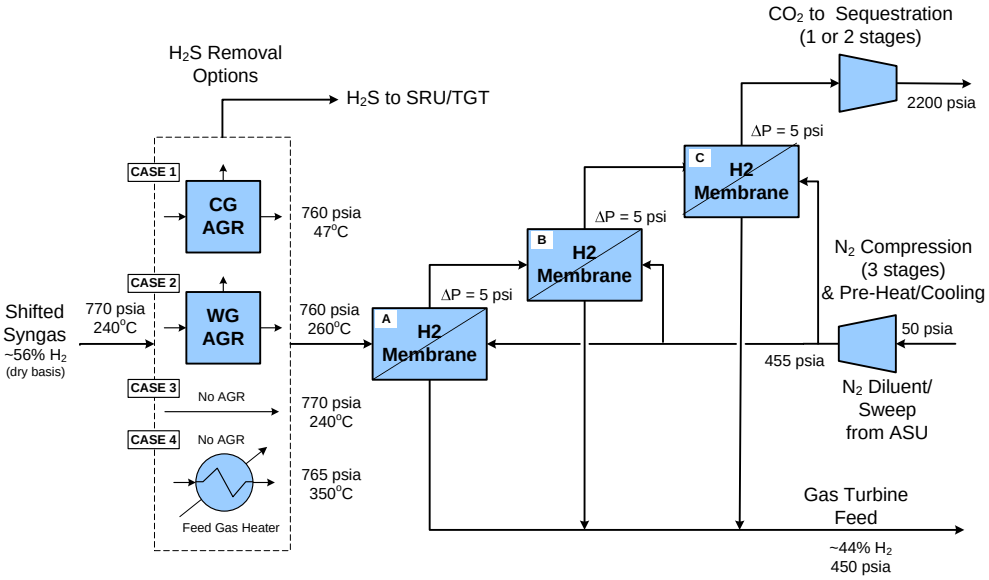

Figure 12. Configuration Ib - Membrane integration post-WGS with permeate sweep

Case Ib3: H_2S is not removed from the syngas, but is co-sequestered with the captured CO_2. This option requires the downstream membranes to be highly impermeable to H_2S. Otherwise, H_2S that permeates the membranes will be combusted in the gas turbine resulting in unacceptable air emissions of SOx. The syngas is fed directly to the first membrane unit at a temperature of 464°F (240°C) and a pressure of 770 psia (52.5 bar).

Case Ib4: This case is similar to Ib3, except that it is assumed the membrane cannot be operated below a temperature of 350°C. A number of membrane material considerations can result in such a limitation (see Section II). For this case, the sour syngas is pre-heated to 662°F (350°C) before being fed to the first membrane unit at a pressure of 765 psia (52.2 bar). Heating the syngas will result in some loss in IGCC plant efficiency.

In all of these cases, nitrogen from the ASU is employed as a sweep gas. As with Case Ia, the recovery of H_2 from the syngas is accomplished using three membrane units in series with the retentate from one unit being fed to the next. Three units were selected in order to minimize the parasitic power needed to compress the H_2 permeate up to the combustion turbine feed pressure of 450 psia (30.7 bar). By staging the permeate recovery pressures such that the first membrane sees the highest pressure and the last sees the lowest pressure, it is possible to minimize compression without significantly increasing membrane area requirements. The N_2 fuel-gas diluent can also be compressed along with the permeate. This dilution has the added benefit of reducing the partial pressure of water present in the permeate from the warm-gas cases, preventing condensation at the compressor discharge.

When compared to IGCC designs employing Selexol for CO_2 capture, the post-WGS membrane design cases with sweep gas described above have the major advantages:

- CO_2 is available for compression at a much higher pressure, ~750 vs. 22 to 300 psia (1.5 to 20.5 bar); thus, reducing equipment and the parasitic power required for CO_2 transportation and storage
- Hydrogen is recovered at the desired pressure ranging from 450 psia, versus only 50 to 216 psia (3.4 to 14.7 bar) for Case Ia1-4. No re-compression of hydrogen is required.

However, the post-WGS membrane design cases also have a significant disadvantage:

- Hydrogen recovery is lower, as is CO_2 purity. This is significantly lower than the Selexol-based design

C. Configuration IIa – Membrane integration with CO_2 compression and permeate sweep

Configuration IIa takes the concepts from Ib one step further, by distributing the membrane system units both post acid-gas removal and between CO_2 compression stages. The bulk of the H_2 recovery occurs before compression and incremental recovery is accomplished at the higher pressures available during the required CO_2 compression for transport and sequestration. This configuration is depicted in Figure 13 below.

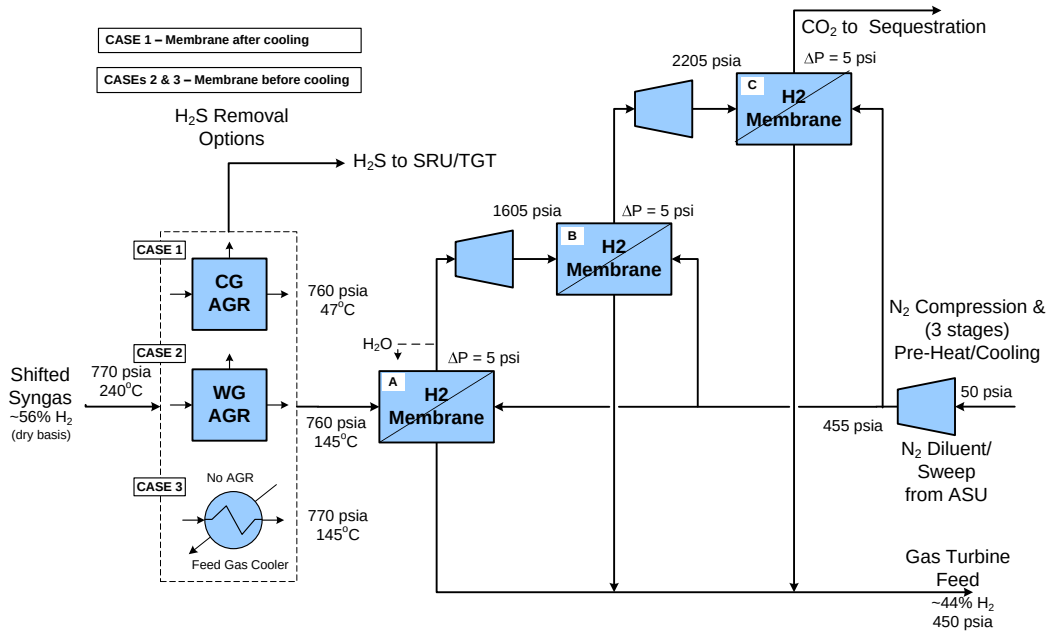

Figure 13. Configuration IIa - Membrane integration with CO_2 compression and permeate sweep

When compared to IGCC designs employing Selexol for CO_2 capture, the membrane integration with compression and sweep has the major advantages:

- CO_2 is available for compression at a much higher pressure, ~750 vs. 22 to 300 psia (1.5 to 20.5 bar); thus, reducing equipment and the parasitic power required for CO_2 transportation and storage

- Hydrogen is recovered at the desired pressure ranging from 450 psia, versus only 50 to 216 psia (3.4 to 14.7 bar) for Case Ia1-4. No re-compression of hydrogen is required.
- Higher H_2 recoveries are obtained relative to Cases Ib1-4. Additional compression of any residual hydrogen in the first membrane bank retentate is minimized.

D. Configuration IIb – PSA & membrane integration with CO_2 compression and permeate sweep

This hybrid PSA-membrane configuration is depicted in Figure 14 below.

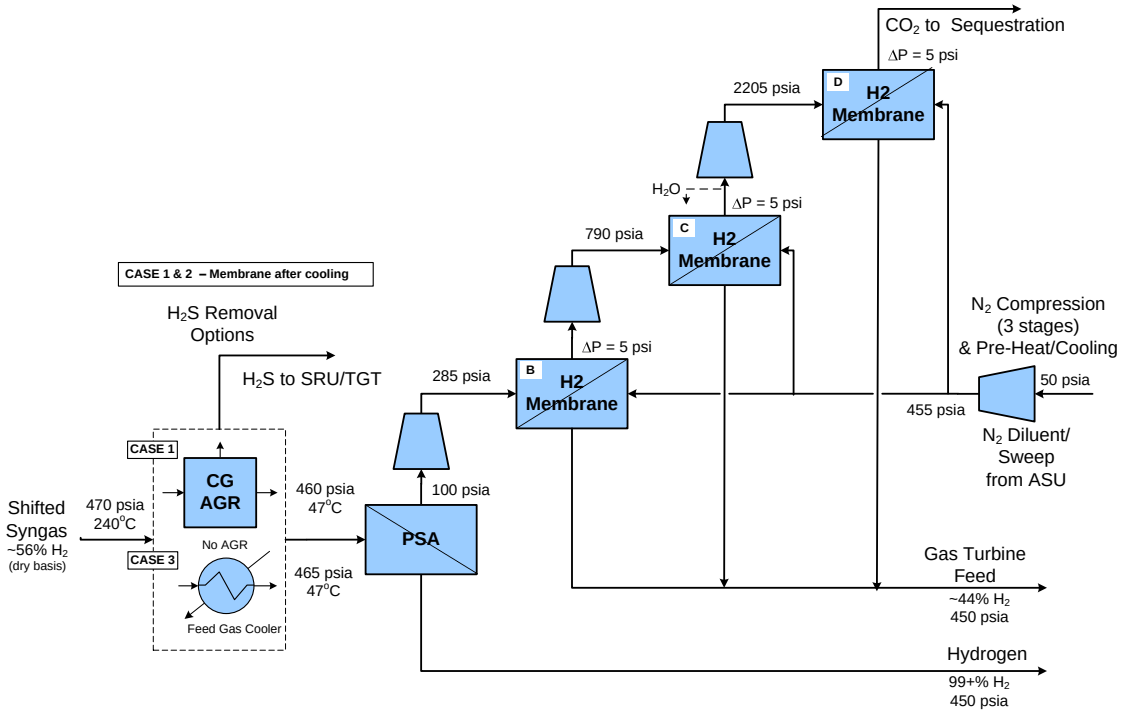

Figure 14. Configuration IIb - PSA & membrane integration with CO_2 compression and permeate sweep

When compared to the Selexol-based design, the hybrid PSA/membrane design has the following potential benefits:

- Eliminates 2nd-stage AGR (possibly 1st-stage and sulfur plant with H_2S co-sequestered)
- The chemical solvent MDEA can still be employed for sulfur removal upstream of the membrane unit, and sulfur tolerance of the membrane may be less critical.
- PSA does bulk hydrogen recovery.
- Hydrogen re-compression is eliminated.
- Hydrogen membrane operates at high pressure with large pressure differential.

- Sweep gas improves driving force and serves as GT diluent, and may also provide some compressor inter-cooling.
- Multiple membrane stages between compression steps are possible.
- Low temperature in front of PSA allows use of current Hg control technologies.
- It is possible to co-produce a high-purity hydrogen stream for sale from the PSA unit.

The hybrid PSA/membrane design also faces some challenges:

- High membrane selectivity for H_2 vs. CO_2 (and possibly H_2S).
- Additional requirements placed on ASU including N_2 purity and delivery pressure.
- There is a loss of power production, since a fuel gas expander is not used and the sweep gas must be compressed.
- Desorption of H_2S from PSA could be a potential problem.
- There is a loss of gross power production, since a fuel gas expander is not used.
- Hydrogen recovery is lower than with Selexol (possibly 98% vs. 99.5%).
- The CO_2 stream contains significant amounts of H_2 (possibly 2-3%).

The integration of the above design introduces some additional constraints. PSA requires low temperatures. Therefore warm-gas clean-up does not provide any advantages.

E. Configuration IIIa – Membrane integration with WGS

The integration of hydrogen-selective membranes with WGS provides for some unique advantages. The removal of H_2 between reactor stages shifts equilibrium for the WGS to the right in the same fashion as does steam injection, improving overall yield of hydrogen. This provides potential process advantages:

- Reduced injection steam requirements
- Higher temperature operation with improved kinetics
- Elimination of one of the reactor stages

However, the integrated WGS-membrane design also has some disadvantages:

- Hydrogen recoveries are lower and it may be necessary to recover additional hydrogen using CO_2 compressor interstage membranes.
- The membrane must be sulfur tolerant and impermeable to water. Lack of sulfur tolerance could be addressed if a hot-gas clean-up technology were available that would remove sulfur upstream of the first reactor. This would allow the CoMo catalyst currently employed in the sour gas shift to be replaced with a higher activity iron catalyst.

In addition, this integration could be improved by combining the reaction and separation in one process (*i.e.* process intensification). This could result in incremental

improvements in CO conversion and H_2 recovery and a reduction in the amount of process equipment. However, this compact device will be more complex, possibly leading to higher equipment costs and operability and reliability issues.

Note on CO_2 Purity. It is essential that the hydrogen content of the CO_2 leaving the IGCC power plant be as low as possible. The transportation of CO_2 containing high concentrations of H_2 may pose an additional risk [16]. Two percent appears to be a reasonable upper limit. This is less than the lower flammability limit of hydrogen in air, which is 4%. Even at these low concentrations, it may be necessary to catalytically combust the remaining H_2, CO and any trace hydrocarbons prior to transportation. This may also pose a difficulty for other capture technologies such as absorption.

System Performance Comparison. Key performance metrics from the analysis of Configurations Ia, Ib, and IIa are reported in Table 10. The state-of-the-art (SOTA) absorption technology can achieve almost complete H_2 recovery; however, CO_2 recovery is at relatively low pressure. The membrane-based systems at best can only achieve about 98% H_2 recovery. A recovery of 95% is probably a practical upper limit. However, Configuration Ib is only able to achieve 90% H_2 recovery at the design conditions considered in the analysis. All of the membrane configurations recover CO_2 at a much higher pressure than possible in the SOTA case. However, for Configuration Ia, H_2 recovery is achieved at much lower pressures, off-setting this advantage.

Table 10. Comparison of Different Membrane Configurations with SOTA CO_2 Capture Technology

	SOTA	Configuration Ia		Configuration Ib		Configuration IIa	
	CGCU	CGCU	WGCU	CGCU	WGCU	CGCU	WGCU
H_2 Recovery	99+%	95%	95%	90%	N/A	95%	N/A
H_2 Purity	75%	93%	61%	43%	N/A	44%	N/A
H_2 Recovery Pressure, psia	725	50-216	50-216	450	450	450	450
CO_2 Recovery	90%	90%	90%	90%	90%	90%	90%
CO_2 Purity	99+%	89%	87%	82%	N/A	88%	N/A
CO_2 Recovery Pressure, psia	50/150	745	745	745	745	745	745
Required H_2/CO_2 Selectivity	-	68	49	68	N/A	56	N/A
Relative Membrane Area	-	1.00	0.82	1.04	N/A	0.56	N/A

SOTA - State-Of-The-Art CGCU - Cold-Gas Clean-Up
WGCU - Warm-Gas Clean-Up

Configurations Ib and IIa are able to recover the H_2 at the desired pressure. Configuration IIa requires the smallest membrane area. Membrane selectivity requirements vary from 49 to 68, with lower selectivities (and smaller areas) required for systems incorporating warm-gas clean-up.

Configuration IIb is a hybrid system which combines membranes with pressure-swing adsorption (PSA). Each of these gas separation technologies has its own distinct advantages and disadvantages, and they can be used together to improve the performance of the overall gas separation system. In particular, Configuration IIb is advantageous in situations where the gasification plant co-produces high-purity H_2 for sale. The PSA unit performs the bulk of the hydrogen separation upstream of the membranes, producing

high-purity hydrogen. Results of the analysis of Configuration IIb indicate that between 50 and 80% of the total hydrogen produced at the plant could be produced at purities exceeding 99%. While hydrogen re-compression is still not required for the fuel gas, use of PSA limits the operating pressure of the upstream gasifier and results in an additional stage of CO_2 compression. Total H_2 recovery for this process configuration is similar to that achieved in Configuration IIa.

The results of this analysis were used to generate performance and cost targets for DOE-sponsored membrane R&D. These targets, which relate directly back to the CCS Program goals, are discussed in the next section of this report.

VI. GAS SEPARATION MEMBRANE R&D TARGETS

Appendix I covers the procedures used to construct cost curves for the various IGCC membrane configurations considered in this assessment. Table 11 below summarizes the targets developed from this analysis. It is a compilation of the results from all five configurations studied.

Table 11. H_2 Membrane R&D Targets for IGCC Applications

	H_2/CO_2 Selectivity	Membrane Cost $/GPU-cm^2×10^3	
	all	Ia	IIa
Has not demonstrated potential to ever be competitive	<40	-	-
May have potential, more fundamental work required	>40	>0.4	>0.8
Has definite potential, exceeds performance of SOTA IGCC w/CC	>40	<0.4	<0.8
Advanced polymers being developed for H2/CO2	~40	1.5 - 2.0	
Commercial polymers for H2/CO, H2/N2, H2/CH4	60-100	0.2 - 0.4	

Interestingly, the selectivity target is roughly 40 in all post-combustion configurations. Membrane costs are more variable, indicating that some configurations are superior to others from a cost standpoint. However it is likely that operating limitations of any materials capable of exceeding the selectivity target will dictate the membrane location and therefore the design configuration.

None of the configurations is capable of achieving the cost goal without additional improvements to other parts of the IGCC process. This is demonstrated in Figure 15 below for Configuration Ia2. However, it can be seen that it is feasible that membranes could out perform the current SOTA technology, if they can achieve the costs associated with polymer membranes.

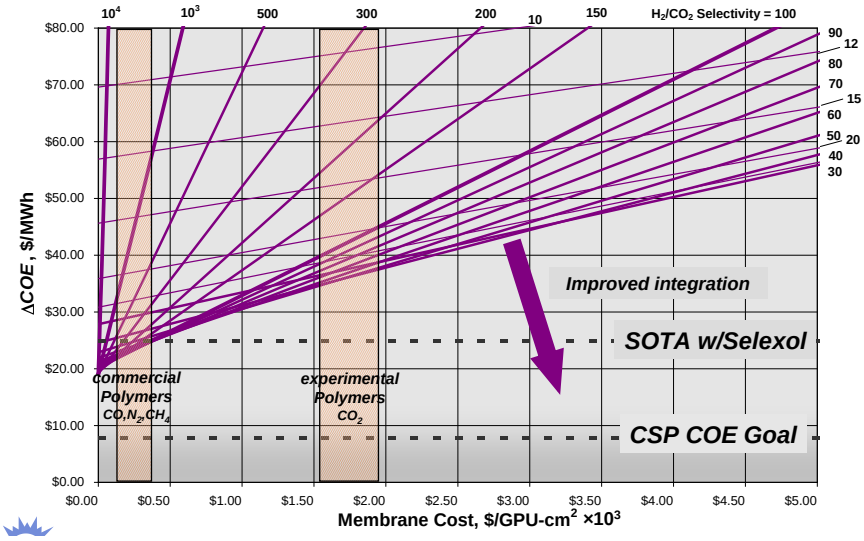

Figure 15. Cost Curves for Configuration Ia2

VII. CONCLUSIONS

This assessment has shown that modular gas separation membranes may be attractively integrated into a number of locations in an IGCC process to separate CO_2 from H_2. More than one type of membrane material will likely be needed, if membranes are to be placed in multiple locations in the process. Syngas cooling, water-gas-shift conversion, syngas clean-up, and CO_2 capture for sequestration operate over a wide range of temperatures (40-1,000^oC). The desired operating temperature for the membrane is a key factor in screening membrane materials for IGCC and hydrogen production applications. Low-temperature membrane applications should not be ruled out for CO_2 capture and may be more achievable in the short term.

High membrane selectivity is a prerequisite for successful process integration. H_2/CO_2 selectivity is directly related to the 90% CO_2 capture goal of the DOE R&D Program, and is still a major hurdle for most gas separation membranes under development. Based on this analysis, the minimum H_2/CO_2 selectivity appears to be on the order of 50. Other issues also remain to be resolved for membranes currently under development. Compared to commercial polymer membranes, cost and foot print will be issues with advanced membranes, and the cost of selective membrane materials and porous supports may be critical. An economic trade-off exists between total membrane area and membrane permeance. A low-cost, low-permeance membrane may be just as, or more attractive than, a high-cost, high-permeance membrane as long as the membrane meets selectivity requirements.

Integrating gas separation membranes into the CO_2 compression train (Configuration IIa) has many benefits, since H_2 and recycle gas re-compression are undesirable for IGCC applications. Major advantages of this integration are the elimination of the 2nd-stage of AGR (and the 1st-stage if H_2S is co-sequestered), chemical solvents can be used for absorption of H_2S, CO_2 is delivered to compression at a much higher pressure, no H_2 re-compression is required, the H_2 separation membranes operate at very high pressures with large membrane pressure differentials, and the sweep gas further improves the pressure driving force and serves as a gas turbine fuel-gas diluent. With further integration of a PSA unit with gas separation membranes, the coal gasification plant can also co-produce high-purity hydrogen for application in fuel cells. Between 50 and 80% of the hydrogen could be produced at high-purity in this hybrid gas-separation system (Configuration IIb).

Finally, membrane integration with the water-gas-shift reaction, up-stream of the acid gas removal system has a number of advantages. Most notably, removal of hydrogen from the syngas before and during the water-gas-shift improves the conversion of CO and H_2O to H_2 and CO_2.

NOMENCLATURE

ΔP_{APP} - Change in membrane partial-pressure approach in psi
ΔP_{P} - Change in membrane permeate pressure in psi
ΔP_{R} - Change in membrane retentate (feed gas) pressure in psi
ΔP_{TG} - Change in PSA unit tail-gas pressure in psi
$\Delta\%_{H2\ P}$ - Change in permeate H_2 concentration, with concentrations expressed in percentages
$\Delta\%_{H2\ Rec}$ - Change in H_2 recovery, with recoveries expressed in percentages

REFERENCES

1. Klett, M.G.; White, J.S., Schoff, R.L.; Buchanan, T.L., *Hydrogen Production Facilities Plant Performance and Cost Comparison, Final Report*, Parsons Corp./NETL Contract No. DE-AM26-99FT40465, March 2002.
2. Klett, M.G.; Rutkowski, M.D.; Schoff, R.L., *Cost and Performance of Hydrogen Separation Membranes* (DRAFT), Parsons Corp./NETL Contract No. DE-AM26-99FT40465, May 2003.
3. Rutkowski, M.D., "Hydrogen Production from Fully Advanced Coal Gasification Plants," Presentation – DOE NETL Hydrogen Program Planning Meeting, Oct. 22, 2003.
4. Gray, D.; Tomlinson, G., *Hydrogen from Coal*, Mitretek Systems, Inc./NETL Contract No. DE-AM26-99FT40465, July 2002.
5. Gray, D.; Tomlinson, G.; Salerno, S., "Coal Hydrogen & Power: Current & Future Configurations," Presentation at NETL Hydrogen Program Planning Meeting, Oct. 22, 2002.
6. Gray, D.; Tomlinson, G.; Salerno, S., Presentation at NETL Hydrogen Program Planning Meeting (untitled), Oct. 22, 2003.
7. Choi, G.N. (Nexant, Inc.), *Novel Composite Membranes for hydrogen Separation in Gasification Processes in Vision 21 Energy Plants, Final Technical Progress Report, 5/26/01-9/30/04*, ITN Energy Systems, Inc./NETL Contract No. DE-FC26-01NT40973, Dec. 2004.
8. Chiesa, P.; Kreutz, T.; Lozza, G., "CO_2 Sequestration from IGCC Power Plants by Means of Metallic Membranes," *Proceedings of GT2005 ASME Turbo Expo 2005*, Reno-Tahoe, NV, June 6-9, 2005.
9. De Lorenzo, L.; Kreutz, T.G.; Chiesa, O.; Williams, R.H., "Carbon-Free Hydrogen and Electricity from Coal: Options for Syngas Cooling in Systems Using a Hydrogen Separation Membrane Reactor," *Proceedings of GT2005 ASME Turbo Expo 2005*, Reno-Tahoe, NV, June 6-9, 2005.
10. Drawing courtesy of B.L. Bischoff, Oak Ridge National Laboratory, 2006.
11. *IGCC Economics Model.xls*, NETL, updated by J.P. Ciferno, June 5, 2007.
12. Buchanan, T.L.; Klett, M.G.; Schoff, R.L., *Capital and Operating Cost of Hydrogen Production from Coal Gasification*, Parsons Corp./NETL Contract No. DE-AM26-99FT40465, April 2003.
13. Personal communication from R.L. Schoff (Parsons Corp.) and J. Ciferno (U.S. DOE), September 2005.
14. Buchanan, T.L.; Delallo, M.; Schoff, R.L.; White, J.S., *Evaluation of Innovative Fossil Fuel Power Plants with CO_2 Removal Interim Report*, Parsons Corp. for EPRI/U.S. DOE, NETL Report No. 1000316, Dec. 2000.
15. *Cost and Performance Baseline for Fossil Energy Plants, Volume 1: Bituminous Coal and Natural Gas to Electricity Final Report* (Original Issue Date, May 2007), Report No. DOE/NETL-2007/1281, Revision 1, August 2007.
16. Ciferno, J.; Newby, R., "Recommended Pressure and Composition for CO_2 Pipeline Transport and Geological Storage for Use in Energy System Studies," *Carbon*

Sequestration System Analysis Technical Note No.2, U.S. DOE National Energy Technology Laboratory, May 2006.

PROJECT-RELATED TECHNICAL PAPERS & PRESENTATIONS

"Integration of Gas Separation Membranes with IGCC," Marano, J.J. and Ciferno, J.P, *9th International Conference on Greenhouse Gas Control Technologies*, Washington, DC, November 16-20, 2008. Published in *Energy Procedia I*, pp.361-368, Elsevier, 2009, available on-line at: *www.sciencedirect.com*.

"Gas Separation Membrane R&D Targets for CO_2 Capture from IGCC Power Plants," Ciferno, J.P. and Marano, J.J., *Seventh Annual Conference on Carbon Capture & Sequestration*, Pittsburgh, PA, May 5-8, 2008.

"Novel Integration of Gas Separation Membranes for CO_2 Capture from IGCC Power Plants," Ciferno, J.P. and Marano, J.J., *2008 AIChE Spring National Meeting*, New Orleans, LA, April 6-8, 2008.

"Membrane Selection & Placement for Optimal CO_2 Capture from IGCC Power Plants (Project Review)," Ciferno, J.P. and Marano, J.J., *ASME Carbon Sequestration Peer Review*, Pittsburgh, PA, Sept. 2007.

"Gas Separation Membrane Systems Analysis," Ciferno, J.P., Marano, J.J. and Grol, E., *NETL Project Status Review*, Pittsburgh, PA, Oct. 18, 2007.

"Membrane Selection and Placement for Optimal CO_2-Capture from IGCC Power Plants," Marano, J.J. and Ciferno, J.P., *Fifth Annual Conference on Carbon Capture & Sequestration*, Alexandria, VA, May 8-11, 2006.

APPENDIX A
Tutorial on Gas Separation Membranes

Tutorial on Gas Separation Membranes

Membrane separation takes advantage of differences in the relative transfer rates of various gases through a membrane barrier, which is influenced by both the relative diffusivity and surface adsorption of the various gases present. The exact mechanisms for transport and adsorption vary for different membrane materials, such as polymers, metals, and ceramics.

History – The earliest experimental studies of gas separation were conducted in the 1850s by Thomas Graham, who measured permeation rates for a large number of gases through a wide assortment of materials. Based on the results of his experiments, Graham developed the solution-diffusion model for permeation and Graham's law of diffusion. The solution-diffusion model is still used today to describe permeation through dense materials, such as polymers. Graham's work was first exploited in the early 1940s as part of the Manhattan project as a means of separating isotopes of uranium. Also in the 1940s and 1950s, gas permeation theory was further developed by Barrer, van Amerongen, Stern, Meares, and others leading to improvements to the solution-diffusion model. Commercial application, however, would not emerge for another twenty years[1].

The development of high flux membranes and large surface area membrane modules for reverse osmosis applications in the late 1960s and early 1970s catalyzed the development of membrane-based gas separation technology. Monsanto was first to commercialize polymer-based gas separation membranes with the introduction of the PRISM™ membrane in 1980. Since then, the application of polymer membranes for hydrogen separations has grown significantly. The success of PRISM resulted in the introduction of other gas separation membrane technologies by companies such as Cynara, Separex, Grace, Dow, Ube, and DuPont/AirLiquide.

Following the successful application of H_2 separation membranes for industrial processes, membranes were introduced for the removal of carbon dioxide from natural gas and for nitrogen separation from air. Since the 1980s, continuous improvements have been made in flux and selectivity through the introduction of advanced polymer materials and improved membrane fabrication technologies, and the cost of gas separation membrane systems have steadily declined. In addition to PRISM membranes currently produced by Air Products, other examples of commercial membranes are MEDAL™ membranes produced by Air Liquide and PolySep™ membranes produced by UOP.

Nomenclature & Units of Measure – Before beginning a discussion of membranes, it is useful to define some of the more important terminology used in describing membrane separation. In membrane-based gas separations, the feed gas is introduced into a membrane unit or module, and comes in contact with the membrane surface. The penetrant or *permeant* is the molecular species in contact with the membrane surface that passes through the membrane. The *permeate* is the stream containing penetrants that leaves the membrane module. The non-permeate or *retentate* is the stream that has been

[1] Baker, R.W., *Membrane Technology and Applications*, Second Edition, Wiley, 2004.

depleted of one or more penetrants that leaves the membrane module without passing through the membrane. Other important definitions include[2]:

Permeability - transport flux per unit trans-membrane driving force per unit membrane thickness. SI units: [kmol-m/m^2-s-kPa]

Permeance - transport flux per unit trans-membrane driving force; permeance equals permeability divided by membrane thickness. SI units: [kmol/m^2-s-kPa]

Pressure Ratio - ratio of the feed pressure to the permeate pressure

Selectivity - ratio of the permeability or permeance of one pure component to another for a given membrane material at stated conditions

Separation Factor - ratio of the compositions of two components in the permeate relative to the composition ratio of these components in the retentate

Stage Cut - the fractional amount of the total feed entering a membrane module that passes through the membrane as permeate

It should be noted that many investigators employ the above terms haphazardly; for example, selectivity as defined above is sometimes referred to as separation factor (see discussion below). Care must be taken in interpreting reported data for permeability, permeance and selectivity.

The following units of measure are frequently employed for permeability:

$$\begin{aligned} 1 \text{ Barrer} &= 10^{-10} \text{cm}^3\text{(STP)-cm / cm}^2\text{-s-cmHg} \\ &= 3.3464\times10^{-14} \text{ g mol-cm / cm}^2\text{-s-Pa} \\ &= 3.3464\times10^{-12} \text{ kg mol-m / m}^2\text{-s-kPa} \quad \text{[SI units]} \end{aligned}$$

and for permeance:

$$\begin{aligned} 1 \text{ GPU} &= 10^{-6} \text{cm}^3\text{(STP) / cm}^2\text{-s-cmHg} \\ &= 3.3464\times10^{-10} \text{ g mol / cm}^2\text{-s-Pa} \\ &= 3.3464\times10^{-6} \text{ kg mol / m}^2\text{-s-kPa} \quad \text{[SI units]} \end{aligned}$$

where standard pressure and temperature (STP) are 0^oC and 1 atmosphere, and GPU stands for Gas Permeation Unit. Barrer and GPU are compound units based on the units of measure selected for quantity transported, membrane thickness, membrane surface area and partial pressure (*i.e.* component fugacity), respectively:

1 kg mol = 1,000 g mol = 76.0 cm^3(STP) = 2.205 lb mol = 836.6 SCF(60^oF)

1 hr = 60 min = 3,600 sec

[2] IUPAC Working Party on Membrane Nomenclature.

1 m = 100 cm = 39.37 in = 3.281 ft

$1\ m^2 = 10^4\ cm^2 = 1{,}550\ in^2 = 10.764\ ft^2$

$1\ atm = 1.013\ bar = 76.0\ cmHg = 14.696\ psi = 1.013\times10^5\ Pa$

Anatomy of a Membrane Separation Factor – For most perm-selective membrane materials, the flux J_i of component *i* through the membrane will be proportional to the difference in partial pressures on either side of the membrane barrier:

$$J_i = (\mathscr{P}_i / l)\Delta p_i \qquad \text{(A1)}$$

where $\mathscr{P}_i$ is the permeability of gas component *i*, *l* is the thickness of the membrane barrier, and Δp_i is the partial pressure driving force across the membrane. Equation A1 is the basis for the definition of permeability given above. Also, the quantity $\mathscr{P}_i / l$ can be viewed as the pressure normalized flux; and is the basis for the definition of membrane permeance:

$$Pi \equiv \mathscr{P}_i / l \qquad \text{(A2)}$$

Permeability is a property of the membrane material; whereas, permeance also depends on the thickness of the membrane. Obviously, it is desirable to minimize the membrane thickness to achieve the highest permeance and flux. The minimum thickness is limited by material properties and membrane fabrication technique, and also depends on mechanical strength requirements for any gas separation application.

Separation Factor is defined as:

$$SF_{ij} \equiv (X_i/X_j)_{\text{permeate}} / (X_i/X_j)_{\text{retentate}} \qquad \text{(A3)}$$

where X_i and X_j are mole fractions of components *i* and *j* on either side of the membrane.

It can be shown for a differential membrane element that[3]:

$$\lim SF_{ij} = (P_i/P_j) \times (\Delta p_i/p_{i\ \text{permeate}}) / (\Delta p_j/p_{j\ \text{permeate}}) \qquad \text{(A4)}$$

Clearly, the separation factor is a function of material properties, membrane thickness and partial pressure driving force. It is useful because it can be directly calculated from experimental data; but is not a good indicator of a membrane's ability to separate gas pairs because it is a function of operating conditions (*i.e.* $\Delta p/p$).

[3] Derivation of equation A4 involves the substitution of A1 for the terms in the numerator, and the ideal gas law for the terms in the denominator. A4 is only applicable for a differential membrane. The true relationship between selectivity and separation factor is more complex and depends on actual geometry of the membrane contactor. For more details see: Koros, W.J.; Fleming, G.K., "Membrane-based gas separation," *Journal of Membrane Science*, 83, pp.1-80, 1993.

Equation A4 can be used as the starting point for considering a number of different definitions for the term selectivity. The ratio (P_i/P_j) in A4 can be defined as the *true selectivity* of components *i* and *j*:

$$S_{ij} \equiv P_i/P_j = \mathscr{P}_i/\mathscr{P}_j \quad \text{(A5)}$$

It is solely a property of the membrane material, and includes any effects of pressure, temperature and interactions between the molecular species present.

An *ideal selectivity* may be defined as:

$$S_{ij}^{o} \equiv \mathscr{P}_i^{o}/\mathscr{P}_j^{o} \quad \text{(A6)}$$

where the superscript 'o' indicates the permeabilities are for transport of pure gas components through membrane. Unlike the true selectivity, the ideal selectivity is not a function of gas composition. Ideal selectivity is also referred to as the *permselectivity*.

It is the true selectivity that is required for the accurate design of commercial gas separation membrane systems. $\mathscr{P}_i$ does not necessarily equal $\mathscr{P}_i^{o}$ nor does $\mathscr{P}_j$ equal $\mathscr{P}_j^{o}$; however, it is much easier to design experiments to measure pure gas permeabilities. Thus, the experimental determination of permselectivity can be a reasonable, cost-effective starting point for screening membrane materials at bench scale, but must be supplemented later on in the development process with testing under realistic operating conditions using the mixed gases of interest.

Finally, if measurements of the pure gas permeabilities, $\mathscr{P}_i^{o}$ and $\mathscr{P}_j^{o}$, are made at the same conditions of temperature, feed and permeate pressure, then based on equation A4, the ideal selectivity S_{ij}^{o} is equivalent to an ideal separation factor, SF_{ij}^{o}.

Theory of Membrane-Based Gas Separation – Conceptually, the behavior of gases permeating a membrane can be considered from the viewpoint of a thin barrier containing a single large pore, which is in contact with a gas containing molecules of two components A and B.

For pore diameters 0.1 μm or larger, flow of the gas through the pore will be by Poiseuille flow and no separation will occur.

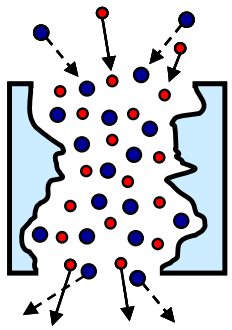

Viscous Flow

As the pore diameter is decreased; a point is reached where the radius of the pore is of the same magnitude as the mean free path of the gas molecules ($\lambda/r \approx 1$).

For λ/r less than one, a gas molecule will experience more collisions with the pore walls than with other gas molecules. Since molecule-to-molecule collisions are rare each molecule moves independently through the micropore. Therefore, for gas mixtures containing components with different average velocities, a gas separation is possible.

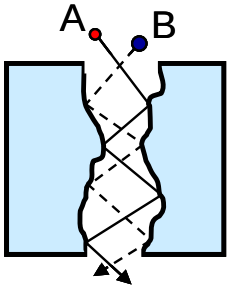

Knudsen Diffusion

This pore flow regime is known as Knudsen diffusion and for an ideal cylindrical pore; the molecular flux of each component is governed by the equation:

$$J_i = \frac{4r\varepsilon}{3}\left(\frac{2RT}{\pi M_i}\right)^{1/2} \frac{(p_{Hi} - p_{Li})}{lRT} \tag{A7}$$

where J_i is the flux of component i in units of kg-mol/m^2-s, r is the pore radius in meters, ε is the porosity of the membrane, R is the ideal gas constant in kg-m^2/s^2-kg-mol-K, T is absolute temperature in Kelvin, M_i is the molecular weight of the gas in kg/kg-mol, l is the pore length in meters, p_{Hi} is the partial pressure at the entrance of the pore in Pascals, and p_{Li} is the partial pressure at the exit of the pore in Pascals. The subscripts H and L designate the high and low partial pressure sides of the pore, respectively.

Based on Equation A7, the gas permeance is defined as:

$$P_i \equiv \frac{4r\varepsilon}{3lRT}\left(\frac{2RT}{\pi M_i}\right)^{1/2} \tag{A8}$$

Equation A8 illustrates that for Knudsen diffusion, the permeance is inversely proportional to the square root of the molecular weight of the gas and also to the square root of the absolute temperature. The former relationship is the basis for Graham's law for predicting the ideal selectivity of Knudsen diffusion membranes:

$$S_{ij} \equiv \frac{P_i}{P_j} = \sqrt{\frac{M_j}{M_i}} \tag{A9}$$

where i and j designate different molecular species present in the gas.

When the pore diameter decreases to between 5 and 10 Å, the *nanoporous* membrane begins to separate gas species via a molecular sieving mechanism.

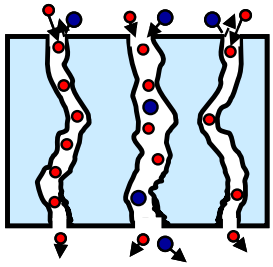

Molecular Sieving

Ideally, for molecular sieving, the flux is related to the ratio of the area of the pore available for transport to the total area of the pore. This is given by:

$$J_i \propto \frac{\left(d_p - d_{ki}\right)^2}{d_{ki}^{\,2}} \tag{A10}$$

where d_p is the diameter of the pore and d_{ki} is the kinetic diameter of the gas molecule. The ideal selectivity is then given by:

$$S_{ij} = \left(\frac{d_p - d_{k,i}}{d_p - d_{k,j}} \right)^2 \tag{A11}$$

In addition to the phenomena described above, Knudsen diffusion and molecular sieving, surface adsorption and diffusion can contribute to molecular transport through membrane pores.

Table A-1 lists molecular parameters for gases typically used in evaluating membrane performance. Also presented are ideal selectivities calculated from these parameters for both molecular sieving and Knudsen diffusion.

Table A-1. Molecular Parameters for Various Gases

Gas Molecule	Kinetic Diameter Å	Mean Free Path (20°C, 1 bar) Å	Molecular Weight	Mol. Sieve (7 Å pore dia.) $\mathcal{P}_{H2}$ / $\mathcal{P}_x$	Mol. Sieve (3.7 Å pore dia.) $\mathcal{P}_{H2}$ / $\mathcal{P}_x$	Mol. Sieve (3.32 Å pore dia.) $\mathcal{P}_{H2}$ / $\mathcal{P}_x$	Knudsen Diffusion $\mathcal{P}_{H2}$ / $\mathcal{P}_x$
He	2.55	-	4.003	0.85	0.50	0.32	1.41
H_2O	2.65	-	18.015	0.89	0.60	0.41	2.99
H_2	2.89	1,744	2.016	1.00	1.00	1.00	1.00
CO_2	3.30	615	44.010	1.23	4.10	330.00	4.67
O_2	3.47	-	31.999	1.35	12.09	∞	3.98
H_2S	3.52	-	34.080	1.40	20.92	∞	4.11
Ar	3.54	-	39.948	1.41	26.28	∞	4.45
N_2	3.64	929	28.013	1.50	182.25	∞	3.73
CO	3.76	923	28.010	1.61	∞	∞	3.73
CH_4	3.80	-	16.043	1.65	∞	∞	2.82
CF_4	4.66	-	88.005	3.09	∞	∞	6.61
C_3H_8	5.12	-	44.097	4.77	∞	∞	4.68
SF_6	5.13	-	146.054	4.82	∞	∞	8.51

Compiled from: Baker, R.W., *Membrane Technology and Applications*, Second Edition, Wiley, 2004;

Handbook of Chemistry & Physics, 56th Edition 1975-1976, CRC Press, 1975;
Skelland, A.H.P., *Diffusional Mass Transfer*, Krieger Publishing Company, 1985.

As the pore diameter is decreased, selectivities can become quite large, approaching infinity when the molecule becomes larger than the pore opening. However, the rate of transport/permeance will also decrease for the smaller gas specie as the pore opening decreases. It can also be seen that H_2 and CO_2 are nearly the same size, making them difficult to separate from each other based on molecular size alone. Most porous materials other than zeolites do not possess precise pore sizes, making their use impractical with small gas molecules. Molecular weight-based separation based on Knudsen diffusion is also an inefficient means of separating H_2 and CO_2.

Adsorption may become significant when the pore diameter drops below about 100 Å. In particular, if a gas species is condensable, the amount of gas adsorbed can be significantly greater than that occupying the free pore volume, and surface diffusion can be the dominant transport mechanism. When the diameter of the adsorbed species is of the same magnitude as the pore diameter, it is also possible for the adsorbed species to effectively block the pores, significantly decreasing or entirely preventing the transport of other gaseous species.

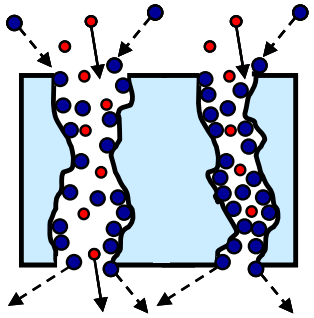

Surface Adsorption with Surface Diffusion

Transport by surface diffusion is complex, since it is also likely to occur in parallel with either Knudsen diffusion or molecular sieving. The combined phenomena cannot be easily modeled using a single equation for predicting the total molecular flux.

At pore diameters less than about 5 Å, the membrane transport mechanism may again change from molecular sieving to one dominated by molecular diffusion. This is the mechanism for transport in most polymer membranes, where the molecular species first adsorbs onto the membrane surface, dissolves in the membrane material, and then diffuses across the membrane (*i.e.* solution-diffusion).

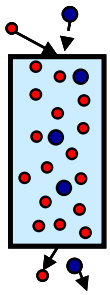

Surface Adsorption with Molecular Diffusion

For molecular diffusion the flux of each component is governed by the equation:

$$J_i = \mathcal{S}_i \mathcal{D}_i \frac{(p_{Hi} - p_{Li})}{l} \qquad \text{(A12)}$$

where $\mathcal{S}_i$ is the surface solubility of component *i*, in units of kg-mol/m^3-Pa, and $\mathcal{D}_i$ is the diffusivity of *i* in bulk membrane material, in units of m^2/s. Solubility is primarily a function of the chemical composition of the membrane and diffusion of the structure of

the membrane. Gases can have high permeation rates due to high solubility, high diffusivity, or both.

Based on equation A12, the gas permeance is defined as:

$$P_i \equiv \frac{\mathcal{S}_i \mathcal{D}_i}{l} \tag{A13}$$

The ideal selectivity for molecular diffusion in dense membranes is then given by:

$$S_{ij} = \frac{\mathcal{S}_i \mathcal{D}_i}{\mathcal{S}_j \mathcal{D}_j} \tag{A14}$$

The ratio of $\mathcal{D}_i/\mathcal{D}_j$ can be viewed as *mobility selectivity*, reflecting the different sizes of the molecules, and the ratio of $\mathcal{S}_i/\mathcal{S}_j$ can be viewed as *solubility selectivity*, reflecting the relative condensabilities of the gases. In polymers, the diffusion coefficient always decreases with increasing molecular size, because big molecules interact with more segments of the polymer chain. Thus, the mobility selectivity always favors the passage of the smaller molecule. The solubility selectivity favors larger, more condensable molecules.

In addition to molecular diffusion, transport may also occur in dense materials via either an atomic or ionic diffusion mechanism.

Atomic diffusion of hydrogen occurs in palladium and related transition metals and alloys. Molecular hydrogen adsorbs on the metal surface and disassociates into atomic hydrogen, which diffuses through the metal atom matrix. The hydrogen atoms then recombine to form molecular hydrogen and desorb from the surface. When diffusion is the controlling step, the flux is given by Sievert's law:

$$J_i = \mathcal{K}_i \mathcal{D}_i \frac{\left(p_{Hi}^{1/2} - p_{Li}^{1/2} \right)}{l} \tag{A15}$$

Note that the partial pressure driving force is no longer linear. The partial pressure term raised to the 1/2-power results from the disassociation of diatomic hydrogen. The equilibrium constant for disassociation of H_2 on the membrane surface $\mathcal{K}_i$ has units of kg-mol/m^3-Pa$^{1/2}$.

Based on Equation A15, a gas permeance can be defined as:

$$P_i \equiv \frac{\mathcal{K}_i \mathcal{D}_i}{l} \tag{A16}$$

However, permeance as defined above for atomic diffusion is not directly comparable to that for all the other transport mechanisms previously discussed, which take the form of the general flux equation given in Equation A1.

The selectivity of metallic membranes for hydrogen separations is essentially infinite due to the disassociation on the membrane surface of diatomic hydrogen, with a molecular diameter of ~2.9 Å, into atomic hydrogen, with an atomic diameter of less than 1 Å. While size loses much of its meaning on these scales as the wave nature of matter begins to noticeably manifest itself, atomic hydrogen is so small that it can easily diffuse through the dense metal phase.

Ionic diffusion can occur in high-temperature dense ceramics, such as doped rare-earth oxides. In this case, hydrogen adsorbs on the ceramic surface, disassociates, and diffuses as hydrogen ions (protons) through the membrane. The hydrogen ions then recombine to form molecular hydrogen and desorb from the surface. The flow of protons across the membrane must be balanced by an equivalent flow of negatively charged electrons in the same direction to maintain neutrality. The hydrogen flux for this transport mechanism at elevated temperature is given by the equation:

$$J_i = \frac{\sigma_{\text{amb}} RT}{4\mathcal{F}^2 l} \ln\left(\frac{p_{Hi}}{p_{Li}}\right) \tag{A17}$$

where R is the ideal gas constant in units of J/kg-mol-K, T is the absolute temperature in Kelvin, $\mathcal{F}$ is the Faraday constant in Coulomb/kg-mole, and σ_{amb} is the ambipolar conductivity of the material in units of 1/Ohm-m, defined as:

$$\sigma_{\text{amb}} = \frac{\sigma_{\text{H+}}\sigma_{\text{e-}}}{\sigma_{\text{H+}} + \sigma_{\text{e-}}} \tag{A18}$$

where σ_{amb} and σ_{amb} are the protonic and electronic conductivities.

Based on Equation A17, a gas permeance can be defined as:

$$P_i \equiv \frac{\sigma_{\text{amb}} RT}{4\text{F}^2 l} \tag{A19}$$

Again, permeance as defined above for ionic diffusion is not directly comparable to that for all the other transport mechanisms previously discussed.

Based on A18, the flux will be high when σ_{amb} is large. This requires both the protonic and electronic conductivities to be large. Conductivity can be raised by operating the membrane at high temperatures and by doping the membrane material. Ceramic materials normally do not possess high electronic conductivity. Therefore, ceramic/metallic composites, referred to as *cermets*, are being researched to enhance this conductivity.

In general, permeability, and thus permeance, is a function of temperature; however, this dependence will vary based on the exact mechanism of membrane transport. Knudsen diffusion is proportional to the square root of temperature. Molecular sieving in principle does not possess a temperature dependence; but, in real systems an effect is observed due to other interacting phenomena. All mechanisms involving surface adsorption and/or diffusion will show an exponential-type temperature dependence, which can be modeled using an Arrhenius Law expression:

$$P_i(T) = K_i e^{(-\mathcal{E}_i/RT)} \tag{A20}$$

where K_i and $\mathcal{E}_i$ are constants for any given component, and $\mathcal{E}_i$ is the activation energy. The quantity R is the ideal gas constant expressed in energy units and the temperature T is in absolute units. In general, gas adsorption decreases with increasing temperatures; whereas, diffusion increases. These interactions can result in quite complex temperature behavior in systems involving both adsorption and diffusion. Based upon Equation A19, it might appear that permeance is only proportional to temperature. However, ionic conductivity also exhibits an exponential temperature dependence, increasing with increased temperatures.

For membrane systems involving molecular diffusion, most notably polymers, an inverse relationship exists between selectivity and permeability; as the selectivity is increased, the permeability decreases, and vice versa. It has also been shown experimentally that a log-log plot of the permselectivity of a binary gas pair versus the permeability of the "faster" gas molecule, results in a clearly defined upper limit on selectivity for any given value of permeability. Such a plot is referred to a Robeson plot after the membrane researcher to first describe this phenomenon in polymer-based membranes. This relationship is depicted in Figure A-1 for H_2 and CO_2 for a wide range of polymeric membrane materials.

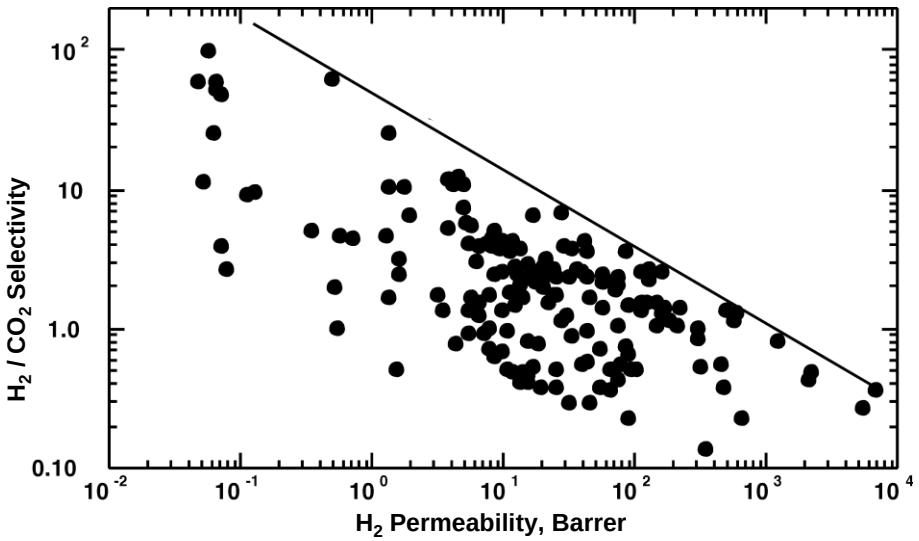

Figure A-1. Robeson Plot for H_2/CO_2 Permselectivity in Polymers

From: Robeson, L.M., "Correlation of Separation Factor Versus Permeability for Polymeric Membranes," *Journal of Membrane Science*, 62, 1991.

No completely theoretical explanation has been identified for the Robeson limit, and many researchers have investigated modified materials with the hope of pushing this limit. However, these efforts have so far only had limited success.

Figure A-2 shows the Robeson limits for H_2/CO_2, H_2/N_2, and H_2/CH_4. These plots clearly demonstrate the difficulty of separating H_2 from CO_2 using purely a solution-diffusion mechanism, relative to H_2/N_2 and H_2/CH_4 membrane-based separations which have been commercialized. As discussed above, both solubility and diffusion are molecular size dependent phenomena, and as can be seen from Table A-1, H_2 and CO_2 molecules have very similar sizes.

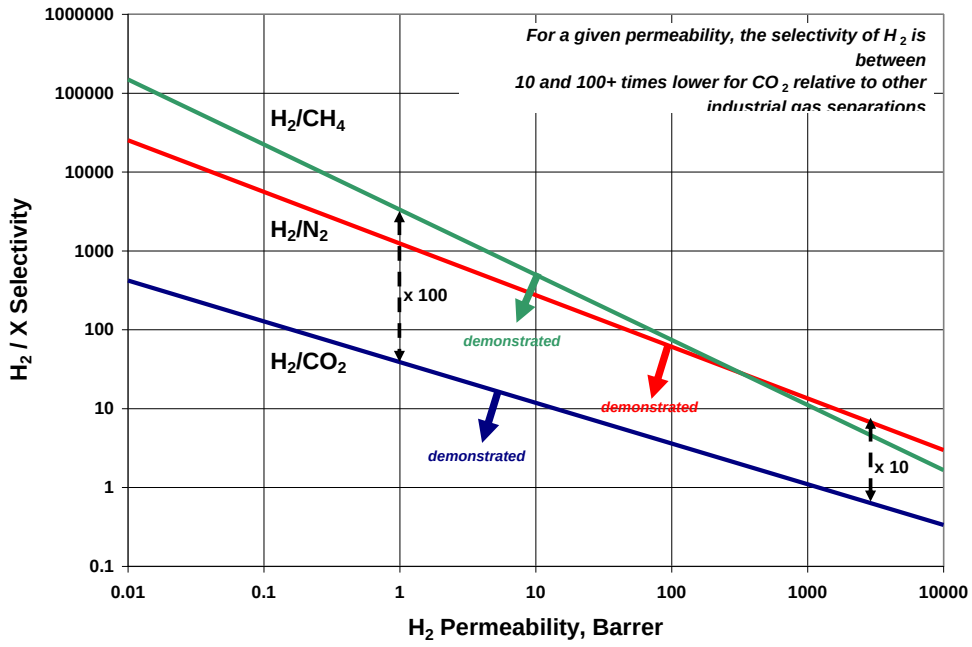

Figure A-2. Robeson Limits for H_2 Permselective Membranes

Based on parameters from: Robeson, L.M., *Polymer*, 35, p.4970, 1994.

Membrane Module Designs – Schematics of the four most common membrane module designs are shown in Figure A-3. Tubular and plate-and-frame designs are common in filtration and water treatment applications. Multiple tubes are often packed into a single cylindrical vessel. This is referred to as a shell-and-tube design. Currently, all industrial, gas separation membrane applications employ polymer membrane technology based on hollow fibers or flat sheets, and these designs will be discussed in more detail below.

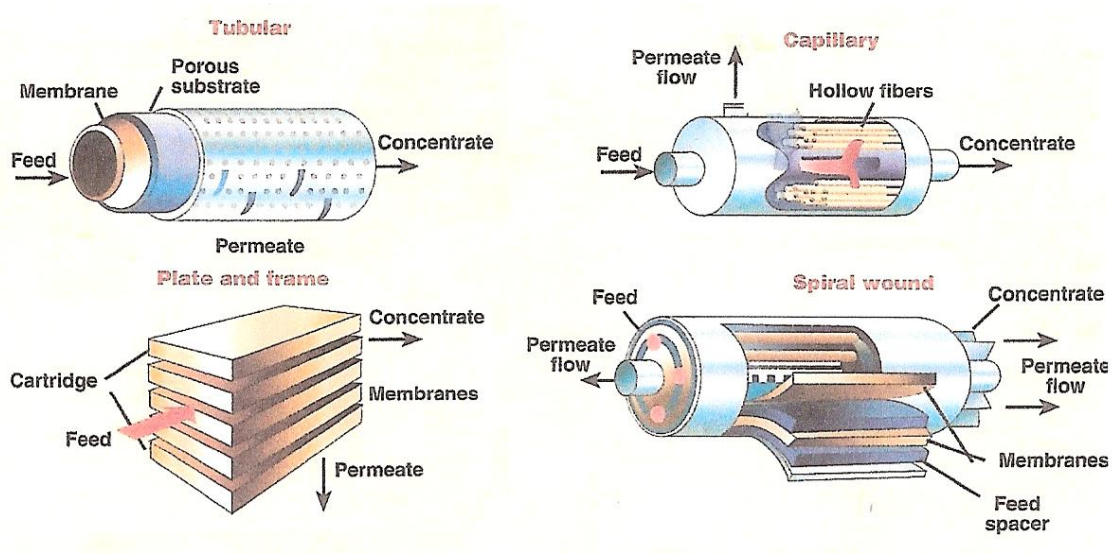

Figure A-3. Common Membrane Module Designs

From: Torzewski, K. (Ed.),"Facts at your Fingertips – Membrane Configuration," *Chem. Eng.*, Mar.1, 2009

In hollow fiber (HF) based modules, the outside layer of the fiber is composed of a dense polymer on the order of 0.05-0.10 μm thick. The separation occurs across this thin layer. The porous sub-layer provides structural support to the fiber so that it can withstand large pressure gradients. Individual fibers are about three times the diameter of a human hair (~125 μm). In a typical membrane module, thousands of fibers are bundled together in a cylindrical arrangement around a central core consisting of perforated tube known as the bore. An epoxy resin seals each end of the cylindrical fiber bundle to a tubesheet, thus separating the feed gas from the permeate. The fiber bundle and bore are enclosed in a shell similar to that used with shell-and-tube heat exchange equipment. Feed gas flows into the shell through the bundle and around the tubes. The retentate, that is the depleted feed gas, exits the membrane module through the bore. If a sweep gas is employed, it is routed through a shell head and distributed to one end of the hollow fiber bundle, exiting at the other end of the module enriched with permeate. If no sweep is used, one end of the fiber bundle may be completely sealed. Flow in this arrangement is predominantly cross flow, though co-current and counter-current arrangements are possible.

An alternative design for polymer membrane equipment uses thin sheets of polymer arranged in spiral wound (SW) modules. The feed gas enters the module and flows between the membrane leaves. Components of the feed gas permeate the membrane and spiral inward toward a central collection pipe. The depleted feed flows across the membrane surface and exits at the other end of the module. The leaves of the membrane alternate between porous membrane sheets and non-porous spacer sheets providing passage for both the retentate and permeate. This arrangement results in cross flow. A less commonly used arrangement involves the use of flat sheets in a plate-and-frame (PF) design.

HF and SW membrane-based systems are typically smaller than other types of gas separation plants, such as absorption and adsorption systems, and have high surface area-to-volume ratios (packing density). Achievable packing densities are much greater for hollow fibers (HF; ~6,000 m^2/m^3 or ~1,800 ft^2/ft^3) versus either spiral-wound sheets (SW; ~650 m^2/m^3 or ~200 ft^2/ft^3) or plate-and-frame sheet arrangements (PF; ~325 m^2/m^3 or ~100 ft^2/ft^3). All of these are greater than what is achievable in for example an absorption column (~260 m^2/m^3 or ~80 ft^2/ft^3). Since membrane units are modular, there is no limit to maximum capacity and plants consisting of over 100 individual modules, with H_2 delivery rates of greater than 50 MM scfd have been built. However, modularity has the drawback that plant costs essentially scale linearly with plant capacity and the economic advantages of membranes versus other processes can be lost at high throughputs. Almost 400 hydrogen gas-separation membrane systems are operating worldwide.

The cost of H_2 recovery systems is proprietary, but may be estimated. Typical costs for hollow fiber and spiral wound sheet membranes are $45-55 and $375 per m^2 ($4-5 and $35 per ft^2), respectively[4]. Housing can be an additional 20% of the surface area cost and final assembly an additional 1%. Installation of the system at the plant site can be assumed to be 20% of the equipment cost due to the modular nature of the equipment. Installed costs of plate-and-frame or shell-and-tube modules utilizing metallic plates or tubes to support the active membrane layer are at least an order of magnitude greater due to higher materials and fabrication costs.

In addition to permeance and selectivity, the useful life of the membrane and module is a critical parameter in evaluating the economic performance of a membrane-based gas separation process. A shortened lifetime results in higher maintenance and replacement costs. Membrane life for H_2 recovery systems with proper operation and maintenance is reported to be high, exceeding 15 years. However, operation in harsh chemical environments can shorten this lifetime to as little as 3-5 years. Reliability can also be extremely high, with on-stream factors exceeding 99%. Modularity coupled with proper valve placement allows individual modules to be taken off-line without shutting down the entire system. This feature also provides large swings in throughput. Individual module turn-down/up ratios as low as 30% and greater than 100% are possible; however, recovery will be compromised. Additional modules may be brought on-stream if additional capacity is required.

Commercial Membrane-Based Gas Separation – Currently, gas separation membranes are used industrially for hydrogen separation within ammonia plants (H_2/N_2 separation) and petrochemical plants (H_2/hydrocarbons); and for separating nitrogen from air, removing CO_2 and water from natural gas, and recovering organic vapors from air or nitrogen. The most widely used membrane materials for gas separation are polymers. Polymers are attractive because they can be processed into hollow fibers or thin sheets with high surface areas per unit volume. Each membrane unit can contain thousands of fibers. As discussed above, this results in compact, modular membrane units having relatively low costs, even when permeance and selectivity are not extremely high.

[4] From Baker, R.W., *op.cit.*, 2004; adjusted for inflation.

The three major providers of membrane technologies for gas separation applications are Air products & Chemicals, Inc. (APCI), Air Liquide and UOP. The APCI PRISM™ membrane is based on the original Monsanto technology commercialized back in 1980. Air Liquide's MEDAL™ membrane was developed by a joint venture between DuPont and Air Liquide. The UOP membrane technology is named PolySep™, and also has its roots in technology developed earlier. The relative permeance of these commercial membranes, based on the open literature, is:

	MEDAL	**PRISM**	**PolySep**
High	H_2O He H_2 NH_3 CO_2 H_2S	H_2O H_2 He H_2	H_2 H_2O H_2S CO_2
Intermediate	O_2 Ar CO N_2 CH_4	H_2S CO_2	CH_4 O_2
Low	C_2H_4 C_3H_6	O_2 Ar CO C_2+ CH_4 N_2	C_2+ N_2

Profiles of these three technologies are described in Table A-2.

Table A-2. Process Profiles for Commercial Polymer Membrane Technologies

	Air Liquide MEDAL™ (polyaramide)	**APCI PRISM™ Membrane** (Monsanto technology)	**UOP PolySep™**	**Generic (from literature)**
Feed H_2 Content (wide range)	-	>25%	-	-
(optimal)	-	40% - 80%	75% - 90%	-
Feed Temperature[a], °F	-	<230	Preheated 20°F above retentate dewpoint	
LP Steam Cons., lb/M scf Feed	2.0	-	-	-
Pretreatment[b]	No liquids in feed or retentate; coalescing filter for particulate & entrained liquid removal; must ensure no condensation			
H_2 Recovery (wide range)	80% - 98%	80% - 98+%	70% - 95+%	>85%
(typical)	95+%	90% - 95%	-	90% - 95%
(one-stage)	-	70% - 90%	-	-
(two-stage)	-	<98%	-	-
H_2 Purity (wide range)	<99.9%	80% - 99+%	70% - 99%	>70%
(typical)	-	90% - 95+%	90% - 98%	>90%
H_2 Contaminants (CO & CO_2)	-	-	-	will be at >ppmv levels
Feed Pressure, psia (wide range)[c]	-	<2500	-	-
psia (H_2 purge gas)	<1741	300 - 1850	1000+	300 - 2300
Pressure Drop, psi	Typically small, but may become significant at high recoveries or low permeate pressures			
Pressure Differential, psi	-	<1650 @ 105°F	-	-
Unit Capacity, M scfd H_2	-	-	unlimited (modular)	1,000 - 50,000+
No.of Modules	-	-	3 - 100+	-
Membrane Life, years	-	>15	-	3 - 5[d]
Reliability (On-Stream Factor)	-	-	99.8%	99.8%
Unit Turndown / up[e]	-	30%	30% - 100+%	30%
Revamp Capacity	-	-	unlimited (modular)	-
No.of Operating Units Worldwide	>60 (*circa.* 1998)	>270 (*circa.* 2004)	>50 (*circa.* 2004)	-

[a] Feed heater usually required to maintain constant operating temperature and constant membrane performance

[b] Some resistence to water exposure & particulates; H_2S or aromatics may damage mebrane

[c] Maximum feed pressure only limited by mechanical design pressure of ANSI flanges on pressure vessel

[d] Under harsh chemical environment

Commercial experience with polymer membranes is summarized below[5].

[5] MacLean, D.L.; Stookey, D.J.; Metzger, T.R., "Fundamentals of gas permeation," *Hydrocarbon Processing*, pp.47-51, Aug. 1983.

Mazur, W.H.; Chan, M.C., "Membranes for Natural Gas Sweetening and CO_2 Enrichment," *Chem. Eng. Prog*., pp.38-43, Oct. 1984.

Hogsett, J.E.; Mazur, W.H., "Estimate membrane system area," *Hydrocarbon Processing*, pp.52-54, Aug., 1983.

Whysall, M.; Picioccio, K.W., "Selection and revamp of Hydrogen Purification Processes," *1999 AIChE Spring Meeting*, Houston, TX, March 13-18, 1999. *continued, next page…*

Gases with high permeabilities such as hydrogen enrich the permeate side of the membrane, and gases with lower permeabilities enrich the retentate side of the membrane because of the depletion of components with high permeability. The first fraction of the gas to permeate the membrane consists primarily of the components with the highest permeability. As a larger fraction of the feed gas is allowed to permeate, the relative amount of the components with lower permeability increases in the permeate stream.

Polymer membranes can be used to process gases containing a wide variation in H_2 content. Feed pretreatment requirements are typically minimal, and are primarily associated with feeding a dry, clean gas to the unit. Since the water and hydrocarbon content of the feed will be increased as hydrogen is removed, it is necessary that the feed gas be heated to above the dew point of the retentate exiting the module to prevent condensation of a liquid phase within the module. Exposure to liquid water or hydrocarbons, particulates and high concentrations of H_2S may permanently damage the polymer material. Polymers in commercial use are limited to temperatures not much greater than the boiling point of water.

For any given membrane, hydrogen recovery is a strong function of the feed H_2 content and pressure, and product requirements in regards to H_2 purity and delivery pressure. Feed compression or permeate re-compression requirements can add significantly to the cost of a H_2 recovery plant. A doubling of the feed pressure can cut H_2 delivery costs by as much as a fourth. Higher purity hydrogen is associated with lower recovery, with this effect much more dramatic with membrane systems versus competing PSA technology. For a membrane with a H_2 selectivity of 30, a 3% increase in product purity results in a 25% decrease in recovery. Higher H_2 recoveries also require more membrane area. For specified feed composition and system pressure levels, the amount of area required increases exponentially at high hydrogen recovery. For a specific membrane system, the recovery versus purity is primarily dependent on the ratio of the retentate to permeate pressure and is largely independent of absolute pressure levels. However, area requirements are inversely proportional to the feed pressure. *Therefore, compressing the feed gas rather than the permeate, even though the permeate flow is smaller, is often preferable when the objective is to achieve a required pressure ratio*.

For properly designed and operated membrane systems, pressure drops are typically small. The pressure differential across the membrane is set by the upstream pressure and the desired H_2 delivery pressure, unless feed compression or permeate re-compression is included. Feed pressures as high as 2,500 psia (170 bar) have been demonstrated. More significantly, cross membrane differentials as high as 1,650 psia (112 bar) can be achieved. However, very high pressure differentials can cause compression of the membrane, detrimentally affecting performance. This effect is temperature dependent,

---

Air Products Product Brochure, Advanced Prism® Membrane Systems for Cost Effective Gas Separations, available at *www.airproducts.com*.

Picioccio, K.; Reyes, E., "Breaking the Hydrogen Barrier with PSA Revamps – Increasing Hydrogen Production of PSA Units," UOP webpage, 2000.

Haggin, J., "Membrane Technology Developments Aim at Variety of Applications," *Chem. & Eng. News*, pp.25-26, April 4, 1994.

and the maximum allowable pressure differential will be lower than 1,650 psia as the operating temperature approaches the maximum allowable operating temperature for the membrane.

Bibliography:

Li, N.N.; Fane, A.G.; Ho, W.S.W; Matsuura, T. (editors), *Advanced Membrane Technology and Application*, Wiley, 2008.

Noble, R.D.; Stern, S.A. (editors), *Membrane Separations Technology, Principles and Applications*, Elsevier Science, 1995.

Ho, W.S.W.; Sirkar, K.K. (editors), *Membrane Handbook*, Chapman & Hall, 19

APPENDIX B
Membrane Screening Methodology

Membrane Screening Methodology

Screening Assumptions – The screening analysis presented in the main body of this report only considers the performance of a single ideal membrane, with a number of other assumptions used to further simplify the analysis:

1) The ideal membrane is only permeable to hydrogen. This allows the following equation derived in Appendix C to be used to estimate H_2 recovery:

$$\text{H}_2\text{ Recovery} = 1 - \frac{\left(1 - y(\text{H}_2)_{Ri}\right)}{y(\text{H}_2)_{Ri}} \frac{\left(P_P + \Delta P(\text{H}_2)_o\right)}{\left(P_R - P_P + \Delta P(\text{H}_2)_o\right)} \quad \text{(B1)}$$

where $y(\text{H}_2)_{Ri}$ is the hydrogen mole fraction at the inlet, P_R is the pressure of the retentate, P_P is the pressure of the permeate, and $\Delta P(\text{H}_2)_o$ is the specified hydrogen partial-pressure pinch. Equation B1 was developed for membrane separators only, and is not applicable to WGS membrane reactors.

2) When considering membrane reactors, Equation B1 is replaced by the following equation derived in Appendix E and used to estimate H_2 productivity:

$$\text{H}_2\text{ Productivity} = \frac{\left(y(\text{H}_2)_{Ri} + y_{\varepsilon,Ri}\right)}{\left(y(\text{H}_2)_{Ri} + y(\text{CO})_{Ri}\right)} - \frac{\left(1 - y(\text{H}_2)_{Ri} - y_{\varepsilon,Ri}\right)}{\left(y(\text{H}_2)_{Ri} + y(\text{CO})_{Ri}\right)} \frac{\left(P_P + \Delta P(\text{H}_2)_o\right)}{\left(P_R - P_P + \Delta P(\text{H}_2)_o\right)} \quad \text{(B2)}$$

where $y(\text{CO})_{Ri}$ is the mole fraction of CO at the reactor inlet, and $y_{\varepsilon,Ri}$ is the molar extent of reaction, which is calculated based upon an assumed approach to WGS reaction equilibrium as described in Appendices D and E. H_2 productivity is defined as the molar ratio of hydrogen recovered in the permeate to the combined H_2 and CO at the reactor inlet. All other variables in Equation B2 are defined the same as given above.

3) Equations B1 and B2 assume that the permeate is pure hydrogen, and therefore, no H_2 concentration gradient exists on the permeate side of the membrane. It follows that the direction of flow of the permeate relative to the retentate is irrelevant. This is not the case when a sweep gas is introduced to reduce the H_2 partial pressure on the permeate side of the membrane. When considering the use of a sweep gas, it is assumed for simplicity that the permeate side is well mixed; that is, the partial pressure of hydrogen is constant.

4) For a hybrid system employing both a membrane and a PSA unit, the H_2 recovery of the PSA unit must be estimated. Public information reported by UOP on their PolySep™ PSA technology was used to develop a performance curve for PSA[1]. Figure B-1 shows the effect of tail gas pressure on H_2 recovery for a syngas with the composition given below in Table B-1.

[1] UOP Hydrogen Recovery Equipment at: *www.uop.com/refining/1101.html* .

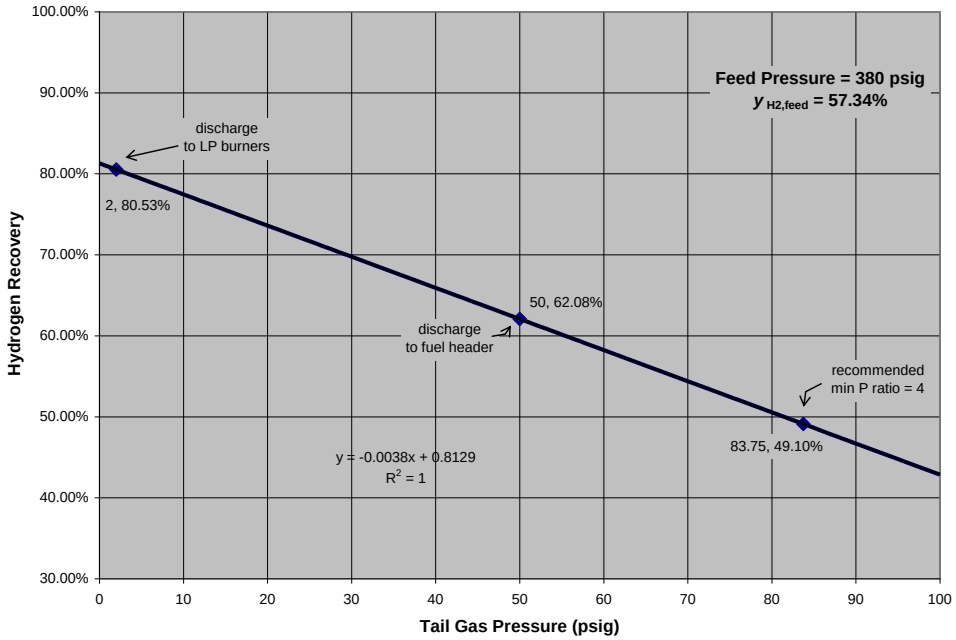

Figure B-1. Common Membrane Module Designs

The PSA performance curve in Figure B-1 can be fit to a linear equation:

$$\text{H}_2\text{ Recovery} = 0.8129 - 0.0038P_{TG} \qquad \text{(B3)}$$

where P_{TG} is the PSA tail-gas pressure, in psig. Equation B3 is only applicable for feed gas pressures near 380 psig and H_2 contents of about 57 vol%, and is valid over a range of tail-gas pressure from 2 to 84 psig.

Note that Equations B1-B3 above do not provide information on equipment size requirements for the membrane separator, WGS reactor or PSA unit. Membrane area, WGS catalyst loading, and PSA sorbent loading can only be determined by formulating and solving more complex models for these systems. What Equations B1-B3 do provide is a means of estimating the best achievable system performance, which can be used to screen alternative H_2/CO_2 separator locations and operating conditions.

Screening Parameters and Inlet Conditions – In addition to the equations given above, stream compositions and conditions, before and after syngas shifting, must be specified for possible feeds to the membrane unit. The flowsheet used for the screening analysis is from a 2000 IGCC conceptual design study performed by Parsons for EPRI and DOE[2]. Unfortunately, this study did not provide compositions for any process streams in the flowsheet. Therefore, stream compositions and specifications from a similar design study

[2] Buchanan, T.L.; Delallo, M.; Schoff, R.L.; White, J.S., *Evaluation of Innovative Fossil Fuel Power Plants with CO_2 Removal Interim Report*, Parsons Corp. for EPRI/U.S. DOE, NETL Report No. 1000316, Dec. 2000.

conducted by Parsons for DOE were used[3]. The WGS exit stream compositions were estimated using additional data provide by Parsons[4], assuming a 10 C° approach to WGS equilibrium. Overall conversion of CO to hydrogen is about 98%.

Figure B-2 is a simple schematic showing locations of possible membrane feed streams downstream of the gasifier and before acid gas removal. Table B-1 reports the corresponding compositions estimated for these streams.

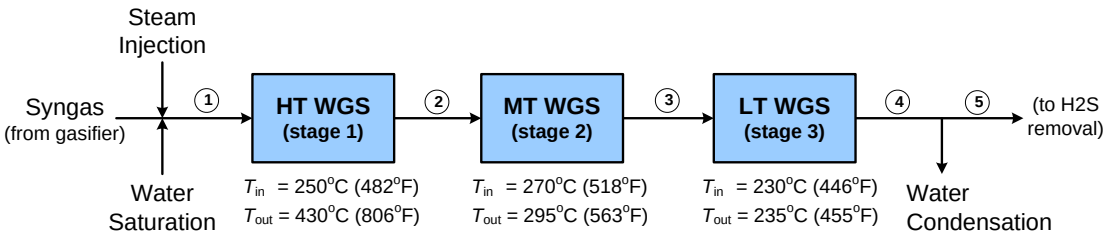

Figure B-2. Location of Streams Considered in Screening Analysis

Based on Parsons' 2000 IGCC conceptual design, the desired gas-turbine fuel-gas conditions are assumed to be 380 psia (26 bar) with a LHV of 120 Btu/scf (4.3 kJ/Nl). These conditions correspond to the estimated performance of a GE "H" turbine at the time the screening study was performed.

Table B-1. Syngas Composition Used in Screening Analysis

Composition, vol%	*Stream 1*	*Stream 2*	*Stream 3*	*Stream 4*	*Stream 5*
H_2	19.33%	39.40%	42.45%	43.20%	57.34%
CO	24.43%	4.36%	1.31%	0.56%	0.75%
CO_2	5.68%	25.75%	28.80%	29.55%	39.22%
H_2S+COS	0.48%	0.48%	0.48%	0.48%	0.64%
NH_3	0.16%	0.16%	0.16%	0.16%	0.21%
CH_4+C_2H_6	0.24%	0.24%	0.24%	0.24%	0.32%
N_2+Ar	0.81%	0.81%	0.81%	0.81%	1.08%
H_2O	48.86%	28.79%	25.75%	25.00%	0.45%
Total	100.00%	100.00%	100.00%	100.00%	100.00%
H_2O/CO Ratio	2.00	6.60	19.61	44.28	0.61
$K_{WGS}(P) = K_{WGS}(T)$	0.09	8.08	36.16	90.46	6612.36
Temperature, °C	250	430	295	235	105
WGS Approach, C°	-	10	10	10	-

[3] Buchanan, T.L.; Klett, M.G.; Schoff, R.L., *Capital and Operating Cost of Hydrogen Production from Coal Gasification*, Parsons Corp./NETL Contract No. DE-AM26-99FT40465, April 2003.
[4] Personal communication from R.L. Schoff (Parsons Corp.) and J. Ciferno (U.S. DOE), September 2005.

Three membrane placement options were considered for screening: post-WGS H_2 recovery, CO_2 compressor-interstage H_2 recovery, and H_2 recovery integrated with WGS. Parameters considered in the screening analysis are reported in Table B-2.

Table B-2. Membrane Screening Parameters

H_2 selective membrane located downstream from WGS reactors		**Range**
Feed Gas H_2 Content, vol%	based on maximum shifting of syngas	57.34%
Permeate H_2 Content, vol%	based on no sweep, partial, or max sweep gas, set by gas turbine	100 / 72 / 44%
Feed Gas Pressure, psia	set by gasifier design pressure and equipment pressure drops	400 / 700
Permeate Pressure, psia	design parameter for membrane; max set by gas turbine	50 / 380
H_2 Partial-Pressure Approach, psi	indicative of membrane area	0 / 10 / 25 / 50
Pressure Diff. Across Membrane, psi	limitation of membrane material and fabrication	20 - 650
H_2 selective membrane integrated with CO_2 compression		
Feed Gas H_2 Content, vol%	based on maximum shifting of syngas	57.34%
Permeate H_2 Content, vol%	based on no sweep, partial, or max sweep gas, set by gas turbine	100 / 72 / 44%
Feed Gas Pressure, psia	CO_2 compression requirements and compression ratios	800 / 1,600 / 2,200
Permeate Pressure, psia	design parameter for membrane; max set by gas turbine	50 / 380
H_2 Partial-Pressure Approach, psi	indicative of membrane area	0 / 10 / 25 / 50
Pressure Diff. Across Membrane, psi	limitation of membrane material and fabrication	420 - 2,150
PSA located downstream from WGS reactors with…		
Feed Gas H_2 Content, vol%	based on maximum shifting of syngas	57.34%
Feed Gas Pressure, psia	design parameter for PSA unit; max set by gas turbine	380
Tail Gas Pressure, psia	design parameter for PSA unit; affects compression requirements	17 / 50 / 100
...H_2 selective membrane integrated with CO_2 compression		
Permeate H_2 Content, vol%	based on no sweep, partial, or max sweep gas, set by gas turbine	100 / 44%
Feed Gas Pressure, psia	CO_2 compression requirements and compression ratios	800 / 1,600 / 2,200
Permeate Pressure, psia	design parameter for membrane; max set by gas turbine	380
H_2 Partial-Pressure Approach, psi	indicative of membrane area	0 / 10 / 25 / 50
Pressure Diff. Across Membrane, psi	limitation of membrane material and fabrication	420 - 1,820
H_2 selective membrane integrated with WGS reactors		
Feed Gas H_2 Content, vol%	based on partial shifting of syngas, set by WGS reactor design	19.3 / 39.4 / 43%
Permeate H_2 Content, vol%	based on no sweep, partial, or max sweep gas set by gas turbine	100 / 44%
Feed Gas Pressure, psia	set by gasifier design pressure and equipment pressure drops	700
Permeate Pressure, psia	design parameter for membrane; max set by gas turbine	50 / 380
H_2 Partial-Pressure Approach, psi	indicative of membrane area	0 / 10 / 25 / 50
Pressure Diff. Across Membrane, psi	limitation of membrane material and fabrication	420 - 650
LTS Exit Temperature, °C	design parameter for LTS WGS; set by inter-cooling	235 / 300
MTS Exit Temperature, °C	design parameter for MTS WGS; set by inter-cooling	270 / 455
HTS Exit Temperature, °C	design parameter for HTS WGS; set by inter-cooling	430 / 550
WGS Temperature Approach, C°	indicative of catalyst requirements	0 / 10 / 20

Screening Methodology **–** The following steps were utilized to estimate H_2 recoveries for the different membrane locations considered:

Step 1: Select membrane/PSA inlet pressure

Feed gas hydrogen content and pressure depend on where the membrane or PSA unit is placed in the IGCC process. Membrane performance is related to the H_2 partial pressure across the membrane, which in turn is related to hydrogen concentration and total pressure. Locations within the IGCC flowsheet with high total pressure and/or high H_2 concentrations are preferred. Optimal performance of PSA units for H_2 recovery is achieved over a pressure range between 200 and 435 psig (14 and 30 bar gauge). In

particular, PSA is well suited to deliver high-purity hydrogen at pressures consistent with gas turbine and petroleum refining applications.

Pressures upstream of the combustion turbine and CO_2 compressors are set by the gasifier design pressure and cumulative pressure drop across any intervening process equipment. For an IGCC plant without CO_2 capture, the gasifier pressure will be set such that the fuel-gas is delivered at the desired inlet pressure of the combustion turbine. The gasifier may also be designed to operate at a higher pressure; in which case, an expander is used to generate power from the fuel gas prior to combustion. If CO_2 capture is included, high-pressure operation of the gasifier may be desirable if the CO_2 can be separated from the fuel gas at elevated pressures, minimizing CO_2 compression requirements.

For a membrane placed between CO_2 compression stages, the feed pressure is based on the CO_2 pipeline inlet pressure, approximately 2,200 psia (150 bar) and the compression ratios of the individual compressor stages.

Step 2: Select membrane/PSA outlet pressure

It is preferred to produce the H_2 fuel gas at the desired combustion-turbine inlet pressure (*i.e.* 380 psia). However for membrane separation, the H_2 permeate pressure must be low enough to obtain a reasonable H_2 partial pressure driving force across the membrane. This may be as low as 5 to10 psi (0.35 to 0.7 bar), which would require re-compression of the hydrogen prior to combustion.

Since the permeate from the membrane unit will be fired in a combustion turbine to produce power and heat, the partial pressure of the permeate can be further lowered by using a sweep gas. As specified above, the desired fuel-gas conditions are to be 380 psia (26 bar) and a LHV of 120 Btu/scf (4.3 kJ/Nl). If the permeate is pure hydrogen with a LHV of 273.87 Btu/scf (9.8 kJ/Nl), it will must be diluted to meet the heating value specification. By also using the diluent as the membrane sweep gas, the minimum allowable H_2 concentration of the permeate is 120/273.87 = 43.82 vol%. Sensitivity cases were run for permeate H_2 concentrations of 36.51% and 80.33%, corresponding to LHVs of 100 and 220 Btu/scf (3.6 and 7.9 kJ/Nl), respectively.

Nitrogen or steam can be used as diluents. Nitrogen is a by-product from the ASU and would require compression to the GT feed pressure of 380 psia. This is an additional parasitic power loss for the IGCC power plant. Medium pressure steam could be used instead of, or as a supplement to nitrogen. Medium pressure steam would be diverted from the steam turbine to provide diluent. This would result in reduction in gross power output from the IGCC power plant.

Typical PSA tail-gas discharge pressures are 2 psig (0.1 bar) when discharging to low-pressure burners used in modern hydrogen plants, or 50 psig (3.4 bar) when recovering H_2 from refinery gas and discharging tail gas to a refinery fuel header. PSA manufacturers recommend a minimum feed-to-tail gas pressure ratio of about four. For the syngas of interest, this sets the minimum hydrogen recovery at 49.1% with a tail-gas pressure of 83.75 psig (5.7 bar). Producing the tail gas at higher pressures is advantageous from a sequestration standpoint, since it reduces CO_2 compression requirements. However, as Figure B-1 shows, there is a trade-off with lower PSA H_2 recovery.

Existing applications for PSA typically involve the purification of relatively high H_2 content streams. Feed H_2 content exceeds 75%, and bulk H_2 recoveries on the order of 70 to 90% are usually acceptable. In the current application, the feed H_2 content will be less than 60%. This limits bulk recoveries to less than about 80%. However, this is not a significant concern, if the PSA is to be primarily used for bulk H_2 recovery and a membrane is to be used to recover the remaining H_2 from the PSA tail gas at high pressures[5].

Step 3: Select membrane and reactor performance parameters

The maximum recovery of hydrogen occurs when the partial-pressure driving force at some point along the membrane unit approaches zero. Theoretically, this point will occur at the retentate end of the membrane, when the membrane is only permeable to hydrogen. As the *pinch point* approaches zero, the membrane area required to achieve the maximum H_2 recovery approaches infinity. Therefore, any real membrane separation must have a H_2 *partial-pressure approach*, ΔP_{H2}, greater than zero. A good indication that the practical limits of membrane performance have been reached is evident from an abrupt slowing of the increase in H_2 recovery as the partial-pressure approach is further reduced.

The WGS reaction approaches equilibrium as the reactor catalyst volume is increased, but can never quite reach equilibrium in a fixed-bed tubular reactor of finite length. Similar to the membrane partial-pressure approach, a temperature approach can be defined for the WGS reaction. The WGS-reaction *temperature approach*, ΔT_{WGS}, is defined as the difference between the theoretical equilibrium temperature, T_{EQ}, and the actual reactor outlet temperature, T_R. When the WGS pinch equals zero, the thermodynamic equilibrium constant $K_{WGS}(P)$ (defined as $P_{H2} \times P_{CO2} / P_{CO} \times P_{H2O}$) equals the equilibrium constant $K_{WGS}(T_{EQ})$ calculated from temperature. For exothermic reactions, such as the WGS, the temperature approach to equilibrium will always be greater than zero. When screening configurations involving WGS membrane reactors, an approach of 10^oC is used, consistent with the estimated base data given in Table B-1

Step 4: Estimate H_2 & CO_2 recoveries and purities

For post-WGS, CO_2 compressor-interstage, and WGS interstage membranes, H_2 recovery is calculated using Equation B-1 above, based on a specified minimum H_2 partial-pressure approach, the feed-gas H_2 content and pressure, and the permeate pressure (see Table B-2 above). If a PSA unit is employed upstream of a compressor-interstage membrane, Equation B3 is used to estimate the H_2 recovery from the PSA unit, which establishes the membrane feed-gas H_2 content. When a sweep gas is used, a pseudo permeate pressure is calculated based upon the specified H_2 content for the combined sweep gas and H_2 permeate.

For predicting the performance of a WGS membrane reactor, a H_2 productivity is calculated using Equation B-2 above, based on a specified minimum H_2 partial-pressure approach, the feed-gas H_2 content and pressure, the permeate pressure, and the WGS

[5] A similar application of PSA was proposed for recovering H_2 from Fischer-Tropsch reactor off-gas in the indirect liquefaction of coal: Bechtel/AMOCO, *Baseline Design/Economics for Advanced Fischer-Tropsch Technology, Topical Report Volume 1* (Process Design), DOE Contract No. DEAC22 91PC90027, October 1994.

reaction temperature and specified approach. A pseudo permeate pressure can also be used if the membrane reactor employs a sweep gas.

A negative H_2 recovery/productivity is an indication that the specified parameters result in a negative H_2 partial-pressure approach. Therefore, the selected operating conditions are infeasible.

APPENDIX C

Derivation of Theoretical Membrane Recovery

(no WGS Activity)

Theoretical Limit for Hydrogen Recovery from Membrane Separation

(no WGS Activity)

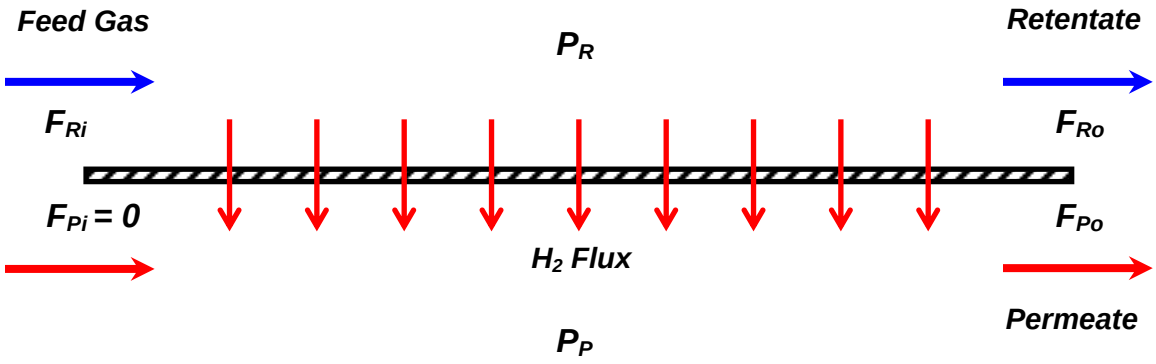

Nomenclature:

F_{Ri}	-	total molar flowrate of retentate at inlet
F_{Ro}	-	total molar flowrate of retentate at outlet
F_{Po}	-	total molar flowrate of permeate at outlet
P_R	-	pressure of retentate stream
P_P	-	pressure of permeate stream
$y_{(H_2)Ri}$	-	mole fraction H_2 in retentate at inlet (feed gas)
$y_{(H_2)Ro}$	-	mole fraction H_2 in retentate at outlet
$\Delta P_{(H_2)o}$	-	hydrogen partial pressure pinch at outlet

Assumptions:

1) No inlet flow to permeate side of membrane unit
2) Pressure drop is negligible in direction of flow for both retentate and permeate
3) Membrane is impermeable to all species other than hydrogen
4) Permeate is pure hydrogen
5) No reactions occur within membrane unit
6) Isothermal conditions maintained within membrane unit
7) Ideal gas behavior, fugacities are equal to partial pressures

The last assumption is justified at higher temperature range of membrane operation (~900°C) and reasonably accurate at lower temperatures (200-250°C)

Material Balances:

Overall: $$F_{Ri} = F_{Ro} + F_{Po} \quad \text{(C1)}$$

Hydrogen: $$y_{(H_2)Ri} F_{Ri} = y_{(H_2)Ro} F_{Ro} + F_{Po} \quad \text{(C2)}$$

Substitution of C1 into C2 and rearrangement yields:

$$\left(1 - y(\mathrm{H}_2)_{Ri}\right) F_{Ri} = \left(1 - y(\mathrm{H}_2)_{Ro}\right) F_{Ro} \tag{C3}$$

$$\frac{F_{Ro}}{F_{Ri}} = \frac{\left(1 - y(\mathrm{H}_2)_{Ri}\right)}{\left(1 - y(\mathrm{H}_2)_{Ro}\right)} \tag{C4}$$

Pinch Specification:

$$y(\mathrm{H}_2)_{Ro} P_R - P_P = \Delta P(\mathrm{H}_2)_o \tag{C5}$$

$$y(\mathrm{H}_2)_{Ro} = \frac{P_P + \Delta P(\mathrm{H}_2)_o}{P_R} \tag{C6}$$

Hydrogen Recovery:

$$\mathrm{H}_2 \text{ Recovery} \equiv \frac{F_{Po}}{y(\mathrm{H}_2)_{Ri} F_{Ri}} \tag{C7}$$

Substitution of C2 into C7:

$$\mathrm{H}_2 \text{ Recovery} = \frac{y(\mathrm{H}_2)_{Ri} F_{Ri} - y(\mathrm{H}_2)_{Ro} F_{Ro}}{y(\mathrm{H}_2)_{Ri} F_{Ri}} = 1 - \frac{y(\mathrm{H}_2)_{Ro} F_{Ro}}{y(\mathrm{H}_2)_{Ri} F_{Ri}} \tag{C8}$$

Substitution of C4 into C8 and rearrangement yields:

$$\mathrm{H}_2 \text{ Recovery} = 1 - \frac{y(\mathrm{H}_2)_{Ro}}{y(\mathrm{H}_2)_{Ri}} \frac{\left(1 - y(\mathrm{H}_2)_{Ri}\right)}{\left(1 - y(\mathrm{H}_2)_{Ro}\right)} \tag{C9}$$

$$\mathrm{H}_2 \text{ Recovery} = 1 - \frac{\left(1 - y(\mathrm{H}_2)_{Ri}\right)}{y(\mathrm{H}_2)_{Ri}} \frac{y(\mathrm{H}_2)_{Ro}}{\left(1 - y(\mathrm{H}_2)_{Ro}\right)} \tag{C10}$$

Substitution of C6 into C10:

$$\mathrm{H}_2 \text{ Recovery} = 1 - \frac{\left(1 - y(\mathrm{H}_2)_{Ri}\right)}{y(\mathrm{H}_2)_{Ri}} \frac{\left(P_P + \Delta P(\mathrm{H}_2)_o\right)}{\left(P_R - P_P + \Delta P(\mathrm{H}_2)_o\right)} \tag{C11}$$

Thus, given the hydrogen mole fraction at the inlet, the membrane operating pressures, and a specified hydrogen partial pressure pinch, the hydrogen recovery can be calculated. However, the membrane area required for this level of recovery is still unknown and can only be determined by solving the ordinary differential equation governing this system.

In the limit as the hydrogen partial pressure pinch approaches zero (*i.e.* the area approaches infinity), the hydrogen recovery approaches:

$$\text{H}_2\ \text{Recovery} = 1 - \frac{\left(-y(\text{H}_2)_{Ri}\right)}{y(\text{H}_2)_{Ri}} \frac{P_P}{\left(P_R - P_P\right)} \qquad \text{(C12)}$$

This is the maximum hydrogen recovery achievable by membrane separation without reaction.

Example Calculation #1 (no sweep):

Input Values - blue
Calc. Values - black

	psia	
Retentate Pressure	700	P_R
Permeate Pressure	50	P_P
H_2 Partial-Pressure Approach	10	$\Delta P\,(H_2)_o$

Feed Gas	mole fraction		partial press
H_2	0.5734	$y\,(H_2)_{Ri}$	401.35
CO	0.0075		5.24
CO_2	0.3922		274.52
H_2O	0.0045		3.18
Other	0.0224		15.70
Total	1.0000		700.00

Permeate	mole fraction		partial press
H_2	1.0000	$y\,(H_2)_{Po}$	50.00

H_2 Recovery	0.9302	from Eq. C11:	$\text{H}_2\ \text{Recovery} = 1 - \frac{\left(-y(\text{H}_2)_{Ri}\right)}{y(\text{H}_2)_{Ri}} \frac{\left(P_P + \Delta P(\text{H}_2)_o\right)}{\left(P_R - P_P + \Delta P(\text{H}_2)_o\right)}$
Retentate	0.4666		
Permeate	0.5334		
Total	1.0000		

Retentate	mole fraction		partial press
H_2	0.0857	$y\,(H_2)_{Ro}$	60.00
CO	0.0161		11.24
CO_2	0.8404		588.30
H_2O	0.0097		6.81
Other	0.0481		33.65
Total	1.0000		700.00

Example Calculation #2 (with sweep approximation):

Input Values - blue
Calc. Values - black

	psia		mole fraction
Retentate Pressure	700	P_R	
True Permeate Pressure	380	Sweep	0.5618
Pseudo Permeate Pressure	167	P_P	=mol.frac. Sweep×True Permeate Pres.
H_2 Partial-Pressure Approach	0	$\Delta P(H_2)_o$	

Feed Gas	mole fraction		partial press
H_2	0.5734	$y(H_2)_{Ri}$	401.35
CO	0.0075		5.24
CO_2	0.3922		274.52
H_2O	0.0045		3.18
Other	0.0224		15.70
Total	1.0000		700.00

Pseudo Permeate	mole fraction		partial press
H_2	1.0000	$y(H_2)_{Po}$	166.52

H_2 Recovery 0.7677 from Eq. C11: $H_2\ \text{Recovery} = 1 - \frac{(-y(H_2)_{Ri})}{y(H_2)_{Ri}} \frac{(P_P + \Delta P(H_2)_o)}{(P_R - (P_P + \Delta P(H_2)_o))}$

Retentate	0.5598	
Permeate	0.4402	Pseudo
Total	1.0000	

Retentate	mole fraction		partial press
H_2	0.2379	$y(H_2)_{Ro}$	166.52
CO	0.0134		9.37
CO_2	0.7006		490.39
H_2O	0.0081		5.68
Other	0.0401		28.05
Total	1.0000		700.00

Ture Permeate	mole fraction		partial press
H_2	0.4382		166.52
Sweep	0.5618		213.48
Total	1.0000		380.00

Retentate	0.5598	
Permeate	1.0046	True
Sweep	-0.5644	
Total	1.0000	

APPENDIX D

Derivation of Theoretical Membrane Productivity

(with WGS Activity)

Theoretical Limit for Hydrogen Productivity from Membrane Separation with Reaction

Nomenclature:

F	- total molar flowrate
n	- component molar flowrate
P	- pressure
ΔP	- pressure pinch
T	- temperature
ΔT	- approach temperature
y	- mole fraction
ε	- molar reaction coordinate or extent of reaction

Subscripts:

eq	- at equilibrium
i	- at inlet
o	- at outlet
P	- permeate
R	- retentate
T	- total

Assumptions:

1) No inlet flow to permeate side of membrane unit
2) Pressure drop is negligible in direction of flow for both retentate and permeate
3) Membrane is impermeable to all species other than hydrogen
4) Permeate is pure hydrogen
5) **WGS reaction approaches equilibrium within membrane unit**
6) Isothermal conditions maintained within membrane unit
7) Ideal gas behavior, fugacities are equal to partial pressures

The last assumption is justified at higher temperature range of membrane operation (~900^{o}C) and reasonably accurate at lower temperatures (200-250^{o}C)

Water-Gas-Shift Reaction:

$$CO + H_2O \leftrightarrow CO_2 + H_2$$

Stoichiometric Relationships:

$$y(\mathrm{CO})_{Ro} = \left(y(\mathrm{CO})_{Ri} - \varepsilon\right) n_{T,Ro} \qquad \text{(E1)}$$

$$y(\mathrm{H_2O})_{Ro} = \left(y(\mathrm{H_2O})_{Ri} - \varepsilon\right) n_{T,Ro} \tag{E2}$$

$$y(\mathrm{CO_2})_{Ro} = \left(y(\mathrm{CO_2})_{Ri} + \varepsilon\right) n_{T,Ro} \tag{E3}$$

$$y(\mathrm{H_2})_{Ro} = \frac{n(\mathrm{H_2})_{Ro}}{n_{T,Ro}} = \frac{P_P + \Delta P(\mathrm{H_2})_o}{P_R} \tag{E4}$$

Equations E1-E3 are the same as D1-D3; D4 has been replaced with C6, the pinch specification for H_2.

Total molar flowrate at inlet:

$$n_{T,Ri} = n(\mathrm{CO})_{Ri} + n(\mathrm{H_2O})_{Ri} + n(\mathrm{CO_2})_{Ri} + n(\mathrm{H_2})_{Ri} \tag{E5}$$

Total molar flowrate at outlet:

$$n_{T,Ro} = n(\mathrm{CO})_{Ro} + n(\mathrm{H_2O})_{Ro} + n(\mathrm{CO_2})_{Ro} + n(\mathrm{H_2})_{Ro} \tag{E6}$$

And, based on E1-E4:

$$\begin{aligned} n_{T,Ro} &= \left(y(\mathrm{CO})_{Ri} - \varepsilon\right) + \left(y(\mathrm{H_2O})_{Ri} - \varepsilon\right) + \left(y(\mathrm{CO_2})_{Ri} + \varepsilon\right) + y(\mathrm{H_2})_{Ro} n_{T,Ro} \\ &= n_{T,Ri} - \left(y(\mathrm{H_2})_{Ri} + \varepsilon\right) + y(\mathrm{H_2})_{Ro} n_{T,Ro} \end{aligned} \tag{E7}$$

Rearranging:

$$\frac{n_{T,Ro}}{n_{T,Ri}} = \frac{\left(1 - y(\mathrm{H_2})_{Ri} - y_{\varepsilon,Ri}\right)}{\left(1 - y(\mathrm{H_2})_{Ro}\right)} \tag{E8}$$

Where $y_{\varepsilon,Ri}$ is defined by:

$$y_{\varepsilon,Ri} \equiv \varepsilon / n_{T,Ri} \tag{E9}$$

Reaction Equilibrium:

As before, the concentration dependence of the equilibrium constant:

$$K_{eq} = \frac{y(\mathrm{CO_2})\, y(\mathrm{H_2})}{y(\mathrm{CO})\, y(\mathrm{H_2O})} \tag{E10}$$

Substitution of E1-D3 into E10 and rearrangement yields:

$$K_{eq} = \frac{\left(y(\mathrm{CO_2})_{Ri} + \varepsilon\right)\left(y(\mathrm{H_2})_{Ro} n_{T,Ro}\right)}{\left(y(\mathrm{CO})_{Ri} - \varepsilon\right)\left(y(\mathrm{H_2O})_{Ri} - \varepsilon\right)} \tag{E11}$$

Upon dividing both the numerator and denominator by $n_{T,Ri}^2$ and substituting E8:

$$K_{eq} = \frac{y(\mathrm{H_2})_{Ro}}{(-y(\mathrm{H_2})_{Ro})} \frac{(y(\mathrm{CO_2})_{Ri} + y_{\varepsilon,Ri})(-y(\mathrm{H_2})_{Ri} - y_{\varepsilon,Ri})}{(y(\mathrm{CO})_{Ri} - y_{\varepsilon,Ri})(y(\mathrm{H_2O})_{Ri} - y_{\varepsilon,Ri})} \tag{E12}$$

Rearranging:

$$(+K'_{eq})y_{\varepsilon,Ri}^{\ 2} + (y(\mathrm{CO_2})_{Ri} + (y(\mathrm{H_2})_{Ri} - 1) - K'_{eq}(y(\mathrm{CO})_{Ri} + y(\mathrm{H_2O})_{Ri}))y_{\varepsilon,Ri} + (y(\mathrm{CO_2})_{Ri}(y(\mathrm{H_2})_{Ri} - 1) + K'_{eq}\, y(\mathrm{CO})_{Ri}\, y(\mathrm{H_2O})_{Ri}) = 0 \tag{E13}$$

Where K'_{eq} is defined by:

$$K'_{eq} \equiv K_{eq}\frac{(-y(\mathrm{H_2})_{Ro})}{y(\mathrm{H_2})_{Ro}} = K_{eq}\frac{(P_R - (P_P + \Delta P(\mathrm{H_2})_{Ro}))}{(P_P + \Delta P(\mathrm{H_2})_{Ro})} \tag{E14}$$

The expression given previously D13, can be used for calculating K_{eq} based on the equilibrium temperature T_{eq} calculated from D15. Then, K'_{eq} can be calculated from E14 and the operating pressures P_R and P_P and approach $\Delta P(\mathrm{H_2})_o$. Finally, K'_{eq} and the inlet concentrations can be used in D13 to solve for $y_{\varepsilon,Ri}$. As before, only one of the two roots of the quadratic equation is realistic.

Material Balances:

Overall: $$F_{Ri} = F_{Ro} + F_{Po} \tag{E15}$$

Hydrogen: $$(y(\mathrm{H_2})_{Ri} + y_{\varepsilon,Ri})F_{Ri} = y(\mathrm{H_2})_{Ro}F_{Ro} + F_{Po} \tag{E16}$$

Note that the flowrates F are equivalent to the n_T used above.
Substitution of E15 into E16 and rearrangement yields:

$$(-y(\mathrm{H_2})_{Ri} - y_{\varepsilon,Ri})F_{Ri} = (-y(\mathrm{H_2})_{Ro})F_{Ro} \tag{E17}$$

$$\frac{F_{Ro}}{F_{Ri}} = \frac{(-y(\mathrm{H_2})_{Ri} - y_{\varepsilon,Ri})}{(-y(\mathrm{H_2})_{Ro})} \tag{E18}$$

Which is equivalent to E8.

Pinch Specification:

This relationship is unchanged from Appendix C:

$$y(\mathrm{H_2})_{Ro} = \frac{P_P + \Delta P(\mathrm{H_2})_o}{P_R} \tag{E19}$$

Hydrogen Productivity:

$$\mathrm{H_2\ Productivity} \equiv \frac{F_{Po}}{\left(y(\mathrm{H_2})_{Ri} + y(\mathrm{CO})_{Ri}\right) F_{Ri}} \tag{E20}$$

Substitution of E16 into E20:

$$\begin{aligned}\mathrm{H_2\ Productivity} &= \frac{\left(y(\mathrm{H_2})_{Ri} + y_{\varepsilon,Ri}\right) F_{Ri} - y(\mathrm{H_2})_{Ro} F_{Ro}}{\left(y(\mathrm{H_2})_{Ri} + y(\mathrm{CO})_{Ri}\right) F_{Ri}} \\ &= \frac{\left(y(\mathrm{H_2})_{Ri} + y_{\varepsilon,Ri}\right)}{\left(y(\mathrm{H_2})_{Ri} + y(\mathrm{CO})_{Ri}\right)} - \frac{y(\mathrm{H_2})_{Ro} F_{Ro}}{\left(y(\mathrm{H_2})_{Ri} + y(\mathrm{CO})_{Ri}\right) F_{Ri}}\end{aligned} \tag{E21}$$

Substitution of E18 into E21 and rearrangement yields:

$$\mathrm{H_2\ Productivity} = \frac{\left(y(\mathrm{H_2})_{Ri} + y_{\varepsilon,Ri}\right)}{\left(y(\mathrm{H_2})_{Ri} + y(\mathrm{CO})_{Ri}\right)} - \frac{\left(-y(\mathrm{H_2})_{Ri} - y_{\varepsilon,Ri}\right) y(\mathrm{H_2})_{Ro}}{\left(y(\mathrm{H_2})_{Ri} + y(\mathrm{CO})_{Ri}\right)\left(-y(\mathrm{H_2})_{Ro}\right)} \tag{E22}$$

Substitution of E19 into E22:

$$\mathrm{H_2\ Productivity} = \frac{\left(y(\mathrm{H_2})_{Ri} + y_{\varepsilon,Ri}\right)}{\left(y(\mathrm{H_2})_{Ri} + y(\mathrm{CO})_{Ri}\right)} - \frac{\left(-y(\mathrm{H_2})_{Ri} - y_{\varepsilon,Ri}\right)\left(P_P + \Delta P(\mathrm{H_2})_o\right)}{\left(y(\mathrm{H_2})_{Ri} + y(\mathrm{CO})_{Ri}\right)\left(P_R - P_P + \Delta P(\mathrm{H_2})_o\right)} \tag{E23}$$

Thus, given the mole fractions of hydrogen, water, carbon dioxide, and carbon monoxide at the inlet of the membrane reactor, the fractional extent of reaction (from the solution of E13 using $K'_{eq}(T+\Delta T)$), the membrane operating pressures, and a specified hydrogen partial pressure pinch, the hydrogen productivity can be calculated. However, the membrane area required for this productivity is still unknown and can only be determined by solving the ordinary differential equations governing this system.

In the limit as the hydrogen partial pressure pinch and the temperature approach to equilibrium approach zero (*i.e.* the membrane area approaches infinity), the hydrogen productivity approaches:

$$\mathrm{H_2\ Productivity} = \frac{\left(y(\mathrm{H_2})_{Ri} + y_{\varepsilon,Ri}\right)}{\left(y(\mathrm{H_2})_{Ri} + y(\mathrm{CO})_{Ri}\right)} - \frac{\left(-y(\mathrm{H_2})_{Ri} - y_{\varepsilon,Ri}\right)}{\left(y(\mathrm{H_2})_{Ri} + y(\mathrm{CO})_{Ri}\right)} \frac{P_P}{\left(P_R - P_P\right)} \tag{E24}$$

where $y_{\varepsilon,Ri}$ is determined from E13 using $K'_{eq}(T)$. This is the maximum hydrogen productivity achievable in a membrane reactor.

Example Calculation:

Input Values - blue
Calc. Values - black

	psia	
Retentate Pressure	700	P_R
Permeate Pressure	50	P_P
H_2 Partial-Pressure Approach	10	$\Delta P\,(H_2)_o$

Feed Gas	mole fraction	
H_2	0.1933	$y\,(H_2)_{Ri}$
CO	0.2443	$y\,(CO)_{Ri}$
CO_2	0.0568	$y\,(CO_2)_{Ri}$
H_2O	0.4886	$y\,(H_2O)_{Ri}$
Other	0.0169	
Total	1.0000	

	°C	K	
WGS Outlet Temperature	430	703	T
WGS Temperature Approach	10	10	ΔT
WGS Equilibrium Temperature	440	713	T_{eq}

K_{eq} = 8.08 from Eq. D13: $K_{eq}(T_{eq}) = \exp\left(4577.8/T_{eq} - 4.33\right)$

K'_{eq} = 86.16 from Eq. E14: $K'_{eq} = K_{eq}\dfrac{\left(P_R - \left(P_P + \Delta P(H_2)_{Ro}\right)\right)}{\left(P_P + \Delta P(H_2)_{Ro}\right)}$

Eq. E13:

$$\left(1 + K'_{eq}\right)y_{\varepsilon,Ri}^{\ 2} + \left(y(CO_2)_{Ri} + y(H_2)_{Ri} - 1\right) - K'_{eq}\left(y(CO)_{Ri} + y(H_2O)_{Ri}\right)y_{\varepsilon,Ri} + \left(y(CO_2)_{Ri}\,y(H_2)_{Ri} - 1\right) + K'_{eq}\,y(CO)_{Ri}\,y(H_2O)_{Ri} = 0$$

Quadratic Coefficients

a	*b*	*c*
8.7164E+01	-6.3906E+01	1.0241E+01

root 1	0.4965
root 2	0.2366
$y_{\varepsilon,Ri}$	0.2366

Eq. D14:

$$-\min\left(y(CO_2)_{Ri}, y(H_2)_{Ri}\right) < y_{\varepsilon,Ri} < \min\left(y(CO)_{Ri}, y(H_2O)_{Ri}\right)$$

-0.4886 < $y_{\varepsilon,Ri}$ < 0.0169

Permeate	mole fraction	
H_2	1.0000	$y\,(H_2)_{Po}$
H_2 Productivity	0.8603	
Retentate	0.6235	
Permeate	0.3765	
Total	1.0000	

from Eq. E23: $H_2\ \text{Productivity} = \dfrac{\left(y(H_2)_{Ri} + y_{\varepsilon,Ri}\right)}{\left(y(H_2)_{Ri} + y(CO)_{Ri}\right)} - \dfrac{\left(-y(H_2)_{Ri} - y_{\varepsilon,Ri}\right)\left(P_P + \Delta P(H_2)_o\right)}{\left(y(H_2)_{Ri} + y(CO)_{Ri}\right)\left(P_R - \left(P_P + \Delta P(H_2)_o\right)\right)}$

Retentate	mole fraction	
H_2	0.0857	$y\,(H_2)_{Ro}$
CO	0.0124	$y\,(CO)_{Ro}$
CO_2	0.4706	$y\,(CO_2)_{Ro}$
H_2O	0.4042	$y\,(H_2O)_{Ro}$
Other	0.0271	
Total	1.0000	

APPENDIX E

Finite-Difference Based Membrane Separator/Reactor Model

Finite-Difference Based Membrane Separator/Reactor Model

A spreadsheet-based model was developed to describe a hydrogen separation membrane. This model has been used to set the design basis for the membrane unit in the system modeling for this project.

The overall objective of the membrane assessment is to quantify which membrane properties and design variables are most critical for the successful commercialization of this technology when integrated with coal-fed gasification systems for either the co-production of hydrogen or power. This information will provide guidance to the Department of Energy as they strive to improve the performance and lower the cost of dense-ceramic hydrogen-separation membranes.

a. ***Membrane Model*** The governing differential equations for hydrogen permeation through a polymer membrane is:

$$\frac{dn''_{H_2}}{dA} = -\mathcal{P}_{H_2}\frac{\left(P'_{H_2} - P''_{H_2}\right)}{l} = -\mathcal{P}_{H_2}\left(P'_{H_2} - P''_{H_2}\right) \tag{4-1}$$

$$-\frac{dn'_{H_2}}{dA} = \pm\frac{dn''_{H_2}}{dA} \tag{4-2}$$

where:

n’	-	molar flowrate of feed gas or retentate
n”	-	molar flowrate of permeate
A	-	membrane area
l	-	membrane thickness
$\mathcal{P}$	-	membrane permeability
$\mathcal{P}$	-	membrane permeance
P’	-	partial pressure of retentate
P”	-	partial pressure of permeate

Similar material balances can be written for all other gases that may permeate across the membrane, CO_2, H_2O, CO, H_2S, etc. In Equation (4-2), the negative sign is used for co-current flow of retentate and permeate, and the positive sign for counter-current flow. To solve Equations (4-1) and (4-2) for the H_2 composition of the permeate and retentate, the differential equations must be integrated along the length of the membrane unit. Unfortunately, an analytic solution to this problem is only possible under certain restrictive assumptions (*e.g.*, linear partial pressure driving force and constant properties), and the solution is algebraically quite complex. For the general case involving multi-component permeation, it is simpler to numerically integrate equations in the form of (1) and (2). This can be performed using standard spreadsheet software such as Excel™. A backward finite difference formulation is used to represent the governing differential equations (4-1) and (4-2) in the spreadsheet model. The solution is represented as a table, with the rows representing different points along the length of the membrane. The values

calculated in any given row of the table for concentration and flowrate are dependent on values in the preceding row. Therefore, iteration is not required to achieve convergence at each point in the grid for co-current flow. For counter-current flow the exit flowrate and composition of the permeate must be assumed, the grid computed, and the assumed conditions updated and iterated to find a solution. The model is particularly convenient in spreadsheet format, since it allows the grid to be expanded by clicking on a row and dragging it downward; thus, copying all cell formulae and updating all cell references.

***Purpose*:**

A schematic of an ion transport membrane is shown in Figure 1.

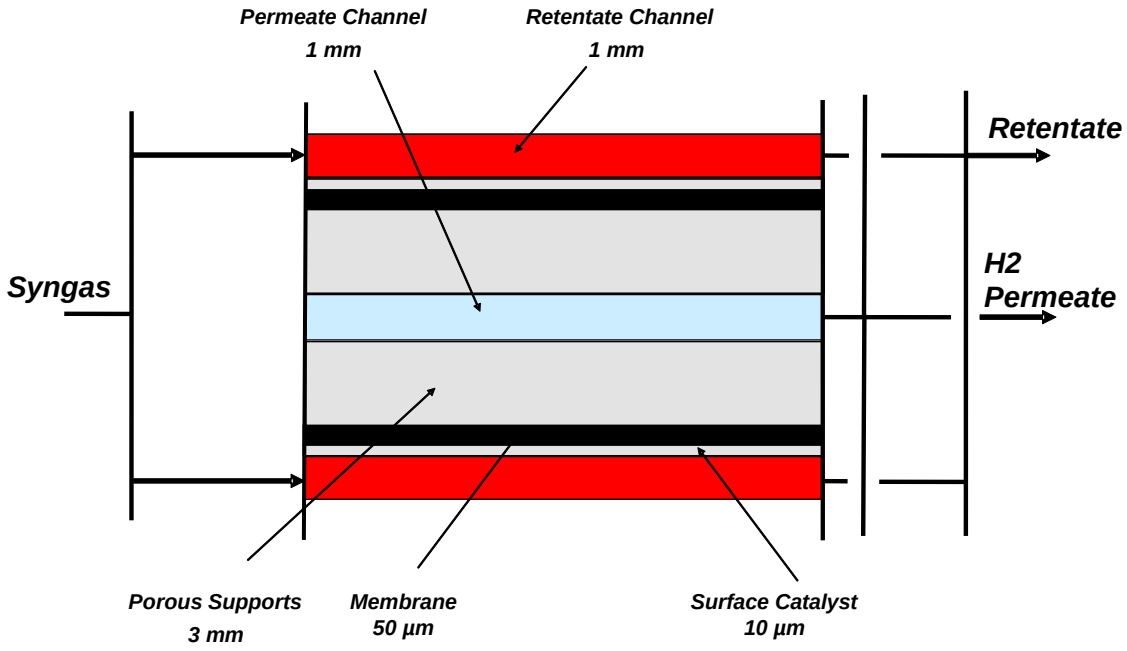

Figure 1. Ion Transport Membrane Unit Schematic

***Model Description*:** The Excel™ workbook *H2M.xls* contains two permanent worksheets. These are *H2-ITM* and *CONSTANTS*. The latter contains predefined constants as Excel Named Cells, which can be accessed throughout the workbook (*e.g.* the molecular weight of H_2, *MW_H2*, one million, *MM*, and the conversion factor for psi to atm units, *psi_to_atm*). The former worksheet, *H2-ITM*, contains the actual membrane unit mathematical model. Neither of these sheets should be deleted, since this would make the model inoperable. In addition, it is recommend that once a feasible solution to a given membrane simulation is complete, it be saved separately, either as a new workbook or as a copy of the *H2-ITM* sheet. Most of the information provided in *H2-ITM* is presented in several different sets of dimensional units.

Worksheet *H2-ITM* is broken into several functionally different sections. Working from the top to the bottom of the active area of the worksheet, Block *A5:M35* summarizes the

inlet and outlet temperatures, pressures, flowrates, and stream compositions, and the membrane performance parameters: CO conversion, hydrogen recovery, flux, and H_2 partial pressure approach. The model assumes a planar membrane geometry consisting of a stack of alternating membrane, membrane supports and flow channels. Block *A37:L59* contains geometry-related parameters for the membrane unit: overall plate dimensions, membrane layer and channel thicknesses, segment size to be used for numerical integration, feed superficial velocity, and computed size characteristics of the complete membrane stack.

Block *A61:H70* contains simplified hydraulic calculations for flow through a single retentate flow channel. Based on a specified feed superficial velocity, the actual flow velocity, pressure drop, and residence time through the unit are estimated. These calculations are used to verify that the conditions specified result in laminar flow with a reasonable pressure drop. Block *A72:J97* contains calculations for estimating the economic performance of the membrane unit. The membrane unit capital investment and annual capital charge are estimated and compared to the relative values of the feed and product streams. The unit profitability is contained in cell *I97*. Excel Solver™ can be used to adjust the superficial velocity to maximize membrane unit profitability by adjusting the number of plates per unit. Other unit profitability maximizations are also possible.

Block *A93:I110* contains membrane specific properties, such as conductivity, activation energy, and technology improvement factor. The technology improvement factor allows the user to easily adjust membrane performance. For example, Excel GoalSeek™ can be used to adjust this parameter to match either experimental results or R&D performance targets. A flag can also be set here to turn the water-gas-shift (WGS) reaction on or off. This flag has been provided because of uncertainty in the kinetic parameters for the WGS reaction at the operating conditions of the ITN membrane. It is also possible that the ITN membrane, currently or with future modifications, may possess catalytic activity. The flag allows sensitivity cases involving the WGS reaction to be modeled.

Finally, the worksheet rows *116* through *1163* contain the actual numerical grid used to integrate and solve the membrane model. The hydrogen partial pressures and flux, and the flowrates and concentrations of all molecular species contained in the retentate are reported for each point along the membrane. The grid has been made larger than the actual dimensions of the membrane, so that the user can change the dimensions of the membrane or the step size of the grid without adding to or modifying the cells and rows in the grid. This region of the worksheet is named *PROFILES*, and built-in Excel Lookup functions are used to extract information from this region that is used in the calculation of some of the model output discussed above. Information reported in the grid cells outside of the physical dimensions of the membrane are ignored in calculating performance parameters. Additional columns of information are calculated when the water-gas-shift reaction is considered. This includes the net rate of production or consumption of H_2 by the water-gas-shift reaction.

Formulas used in the *H2-ITM* worksheet, refer to several Visual Basic for Applications™ coded functions provided with the workbook. These are *RateWGS, KeqWGS,* and *TeqWGS,* which are used to calculate the net rate of reaction, and the equilibrium constant and temperature, respectively, for the water-gas-shift reaction.

***Input Data*:** These data fall into several categories,

- Stream Properties
    1) Feed Pressure (psia)
    2) Feed Temperature (^oC)
    3) Feed Flowrate (lb mol/hr)
    4) Feed Composition for H_2, CO, CO_2, H_2O, other gases (mole %)
    5) Permeate Pressure (psia)
    6) Steam Addition ratio to the feed flow (mol/mol)
- Membrane Assembly Dimensions
    1) Plate Width (cm)
    2) Plate Length (cm, assumed equal to plate length)
    3) Length of segment used for numerical calculations (cm)
    4) Thicknesses (μm) of individual components making up membrane: Feed Channel, Surface Catalyst, Ion Transport Membrane, Porous Support, and Permeate Channel

    The assembly can be easily programmed for other stack arrangements.
- Hydrodynamics
    1) Feed Superficial Velocity per channel (cm/sec)
    2) Viscosity of feed stream (cP)
- Economic Parameters
    1) Equipment manufacturing cost per unit of membrane area ($/sq.ft.)
    2) Cost of installation as percentage of inside-battery limit (ISBL) installed cost
    3) Outside-Battery Limit (OSBL) cost as percentage of total ISBL cost
    4) Other One-Time Costs (OTC) as percentage of total installed costs (ISBL + OSBL)
    5) Annual capital recovery factor as percentage of total investment (ISBL + OSBL + OTC)
    6) Other fixed costs as percentage of total investment
    7) Feed and product values (shadow prices): feed value ($/MM Btu), assumed same as fuel value of waste gas, feed temperature penalty ($/M lb) steam value ($/M lb), permeate value ($/MM Btu), and permeate pressure penalty ($/MM Btu)
- Membrane Properties
    1) Membrane Conductivity (Ohm^{-1}-cm^{-1}) at 900^oC
    2) Energy of Activation (electron-Volts)

3) Technology Improvement Factor
4) Flag for turning on/off Water-Gas-Shift (WGS) reaction

***Output*:** The output is generally reported in several sets of dimensional units. The following information is predicted by the model,

- Permeate and Retentate Molar Flowrates and Compositions
- CO Conversion and H_2 Recovery
- Average Flux across membrane and H_2 Partial Pressure Pinch at outlet
- Membrane Unit Mechanical Design
    1) Number of Flow Channels
    2) Total Stack Height
    3) Total Stack Area
    4) Total Stack Volume
    5) Stack Area-to-Volume Ratio
- Hydraulics
    1) Average velocity at flowing conditions
    2) Reynolds Number
    3) Pressure Drop
    4) Average Residence Time
- Unit Economics
    1) Membrane Unit Cost
    2) Cost of Installation
    3) OSBL Costs
    4) Other One-Time Costs
    5) Capital Charge
    6) Other Fixed Costs
    7) Feed Costs
    8) Product Revenues
    9) Unit Profitability
- Profiles through Membrane Unit (per channel)
    1) H_2 Partial Pressure in Retentate (psia)
    2) H_2 Partial Pressure in Permeate (psia)
    3) H_2 Flux across membrane (g-mole/cm^2-s)
    4) Incremental H_2 transport across membrane (g-mole/cm^2)
    5) Incremental H_2 production from WGS reaction (g-mole/cm^2)
    6) H_2 Flow in retentate (g-mole/-s)
    7) CO Flow in retentate (g-mole/-s)
    8) CO_2 Flow in retentate (g-mole/-s)
    9) H_2O Flow in retentate (g-mole/-s)
    10) Flow of Inerts in retentate (g-mole/-s)
    11) Total Retentate Flow (g-mole/-s)

12) Mole Fraction H_2 in Retentate
13) H_2 Flow in Permeate (g-mole/-s)
14) Cumulative H_2 Productivity, H_2 recovered / H_2+CO in feed
15) Total Concentration in Retentate, (g-mole/liter)
16) H_2 Concentration in Retentate, (g-mole/liter)
17) CO Concentration in Retentate, (g-mole/liter)
18) CO_2 Concentration in Retentate, (g-mole/liter)
19) H_2O Concentration in Retentate, (g-mole/liter)
20) Inerts Concentration in Retentate, (g-mole/liter)
21) Net Rate of Production of H_2 from WGS reaction , (g-mole/liter-s)

***Equations & Theory*:** The following assumptions have been used in the development of the hydrogen separation membrane model:

- Steady-state, 1-dimensional, finite-difference model
  - H_2 flux calculated from ΔP across membrane
  - Ion transport step rate controlling
  - Flux proportional to $\ln(P_{H2}(\text{retentate}))/\ln(P_{H2}(\text{permeate}))$
  - No leakage of other gases (CO, CO_2, H_2O & Inerts) across membrane
- Homogeneous WGS reaction kinetics are included, but may be turned 'on' or 'off'
- Deactivation and other side reactions are ignored, including
  - Effect of contaminants
  - FT synthesis, coking, etc.

Governing differential equation[1]:

$$\frac{dn_{H_2}}{dA} = -\frac{\sigma RT}{4F^2 l}\ln\left(\frac{P'_{H_2}}{P''_{H_2}}\right) \qquad (1)$$

where:

n	-	molar flowrate of feed gas
A	-	membrane area
σ	-	membrane conductivity
R	-	ideal gas constant
T	-	absolute temperature
F	-	Faraday's constant
l	-	thickness of ion transport membrane
P'	-	partial pressure of retentate

[1] See "Ceramics for Advanced Power Generation," by Sarah Benson, IEA Coal Research 2000 (ISBN 92-9029-349-7), August 2000.

P” - partial pressure of permeate

The spreadsheet model can be easily recoded to consider other mechanisms for membrane transport using other flux relationships (by recoding the right-hand side of (1) which appears in Column E of the cell block named *PROFILES*).

A backward finite difference formulation is used to represent the governing differential equation (1) in the spreadsheet model. The values calculated in any given row are only dependent on values in the preceding row. Therefore, iteration is not required to achieve convergence at each point in the grid. This is particularly convenient in the spreadsheet format, since it allows the grid to be expanded by clicking on a row and dragging it downward; thus, copying all cell formulae and updating all cell references.

example output from the *H2M.*x*ls* spreadsheet.

APPENDIX F
IGCC System Analysis Methodology

IGCC System Analysis Methodology

***Modeling Parameters and Inlet Conditions* –** In order to simulate the performance of gas separation membranes using the numerical model described in Appendix E, stream compositions and process conditions must be specified for the membrane feed streams that correspond to the various membrane configurations under consideration. The flowsheet used for the system analysis is derived from the NETL 2007 baseline IGCC plant design with CCS[1] report *Cost and Performance Baseline for Fossil Energy Plants* [15]. The WGS exit stream compositions were estimated using additional data provided by Parsons[2], assuming a 10 C^{o} approach to WGS equilibrium. Overall conversion of CO to hydrogen is about 98%.

Figure F-1 is a simple schematic showing locations of possible membrane feed streams downstream of the gasifier and before acid gas removal. Table F-1 reports the corresponding compositions estimated for these streams.

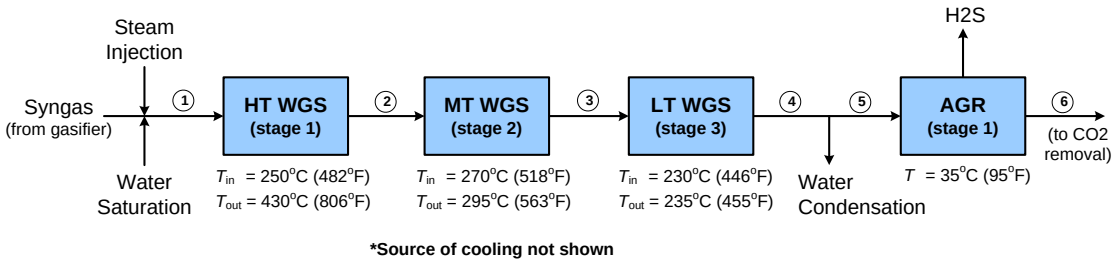

Figure F-1. Location of Streams Considered in System Analysis

Based on the 2007 NETL baseline design, the desired gas-turbine fuel-gas conditions are assumed to be 450 psia (31 bar) with a LHV of 120 Btu/scf. These conditions correspond to the estimated performance of a GE "F" turbine at the time the screening study was performed.

[1] Case 4, *Cost and Performance Baseline for Fossil Energy Plants, Volume 1: Bituminous Coal and Natural Gas to Electricity Final Report* (Original Issue Date, May 2007), Report No. DOE/NETL-2007/1281, Revision 1, August 2007.
[2] Personal communication from R.L. Schoff (Parsons Corp.) and J. Ciferno (U.S. DOE), September 2005.

Table F-1. Syngas Composition Used in Screening Analysis

Composition, vol%	*Stream 1*	*Stream 2*	*Stream 3*	*Stream 4*	*Stream 5*
H_2	19.33%	39.40%	42.45%	43.20%	57.34%
CO	24.43%	4.36%	1.31%	0.56%	0.75%
CO_2	5.68%	25.75%	28.80%	29.55%	39.22%
H_2S+COS	0.48%	0.48%	0.48%	0.48%	0.64%
NH_3	0.16%	0.16%	0.16%	0.16%	0.21%
CH_4+C_2H_6	0.24%	0.24%	0.24%	0.24%	0.32%
N_2+Ar	0.81%	0.81%	0.81%	0.81%	1.08%
H_2O	48.86%	28.79%	25.75%	25.00%	0.45%
Total	100.00%	100.00%	100.00%	100.00%	100.00%
H_2O/CO Ratio	2.00	6.60	19.61	44.28	0.61
$K_{WGS}(P) = K_{WGS}(T)$	0.09	8.08	36.16	90.46	6612.36
Temperature, °C	250	430	295	235	105
WGS Approach, C°	-	10	10	10	-

Three membrane placement options were considered for screening: post-WGS H_2 recovery, CO_2 compressor-interstage H_2 recovery, and H_2 recovery integrated with WGS. Parameters considered in the screening analysis are reported in Table F-2.

***Screening Methodology* –** The following steps were utilized to estimate changes in equipment capacity due to the different membrane configurations considered:

1) Remove 2nd-stage of Selexol unit
2) Add membranes and determine area requirements
3) Determine new CO_2 compression requirements: number of stages and flow
4) Remove humidification if not needed
5) Add hydrogen compression if necessary
6) Determine changes to auxiliary power load
7) Determine changes to auxiliary steam load and estimate power loss

Table F-2. Membrane Screening Parameters

H_2 selective membrane located downstream from WGS reactors		**Range**
Feed Gas H_2 Content, vol%	based on maximum shifting of syngas	57.34%
Permeate H_2 Content, vol%	based on no sweep, partial, or max sweep gas, set by gas turbine	100 / 72 / 44%
Feed Gas Pressure, psia	set by gasifier design pressure and equipment pressure drops	400 / 700
Permeate Pressure, psia	design parameter for membrane; max set by gas turbine	50 / 380
H_2 Partial-Pressure Approach, psi	indicative of membrane area	0 / 10 / 25 / 50
Pressure Diff. Across Membrane, psi	limitation of membrane material and fabrication	20 - 650
H_2 selective membrane integrated with CO_2 compression		
Feed Gas H_2 Content, vol%	based on maximum shifting of syngas	57.34%
Permeate H_2 Content, vol%	based on no sweep, partial, or max sweep gas, set by gas turbine	100 / 72 / 44%
Feed Gas Pressure, psia	CO_2 compression requirements and compression ratios	800 / 1,600 / 2,200
Permeate Pressure, psia	design parameter for membrane; max set by gas turbine	50 / 380
H_2 Partial-Pressure Approach, psi	indicative of membrane area	0 / 10 / 25 / 50
Pressure Diff. Across Membrane, psi	limitation of membrane material and fabrication	420 - 2,150
PSA located downstream from WGS reactors with…		
Feed Gas H_2 Content, vol%	based on maximum shifting of syngas	57.34%
Feed Gas Pressure, psia	design parameter for PSA unit; max set by gas turbine	380
Tail Gas Pressure, psia	design parameter for PSA unit; affects compression requirements	17 / 50 / 100
...H_2 selective membrane integrated with CO_2 compression		
Permeate H_2 Content, vol%	based on no sweep, partial, or max sweep gas, set by gas turbine	100 / 44%
Feed Gas Pressure, psia	CO_2 compression requirements and compression ratios	800 / 1,600 / 2,200
Permeate Pressure, psia	design parameter for membrane; max set by gas turbine	380
H_2 Partial-Pressure Approach, psi	indicative of membrane area	0 / 10 / 25 / 50
Pressure Diff. Across Membrane, psi	limitation of membrane material and fabrication	420 - 1,820
H_2 selective membrane integrated with WGS reactors		
Feed Gas H_2 Content, vol%	based on partial shifting of syngas, set by WGS reactor design	19.3 / 39.4 / 43%
Permeate H_2 Content, vol%	based on no sweep, partial, or max sweep gas set by gas turbine	100 / 44%
Feed Gas Pressure, psia	set by gasifier design pressure and equipment pressure drops	700
Permeate Pressure, psia	design parameter for membrane; max set by gas turbine	50 / 380
H_2 Partial-Pressure Approach, psi	indicative of membrane area	0 / 10 / 25 / 50
Pressure Diff. Across Membrane, psi	limitation of membrane material and fabrication	420 - 650
LTS Exit Temperature, ^oC	design parameter for LTS WGS; set by inter-cooling	235 / 300
MTS Exit Temperature, ^oC	design parameter for MTS WGS; set by inter-cooling	270 / 455
HTS Exit Temperature, ^oC	design parameter for HTS WGS; set by inter-cooling	430 / 550
WGS Temperature Approach, C^o	indicative of catalyst requirements	0 / 10 / 20

APPENDIX G
Economic Analysis Methodology

Economic Analysis Methodology

Costing Methodology – The following steps were utilized to estimate changes to the cost of electricity for the different membrane configurations considered:

1) Adjust costs for WGS due to changes in operating pressure
2) Remove costs associated with 2nd-stage of Selexol unit
3) Add assumed membrane cost for membranes
4) Determine new costs for CO_2 compression
5) Remove costs associated with humidification if not needed
6) Add costs for hydrogen compression if necessary
7) Adjust plant to auxiliary power load due to power losses

APPENDIX H

Primer on Targeting Membrane Cost & Performance

Primer on Targeting Membrane Cost & Performance

This primer provides details on the approach used in establishing R&D targets for gas separation membrane technologies being applied to pre-combustion removal of CO_2 from coal-derived syngas for Integrated-Gasification Combined-Cycle (IGCC) power generation.

Why Set R&D Goals? – The primary purpose of applied R&D is the solution of current and future societal, environmental, and economic problems based on the discovery and application of new technologies. In contrast, pure R&D is focused on a search for knowledge and truth for their own merit. Pure R&D by its nature can and should wander into new and exciting areas. Applied R&D, however, must remain focused on the problem at hand, or risk not fulfilling its mission of solving the problem identified in a timely and cost-effective manner[1]. Therefore, it is appropriate to set goals and targets for applied R&D programs and projects. This is especially true when society as a whole (*i.e.* the tax-payer) is asked to fund these programs and projects.

A well thought-out applied R&D program will have well-defined goals. These goals will relate directly to the problem at hand. For example, and of direct bearing to this discussion, is the problem of anthropologically-driven global climate change. This problem is so large and complex that some cannot accept the current evidence for its existence. To address this problem, the U.S. DOE, and other organization that sponsor R&D worldwide, have identified and developed R&D programs to specifically address certain critical aspects of the problem.

CCS Program IGCC R&D Goals –The DOE's CCS (Carbon Capture and Sequestration) R&D Program has established a goal of developing and demonstrating by 2020, technologies that can capture and sequester 90% of the CO_2 generated by future IGCC plants, at a cost of electricity (COE) increase of less than 10% above current technology without CCS.

The CCS Program goal is relative to the performance of current state-of-the-art (SOTA) IGCC technology. A reference plant design for making comparisons has been established based on analysis conducted at DOE's National Energy Technology Laboratory (NETL)[2]. As a part of this baseline, NETL has also estimated the increase in the COE for 90% CO_2 capture from a SOTA IGCC plant fitted with the best available CO_2 capture technology, currently considered to be a physical absorption system employing the commercial solvent Selexol™.

[1] It is often the case that pure and applied R&D alike often inadvertently result in the discovery of new technologies (or ones different from those intended) that have direct application to existing or future problems.

[2] *Cost and Performance Baseline for Fossil Energy Plants: Volume 1 - Bituminous Coal and Natural Gas to Electricity* (Original Issue Date, May 2007), Report No. DOE/NETL-2007/1281, Revision 1, August 2007.

The COE from the DOE baseline design report, with and without CCS are:

Reference IGCC plant with CCS	10.29 ¢/kWh
Reference IGCC plant without CCS	− 7.80
Reference IGCC plant increase in COE	2.49 ¢/kWh

The COE for the reference plant with SOTA CCS is 32% above that for the same plant without CCS. This increase in COE is the result of a number of factors:

- Addition of water-gas-shift (WGS) reactors to convert CO in the syngas to H_2 and CO_2.
- Replacement of the single-stage MDEA acid gas removal (AGR) unit used for H_2S removal with a two-stage Selexol system for H_2S and CO_2 removal.
- Addition of CO_2 compression, transport, injection and CCS site monitoring.

The DOE Program R&D goal for COE is:

Reference IGCC plant without CCS	7.80 ¢/kWh
Goal for future IGCC plants with CCS	+0.78
Maximum incremental increase in COE	8.58 ¢/kWh

The above goal corresponds to a 17% reduction in COE relative to the best currently available CCS technology for IGCC. The goal is not meant to establish future policy or regulations, especially since R&D success cannot be guaranteed. Nor is it meant to be applied generally to determine the economic feasibility of any new real-world IGCC project. Rather, the 10% COE goal for 90% capture is solely intended for use in measuring the progress of pre-combustion CCS technology development under the DOE CCS R&D Program.

Other DOE Fossil-Energy R&D Programs have their own goals relating to CCS. In particular, alternative-fuels programs, such as coal-to-liquids and coal-to-hydrogen that employ coal gasification, have adopted the 90% capture target, but are subject to economic metrics tied to existing technologies for producing hydrogen and conventional liquid fuels. In addition, specific capture technologies, such and gas separation membranes, will in general have different numerical targets for their key performance parameters based on the application.

In addition to chemical and physical absorption, other pre-combustion capture technologies being investigated by the DOE R&D Program include gas-solid adsorption and membrane separation. Outside of the CO_2 capture component, next-generation and future technologies relating to gasification, syngas clean-up, water-gas-shift, CO_2 compression and gas turbines can also contribute to achieving the COE goal established by the DOE CCS R&D Program.

Establishing Membrane R&D Targets – An R&D program goal by itself does not provide much guidance to researchers and technology developers. The goal must be

translated into meaningful numerical targets related to the type of technology being investigated. Specific to H_2-separation membranes, the DOE CCS goal must be related to process and cost parameters that are meaningful in membrane-based gas separations. These parameters are H_2 permeance, H_2 selectivity, and membrane cost.

The conversion of the COE goal for CCS into membrane R&D targets is an exercise in reverse engineering. One imbeds the technology under consideration into the IGCC process, assumes the technology can attain 90% CO_2 capture, and then back calculates the range of membrane parameters satisfying the COE goal. While in principle simple, the procedure requires a parametric study to determine H_2 recovery as a function of the unique set of membrane permeances/selectivities that result in 90% CO_2 capture. This data set is used to construct a cost curves for the membrane system being investigated. The cost curves are then used to establish targets for H_2 permeance, H_2 selectivity, and membrane cost. Figure H-1 shows example cost curves for illustrative purposes.

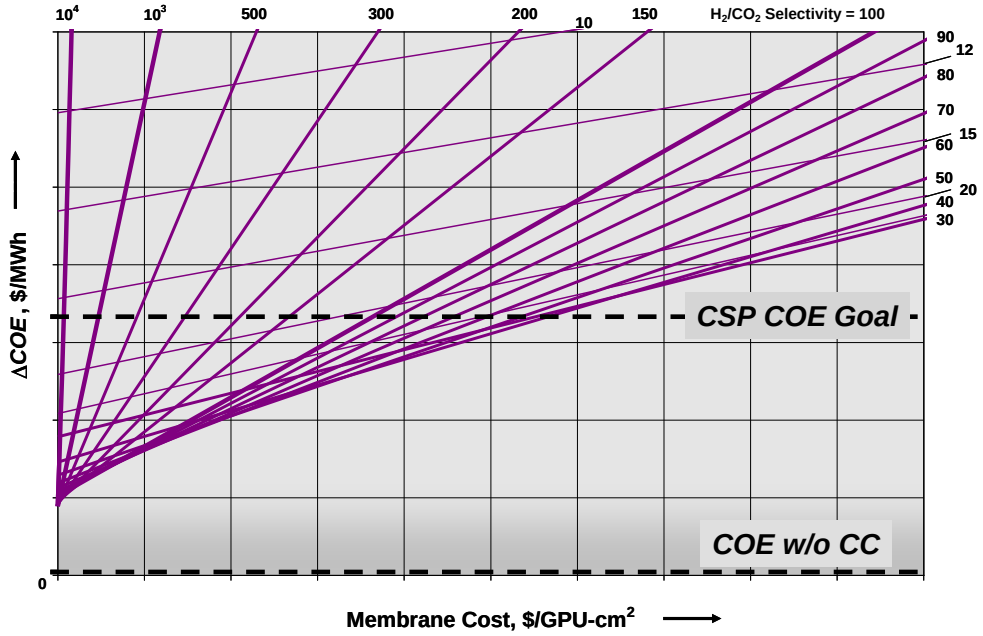

Figure H-1. Illustrative Membrane Cost Curves for IGCC with CCS

The following steps are used in construction of the cost curves depicted above:

Step 1: Select membrane configuration

Each membrane configuration integrated into the IGCC process design will result in a unique set of membrane targets, requiring each system to be analyzed individually. In this assessment five unique configurations were considered:

Configuration Ia – Membrane integration post-WGS with H_2 re-compression

Configuration Ib – Membrane integration post-WGS with permeate sweep

Configuration IIa – Membrane integration with CO_2 compression and permeate sweep

Configuration IIb – PSA and membrane integration with CO_2 compression and permeate sweep

Configuration III – Membrane integration with medium-temperature WGS

In addition, each configuration considered a number of flowsheet variations, such as cold versus warm-gas clean-up for H_2S removal, CO_2/H_2S co-sequestration with no H_2S removal, and the effects of having to re-heat the membrane feed gas due to possible membrane operating limitations. Sensitivities were also run to examine the impact of relaxing or tightening the 90% CO_2 capture requirement.

Step 2: Predict Membrane Performance

The key components for the gas separation are H_2 and CO_2. For size-selective membranes, H_2 is the more permeable of these two gases, and the ideal selectivity (*i.e.* permselectivity) of H_2 relative to CO_2 is greater than one. With the exception of H_2O, all of the other syngas components possess H_2 permselectivities which are greater than that of CO_2. If the gas separation is solely based on molecular size, then the permselectivity of H_2 relative to H_2O is less than one. However, for certain materials such a silica glass and certain zeolites, the permselectivity of H_2 relative to H_2O can be greater than one; and for palladium, permselectivity is essentially infinite.

In order to develop unique permselectivity targets for the key gas components, H_2 and CO_2, it is necessary to make assumptions regarding the selectivities of the other syngas components. The permselectivity of H_2 relative to the gases: H_2S, CO, N_2 and CH_4, will be assumed to be large. For H_2O, the H_2 permselectivity will be assumed to be 0.25 for post-WGS membrane configurations, and large for integrated membrane-WGS configurations. The former value is typical of many polymer-based gas separation membranes; whereas, the latter is required for WGS interstage membranes, since loss of reaction water has a negative impact on WGS equilibrium.

The numerical values assumed for the selectivities of all non-key components of the syngas are listed in Table I-1. The assumed selectivities constitute additional performance targets for membrane R&D (thus the '<' and '>' signs used in the table).

In regards to the permselectivity of H_2 relative to CO_2, that is $S_{H2,CO2,}$ specifying the membrane system total H_2 and CO_2 recoveries results in a unique set of values for $S_{H2,CO2}$ and *PA*, which minimize *PA*. Where, *PA* is the product of the H_2 permeance P_{H2} and the membrane area *A*. For any fixed CO_2 recovery (in this case 90%), an increase in H_2 recovery will require both an increase in $S_{H2,CO2}$ and in *PA*.

The membrane numerical model described in Appendix F is used to construct a table of values for H_2 recovery as a function of $S_{H2,CO2}$ and *PA*. Typically, H_2 recovery values of 80, 85, 90, and 95% were used. Above about 95%, selectivity and *PA* requirements increase rapidly, approaching a limiting asymptote for H_2 recovery that is unique for any given membrane configuration. A series model runs were also made above 95% in order to estimate the maximum achievable H_2 recovery.

It is impractical to minimize *PA* within the membrane model. Therefore, heuristic arguments where used to avoid rigorous optimization. All configurations considered the integration of three banks of membrane modules. Membrane areas of the first two banks were kept equal, %recovery was kept equal, sweep gas when considered was distributed. While these assumptions do not gareetee the true minimum PA, they do seem to produce a low value .

Step 3: Predict Membrane Cost

The procedure outlined in Appendix G is used to analyze the performance of the IGCC plant incorporating H_2 selective membranes for CO_2 capture. This analysis provides changes to plant parasitic energy requirements (*i.e.* steam and electric power) and to plant equipment capacity requirements, for each of the H_2 recovery levels considered in Step 2. In turn, the procedure from Appendix F is used to convert this information into a lelvelized-cost of electricity (COE), using the NETL IGCC economics model.

The change in COE relative to the baseline IGCC plant without CCS is related to the cost of the membrane per unit area per unit permeance, C_{PA}, by a straight line:

$$\Delta COE = a + b_A c_A A = a + b_A \times (c_A / P) \times (PA) = a + (b_A (PA)) \times (c_A / P) \quad \text{(C1)}$$

or

$$\Delta COE = a + b_{PA} C_{PA} \quad \text{(C2)}$$

where a and b are constants, and c_A is the cost of the membrane per unit area only. The subscripts A and PA refer to quantities either on a per unit area or a per unit area per unit permeance basis, respectively.

A plot of ΔCOE versus C_{PA} results in a family of lines with $S_{H2,CO2}$ as a parameter. By assuming two vales for C_{PA}, the IGCC economics workship can be used to determine two values for ΔCOE, from which the constants a and b_{PA} can be determined. Plotting of these data results in membrane cost curves, such as those shown in Figure H-2.

Step 4: Establish Membrane R&D Targets

By examining the cost curves established in Step 3, a number of membrane cost and performance regimes may be identified.

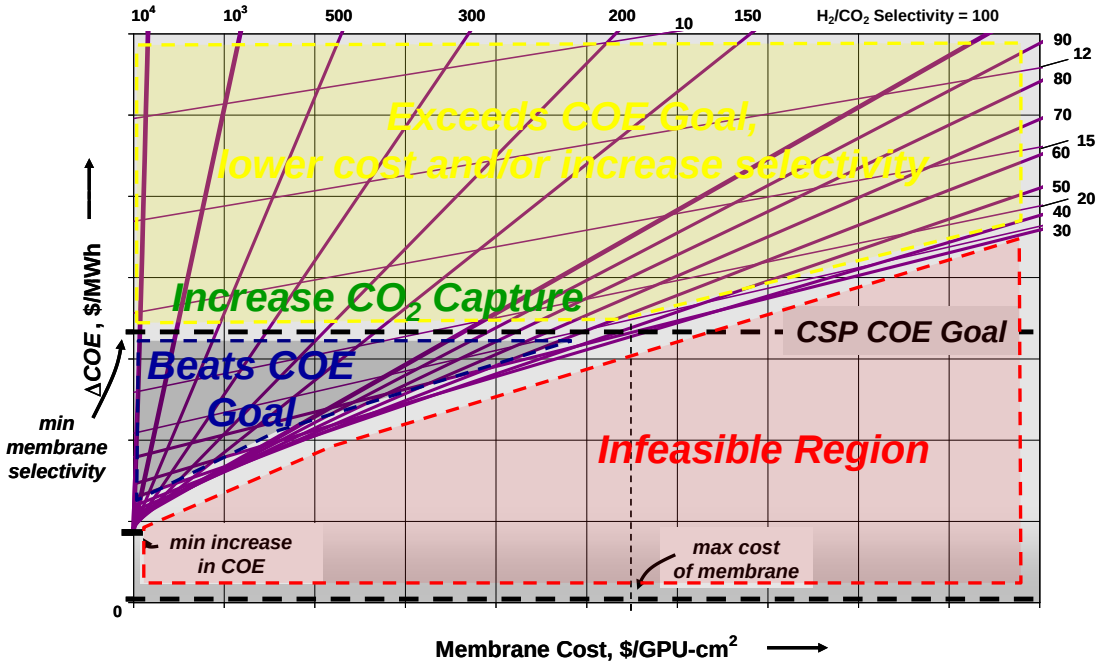

Figure H-2. Membrane Performance Regimes for IGCC with CCS

Interpreting Membrane R&D Targets – Figure H-3 depicts the performance three hypothetical membranes. The point labeled S_1, does not meet the membrane goals. Researchers developing this membrane have three distinct options for improvement. They can try to maintain selectivity and either lower the cost per unit area or increase the permeance, or they can try to increase selectivity while maintaining cost and permeance (thus, shifting the line labeled *Selectivity* 1 down). Interestingly, the point labeled S_2, can never meet the goal without improving selectivity.

Since membrane technology will be employed with other advanced technologies, it will not be required to achieve all of the cost reduction alone. The red dashed-line labeled "Membrane Goal" lies between the baseline IGCC plant retrofitted with a currently available carbon capture system (green-dashed line) and the program goal (blue dashed-line). For a membrane technology to achieve the program's membrane goal for a given selectivity (*e.g.*, the line labeled *Selectivity* 1), its cost in units of dollars per membrane area per unit of membrane permeance must lie to the left of the vertical orange dashed-line. Note that a trade-off thus exists between permeance and cost per unit of area. A membrane could achieve the target with either a "low" cost per unit area or a "high" permeance.

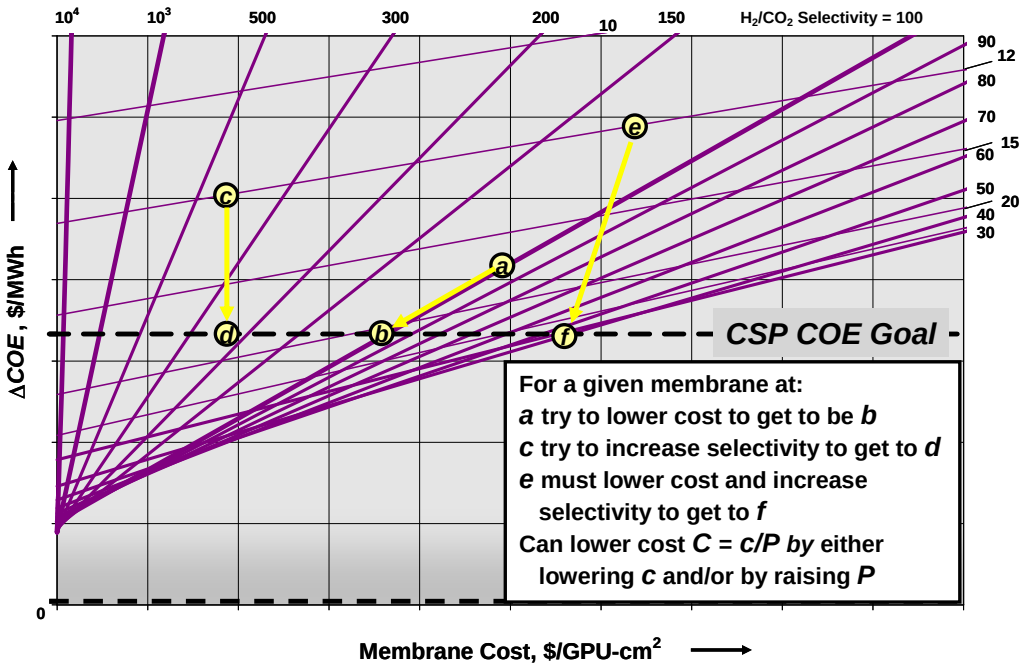

Figure H-3. Illustrative Membrane R&D Strategies for IGCC with CCS

Table H-2 shows on the targets described above can be used to establish metrics for following the progress of membrane R&D.

	H_2/CO_2 Selectivity	Membrane Cost $/GPU-cm^2
Has not demonstrated potential to ever be competitive	$< S_{min}$(SOTA)	-
May have potential, more fundamental work required	$> S_{min}$(SOTA)	$< C_{max}$ (SOTA)
Has definite potential but does not meet IGCC targets w/CC	$> S_{min}$(SOTA)	$< \frac{\Delta COE \text{ (SOTA)} - a(S)}{B(S)}$
Has definite potential and meets IGCC targets w/CC	$> S_{min}$(CSP Goal)	$< \frac{\Delta COE \text{ (Goal)} - a(S)}{B(S)}$